The Abdus Salam International Centre for Theoretical Physics

United Nations Educational, Scientific and Cultural Organization

IAEA International Atomic Energy Agency

2269-19

Workshop on New Materials for Renewable Energy

17 - 21 October 2011

Charge carrier transport in organic photovoltaic devices (Transport phenomena in organic photovoltaic diodes)

Niyazi Serdar SARICIFTCI

Linz Institute for Organic Solar Cells LIOS
Institute for Physical Chemistry, Johannes Kepler University
Linz
Austria

Transport Phenomena in Organic Photovoltaic Diodes

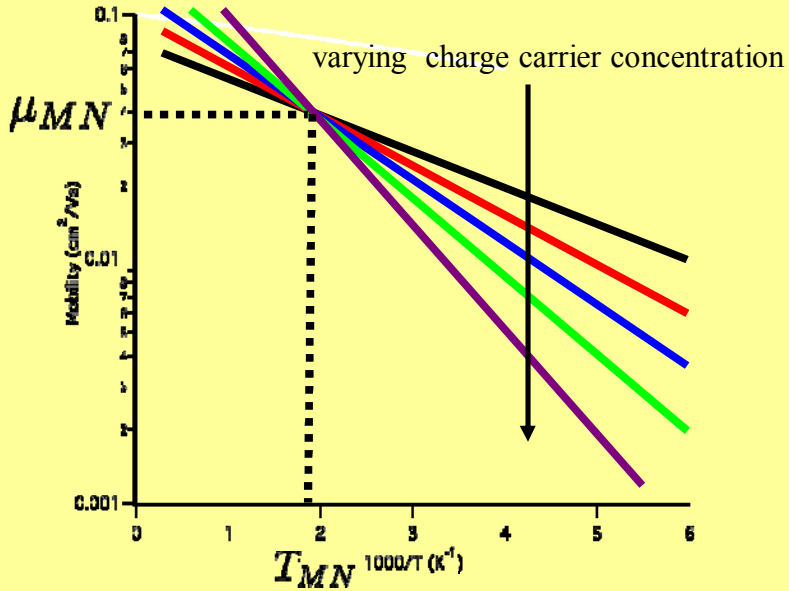

Niyazi Serdar SARICIFTCI

Linz Institute for Organic Solar Cells (LIOS),

Physical Chemistry, Johannes Kepler University Linz

Austria

Transport and Order

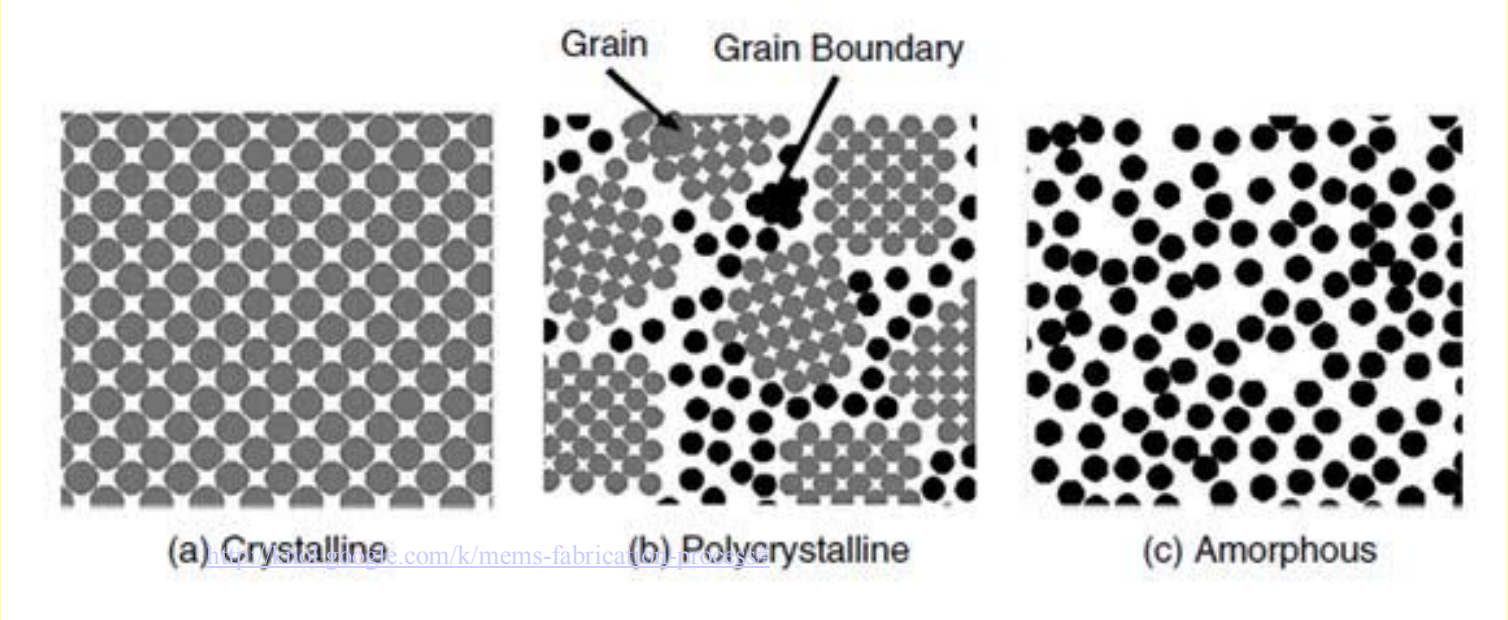

What are the differences in charge transport crystalline versus disordered media?

Crystals

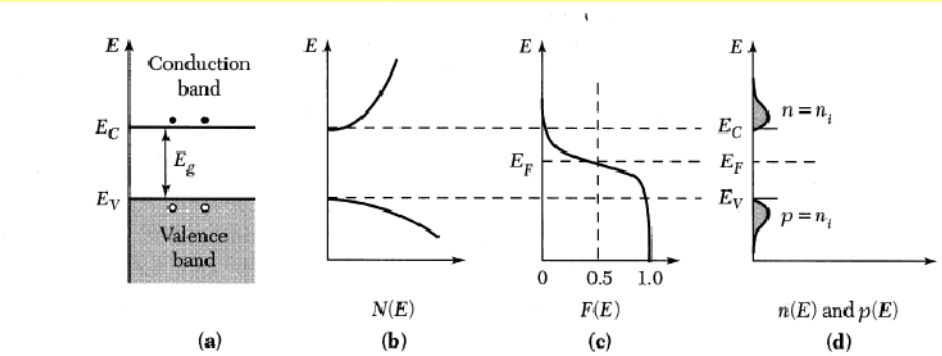

Fig. 21 Instrinsic semiconductor. (*a*) Schematic band diagram. (*b*) Density of states. (*c*) Fermi distribution function. (*d*) Carrier concentration.

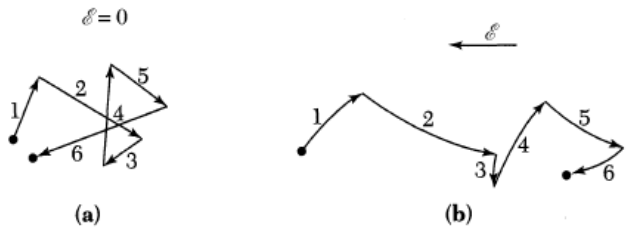

Fig. 1 Schematic path of an electron in a semiconductor. (*a*) Random thermal motion. (*b*) Combined motion due to random thermal motion and an applied electric field.

Sze, Semiconductor Devices_Physics and Technology 2ndEd_Wiley

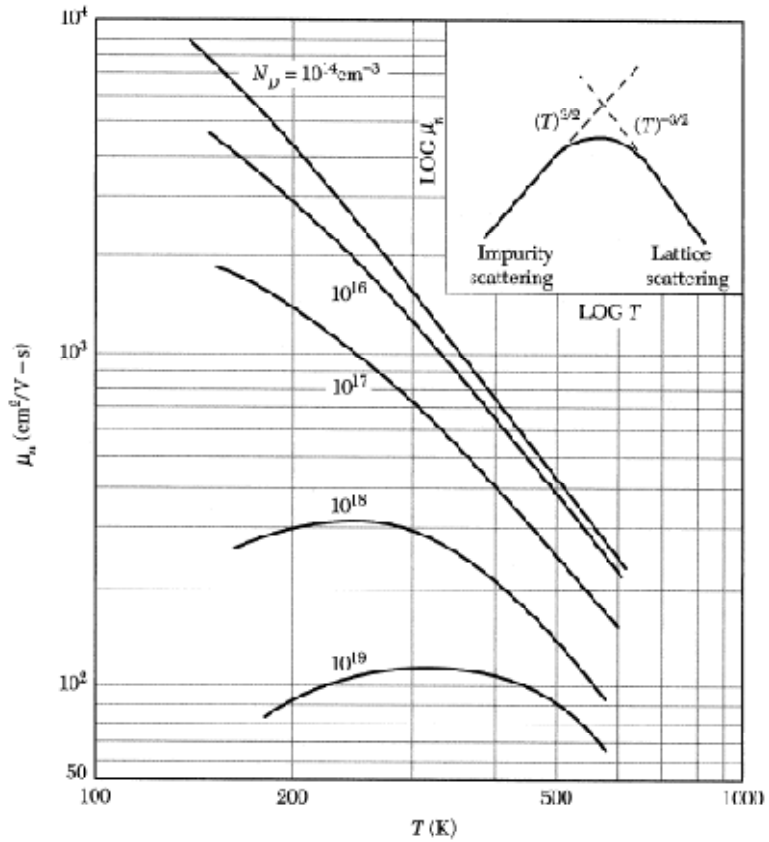

LV. F. Beadle, J. C. C. Tsai, and R. D. Plummer, Eds., Quick Reference Manual for Semiconductor Engineers, Wiley, New York, 1985.

Bulk Heterojunction Device Structure

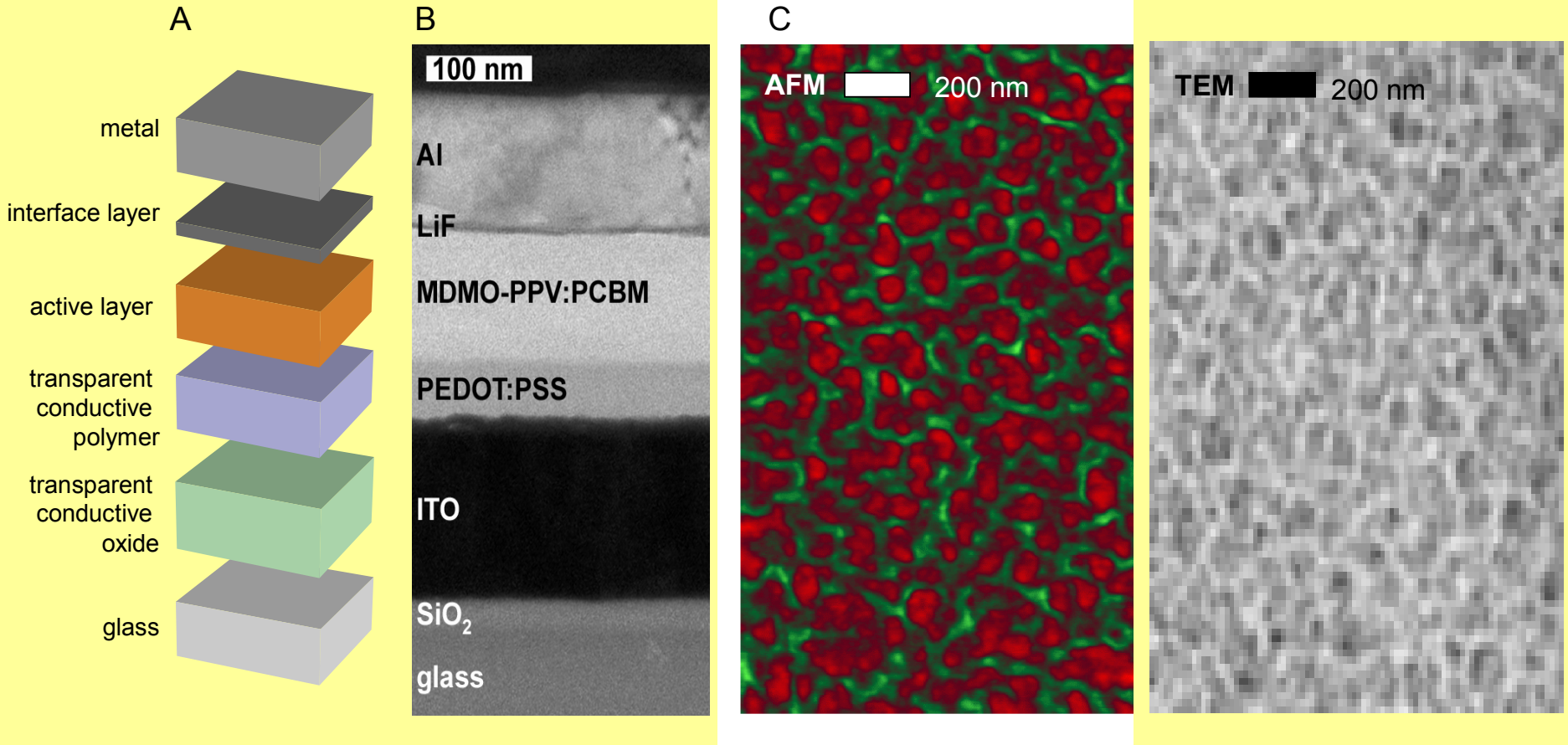

Rene Janssen *et al*, 2004

Bulk Heterojunctions

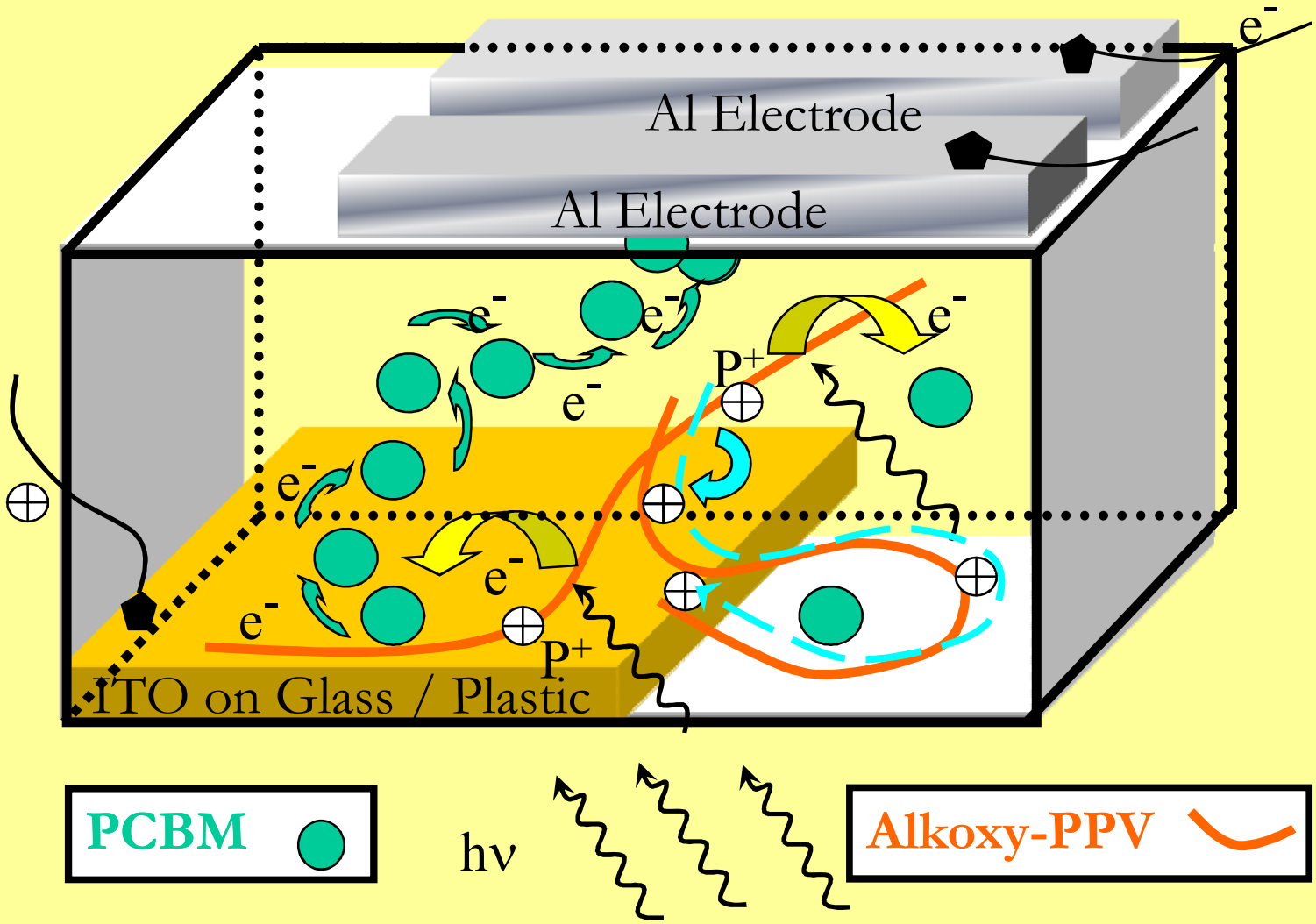

3-D Percolation

Strong luminescence quenching occurs at appr. 1 mol% of PCBM in alkoxy-PPV. Photocurrent onset at appr. 17 mol% PCBM, in accordance with percolation theory.

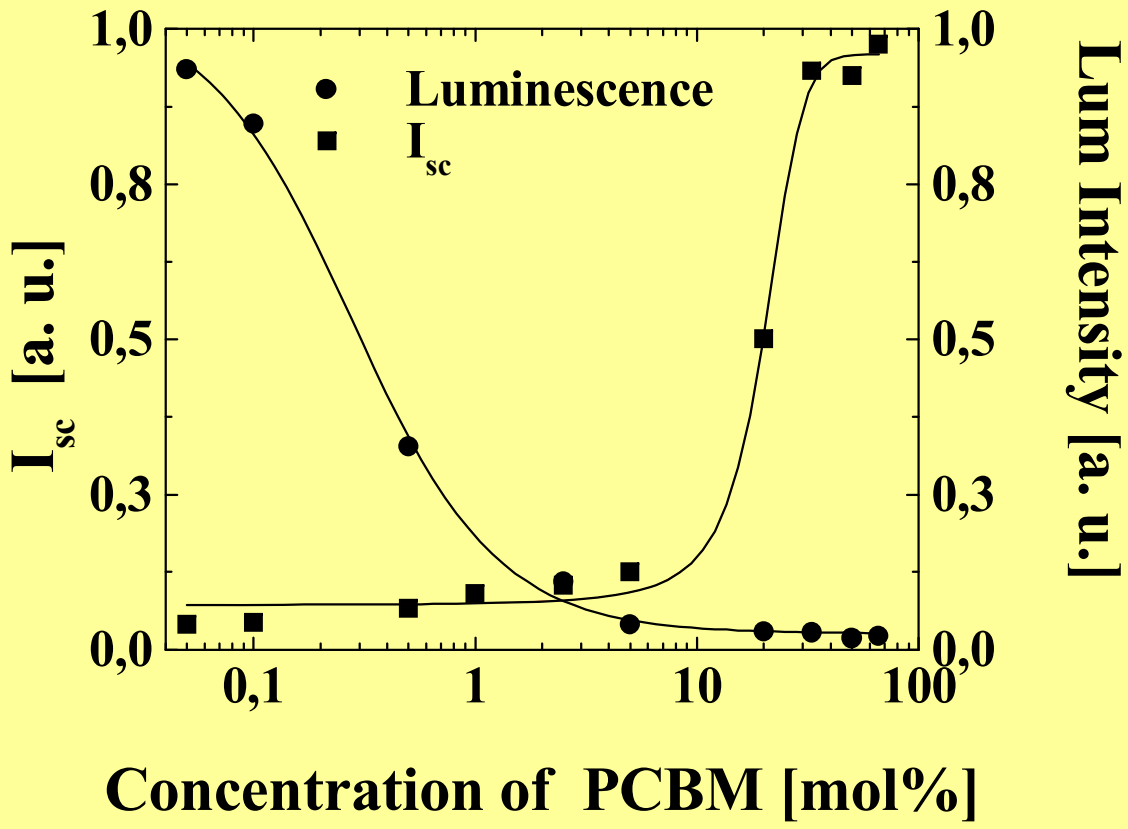

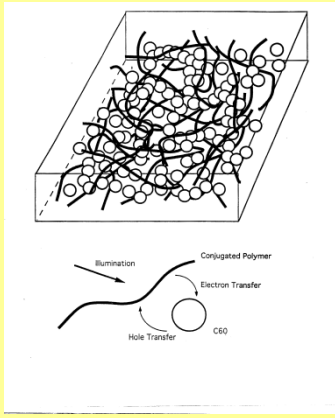

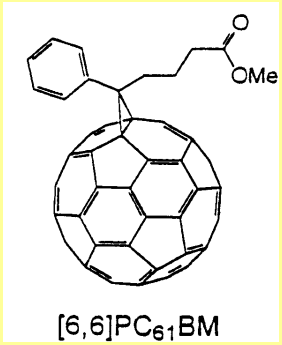

Property Optimization

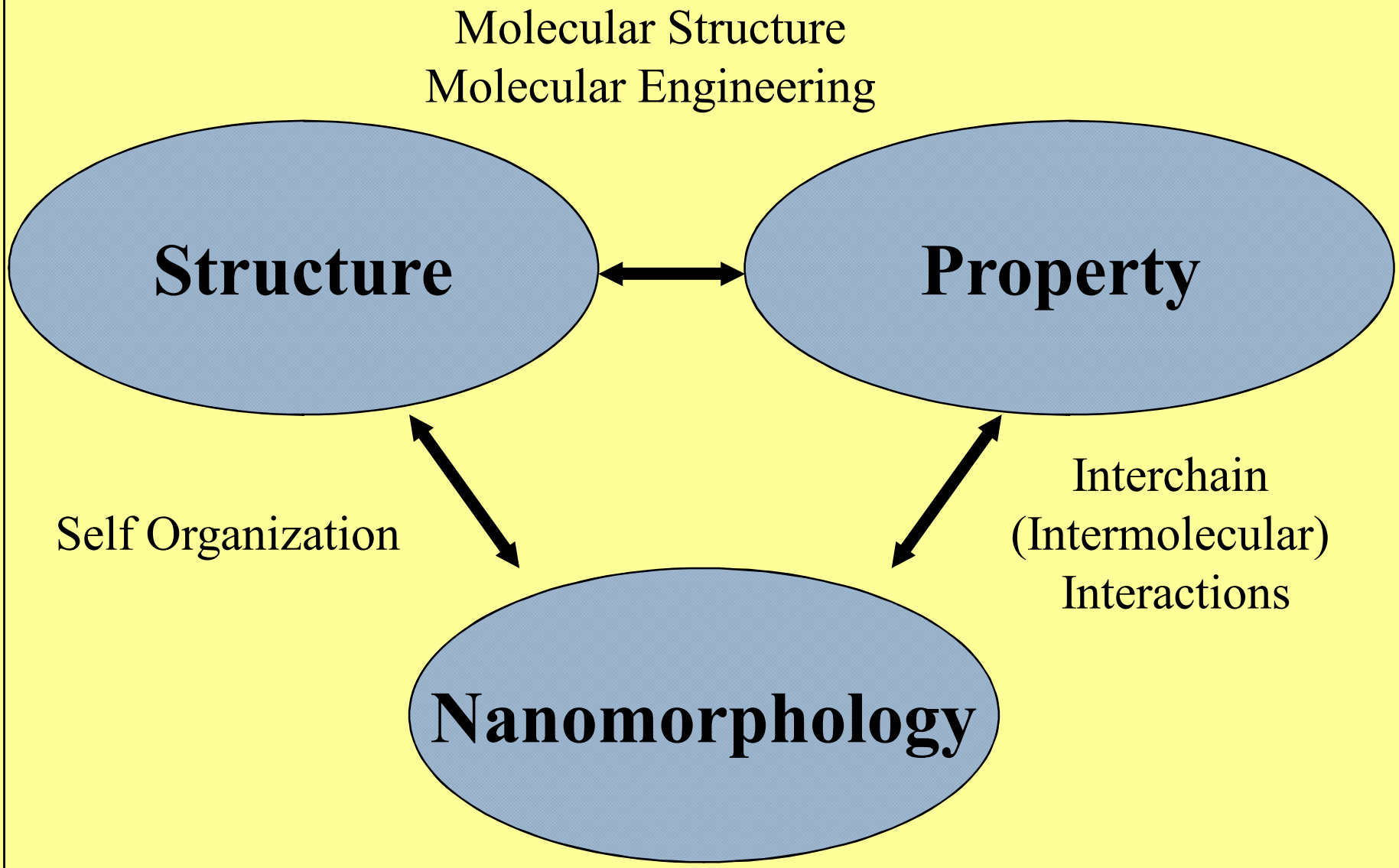

Nanomorphology vs Efficiency

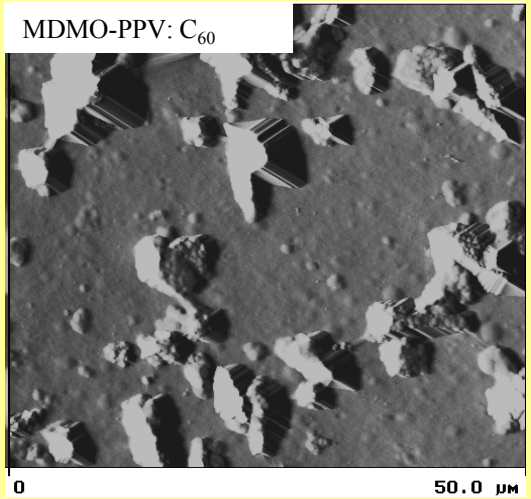

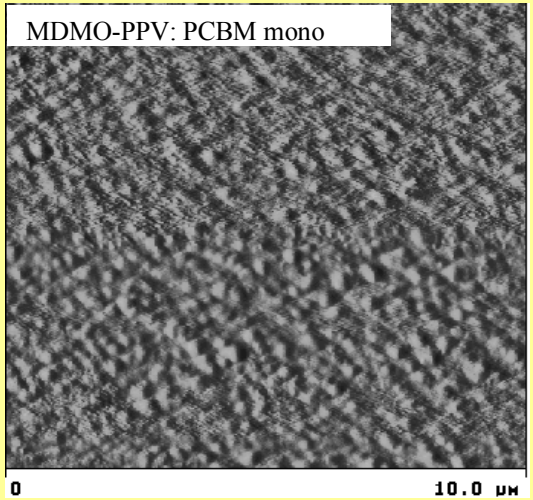

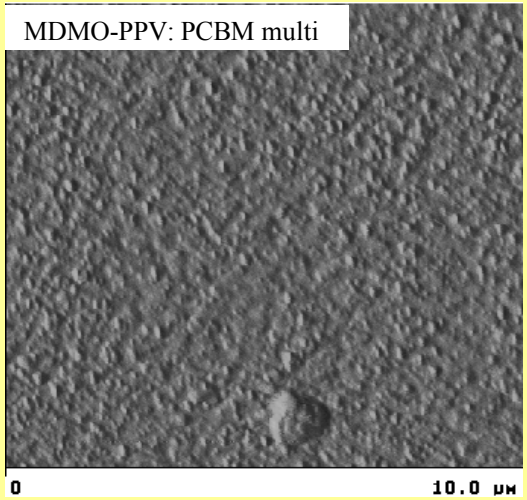

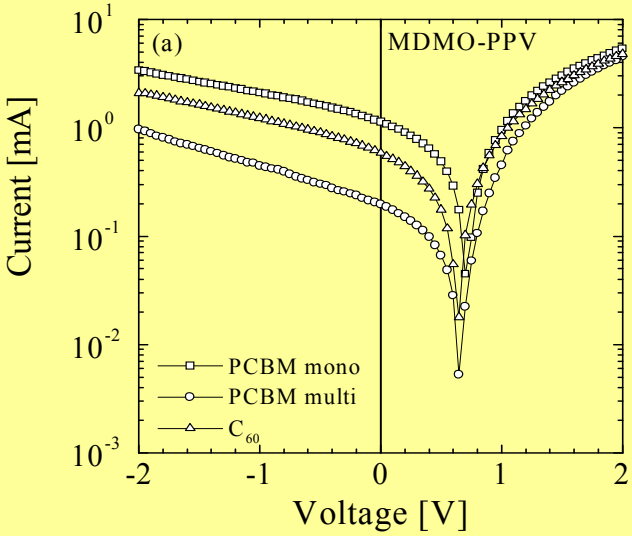

Nanomorphology: Solvent Effects

a

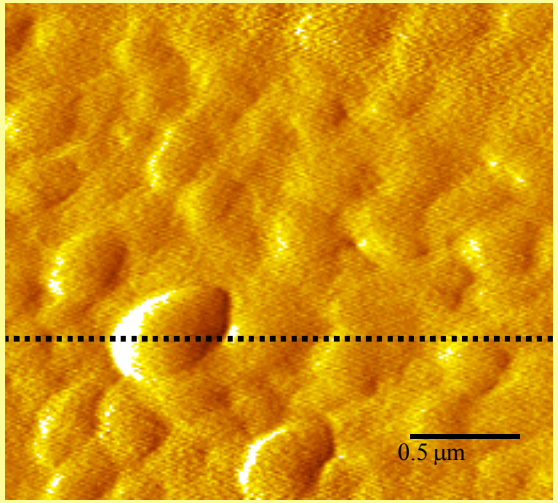

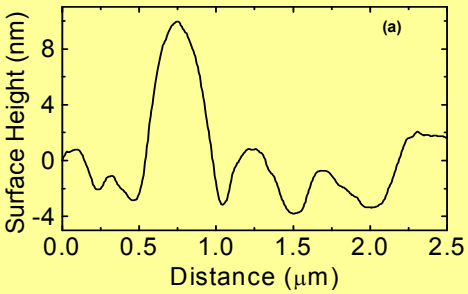

Toluene cast film

b

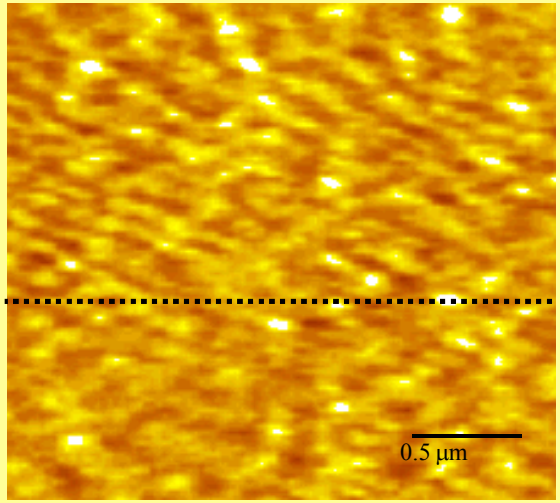

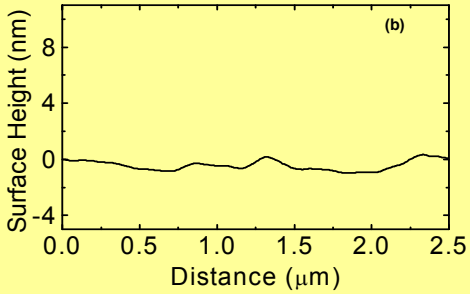

Cholorobenzene cast film

Morphology: Solvent effects

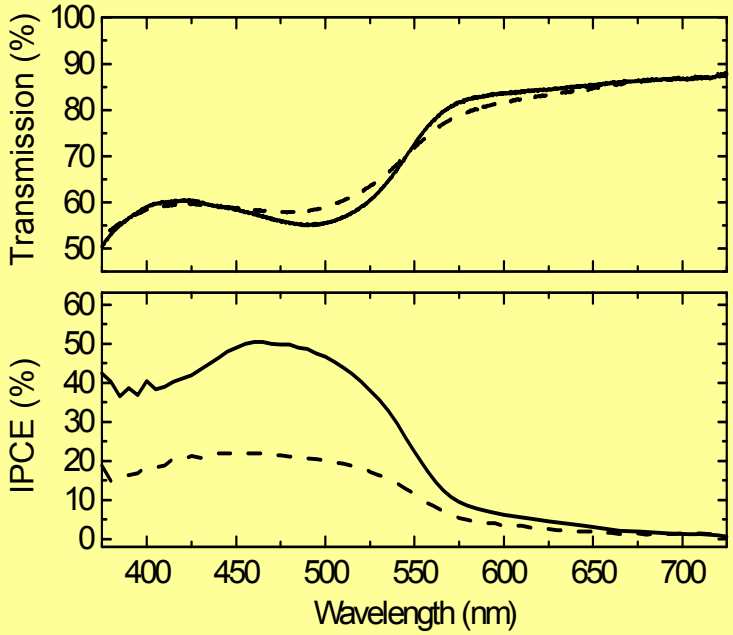

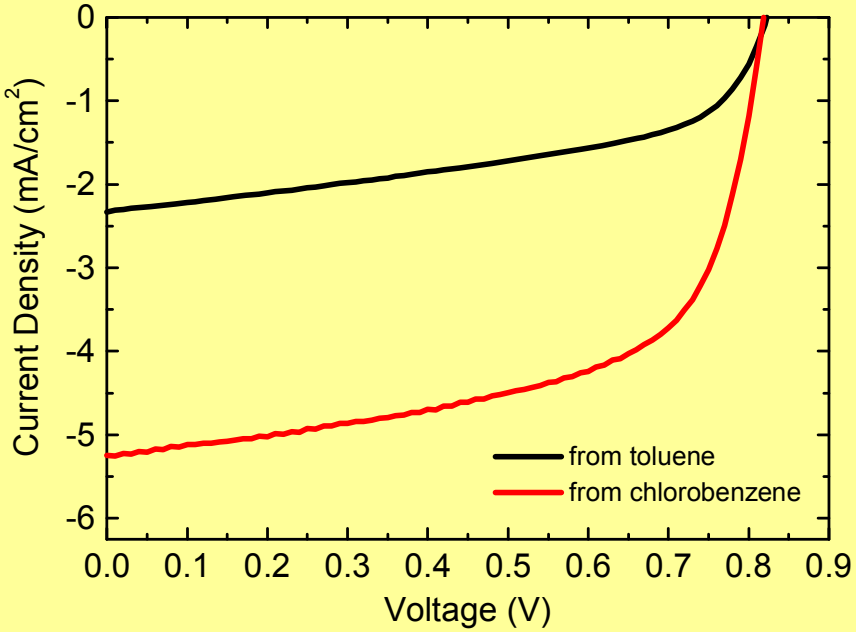

A 2-3 fold increase of the IPCE and short circuit current was observed by S.E. Shaheen et al.* due to the change from toluene to chlorobenzene as solvent, while by AFM measurements a decrease in the surface roughness was detected.

*S.E. Shaheen, C.J. Brabec, N.S. Sariciftci, F. Padinger, T. Fromherz, J.C. Hummelen, *Appl. Phys. Lett.* **78**, 841 (2001)

Nanomorphology: Solvent Effects

Improved performance: higher mobility

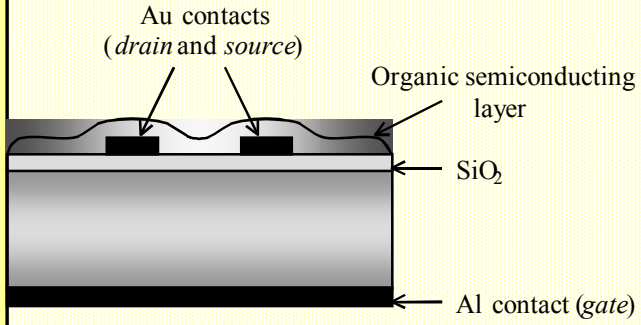

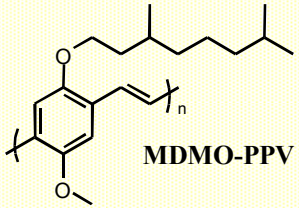

MDMO-PPV

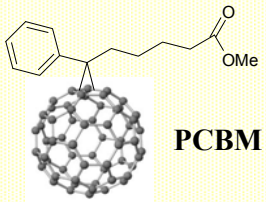

PCBM

$$I_{ds_{sat}} = \frac{\mu_{FE} W C_{ox}}{2L}\left(V_{gs} - V_t\right)^2$$

$$I_{ds_{lin}} = \frac{\mu_{FE} W C_{ox}}{L}\left(V_{gs} - V_t\right)V_{ds}$$

Field Effect Transistors with Conjugated Polymer as Active Layer

Mobility calculated from linear and saturation regime using long integration times

Wim Geens *et al*, *Organic Electronics* **3**, 105 (2002)

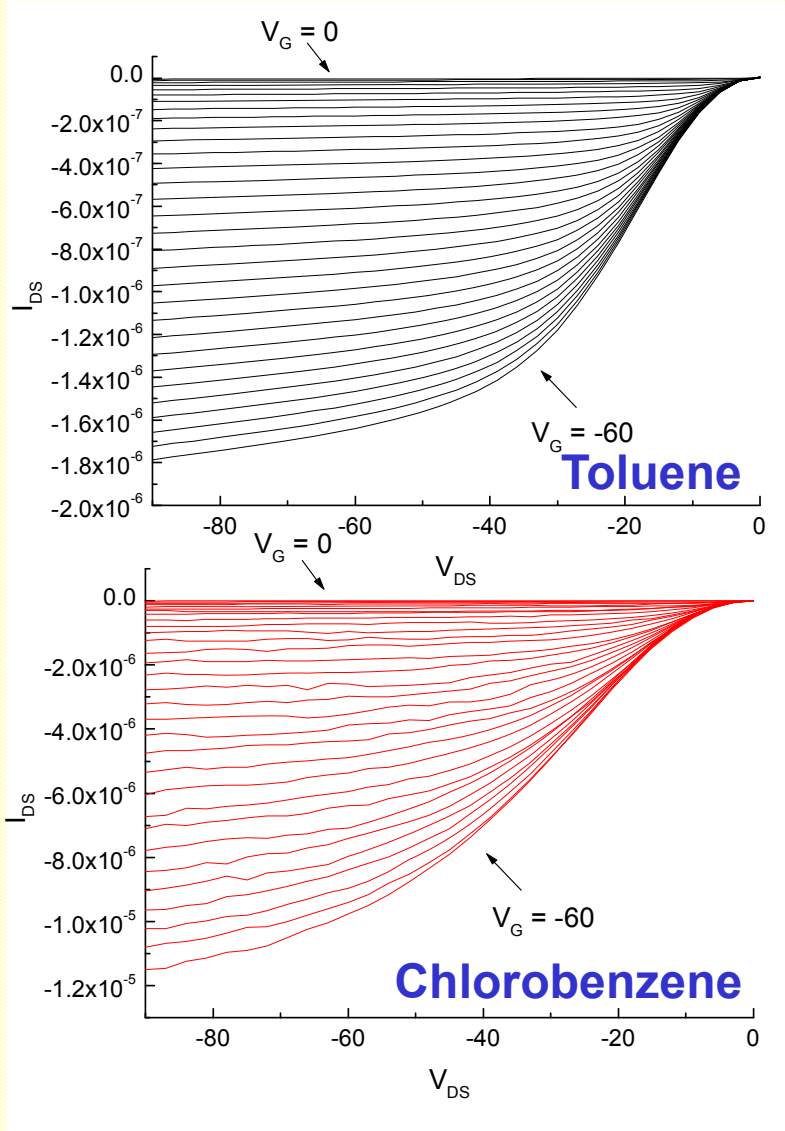

Nanomorphology Effects-AFM Studies

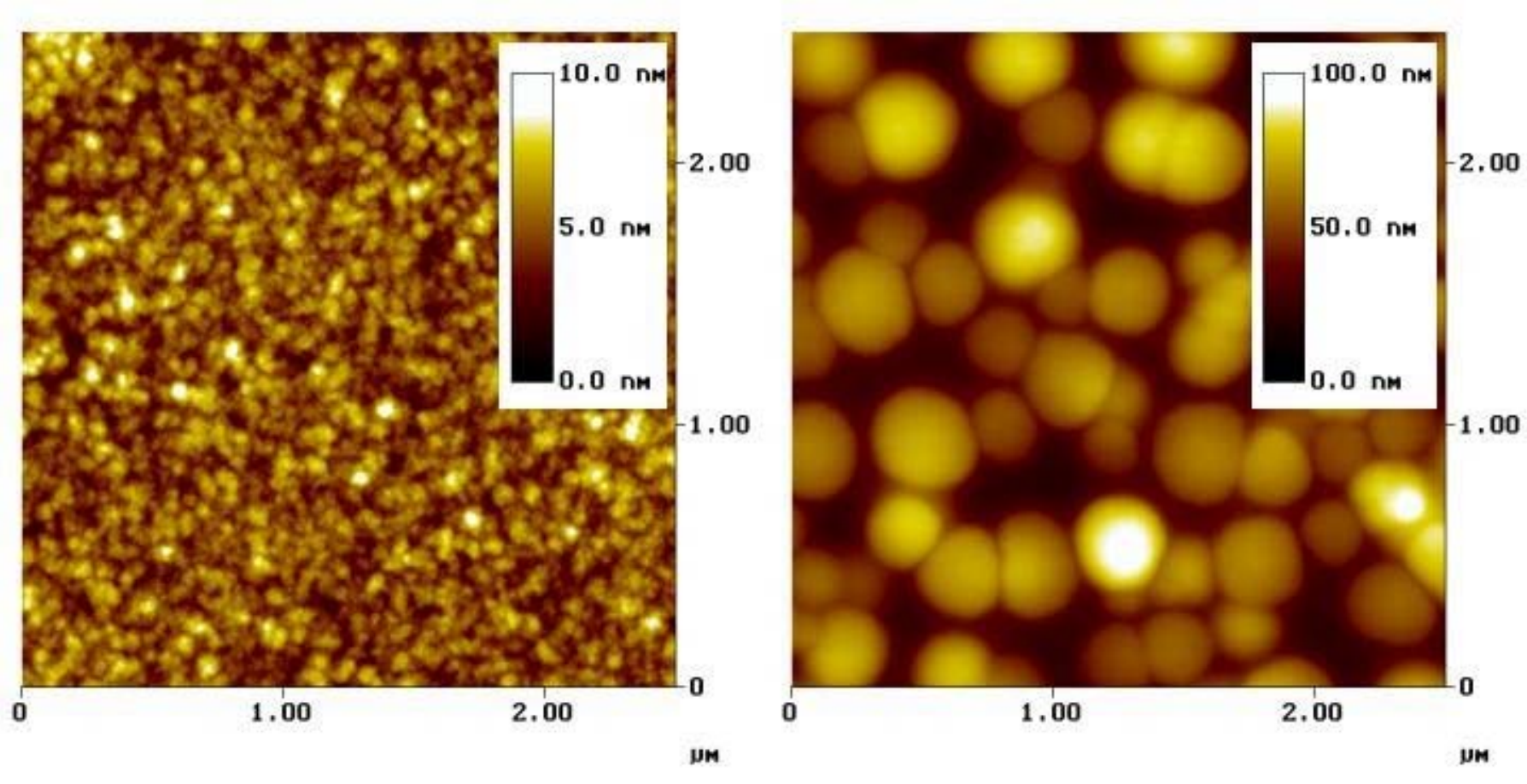

Harald Hoppe *et al*. *Adv. Func. Mater*. **14**, (2004) 1005,

Toluene concentration series – (top view) MDMO-PPV:PCBM by weight

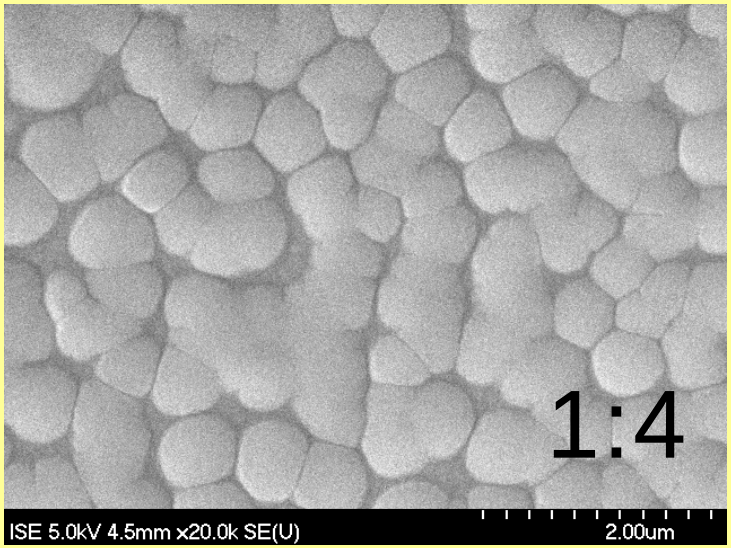

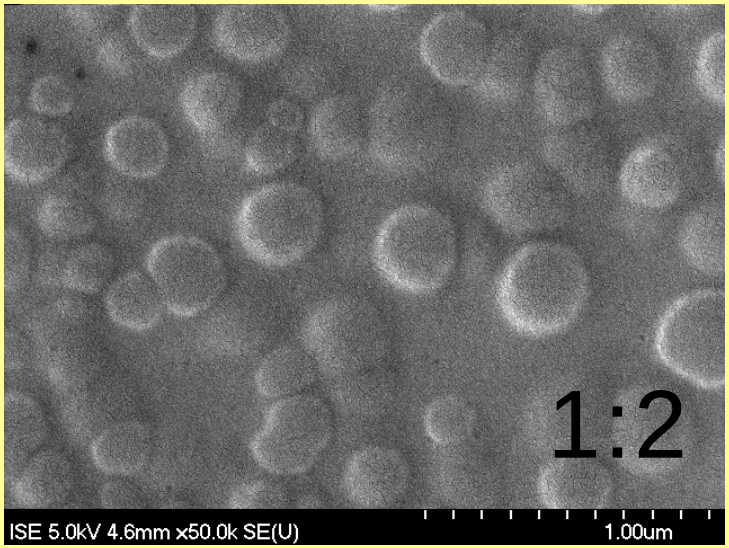

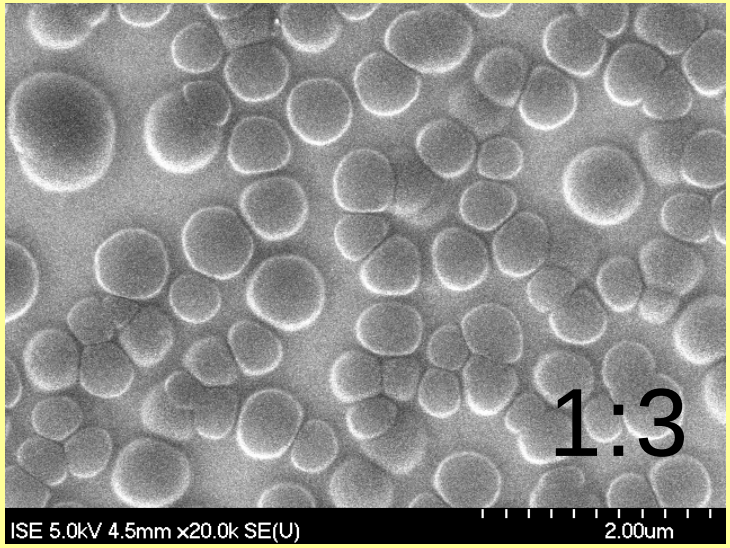

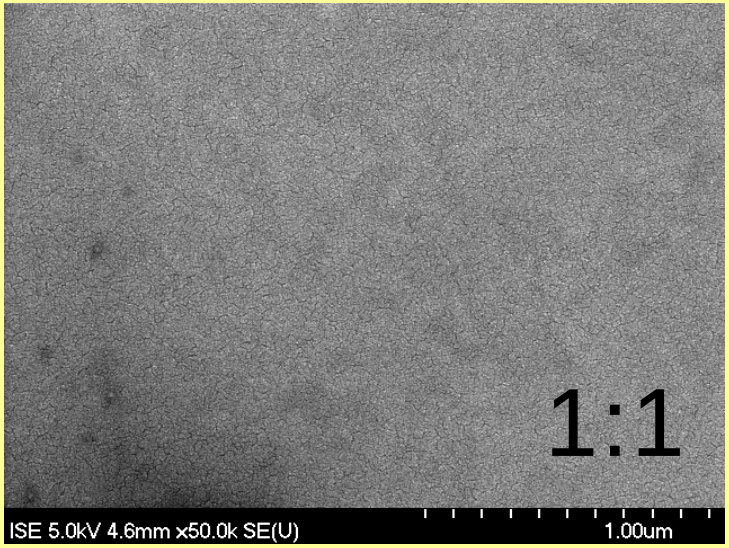

Nanomorphology Effects-SEM Studies

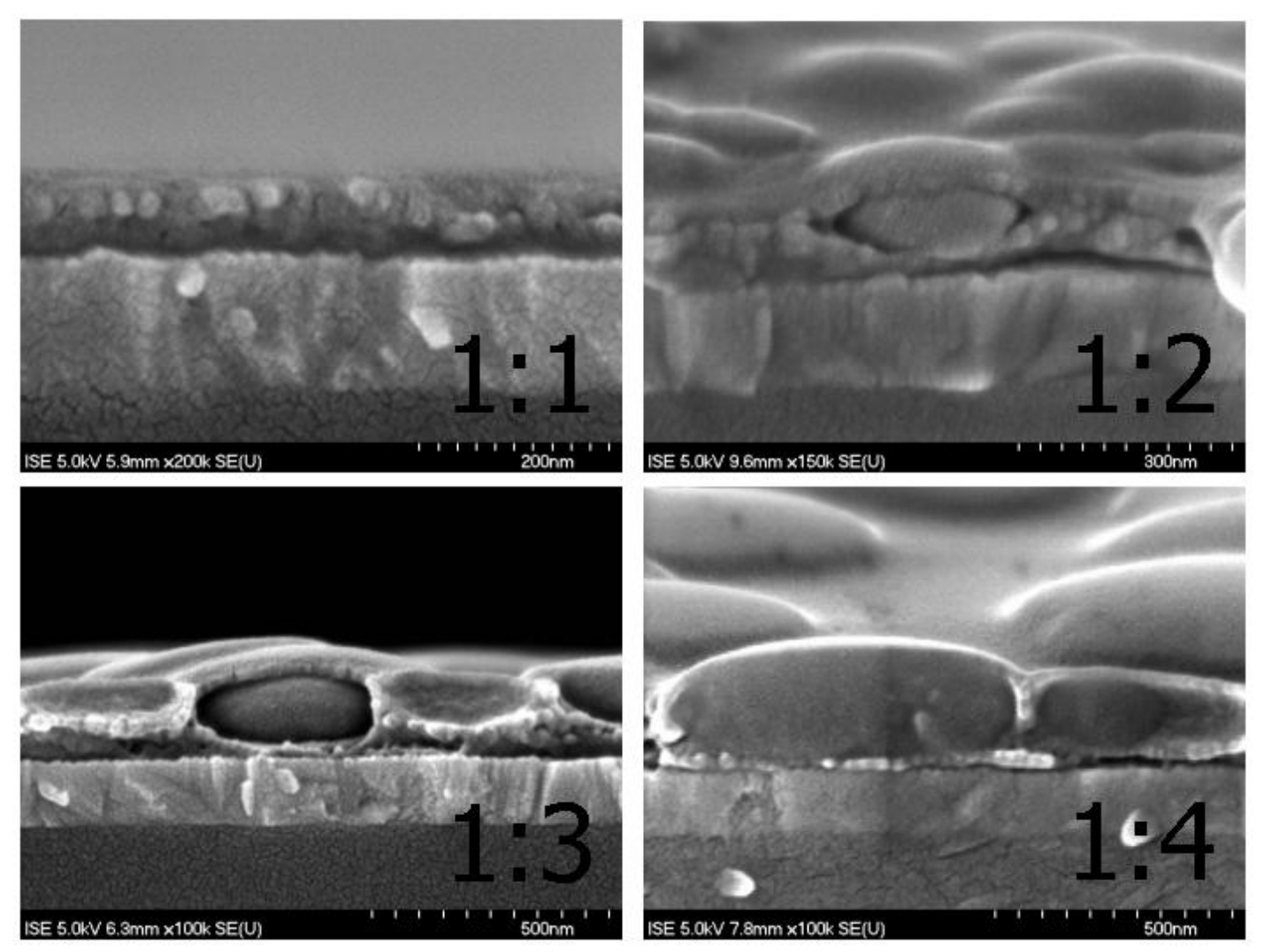

Harald Hoppe *et al*. *Adv. Func. Mater*. **14**, (2004) 1005,

Nanomorphology Effects-SEM Studies

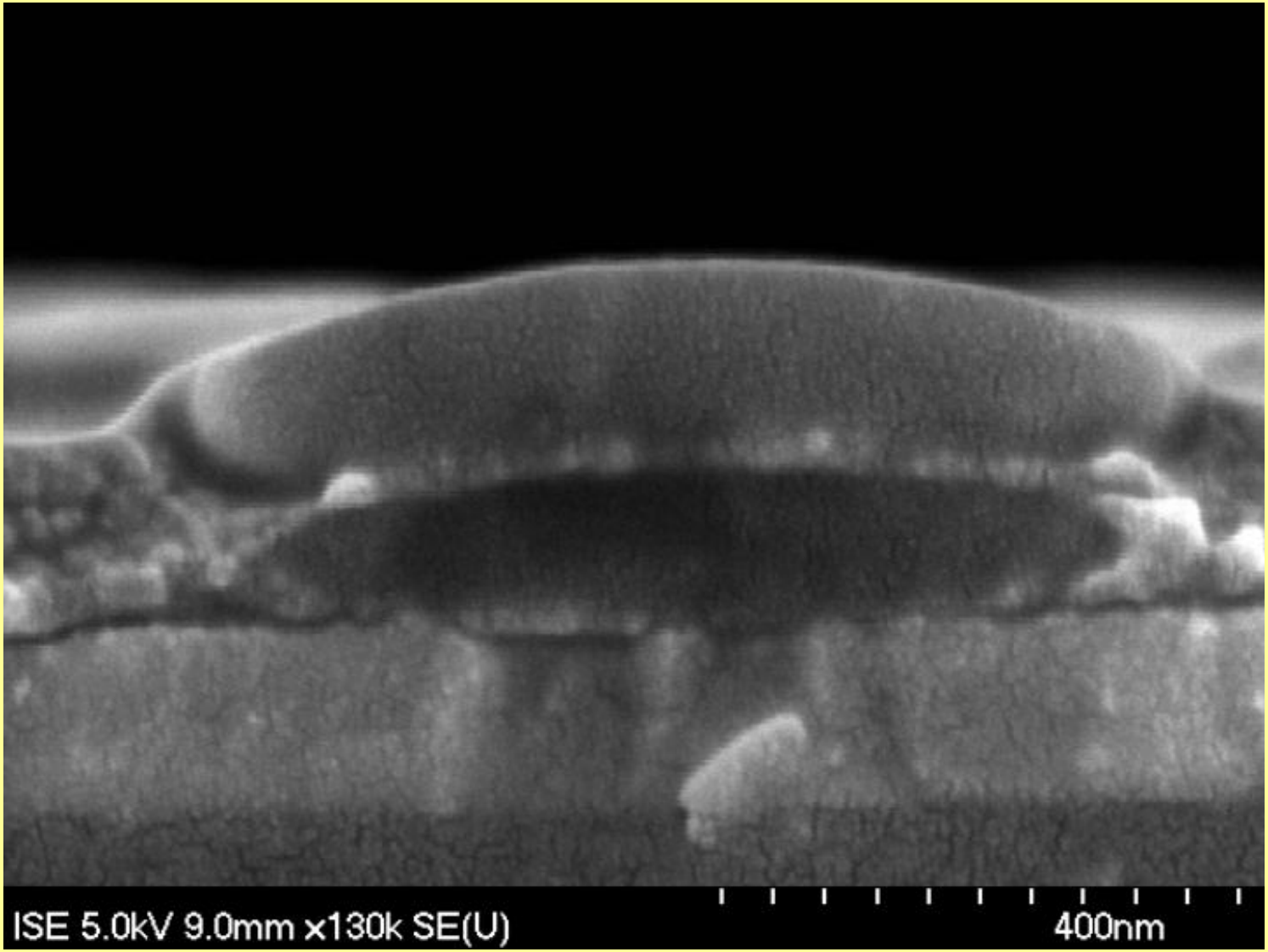

Harald Hoppe, et al. *Adv. Func. Mater*. **14**, 1005 (2004)

Nanomorphology Effects-AFM Studies

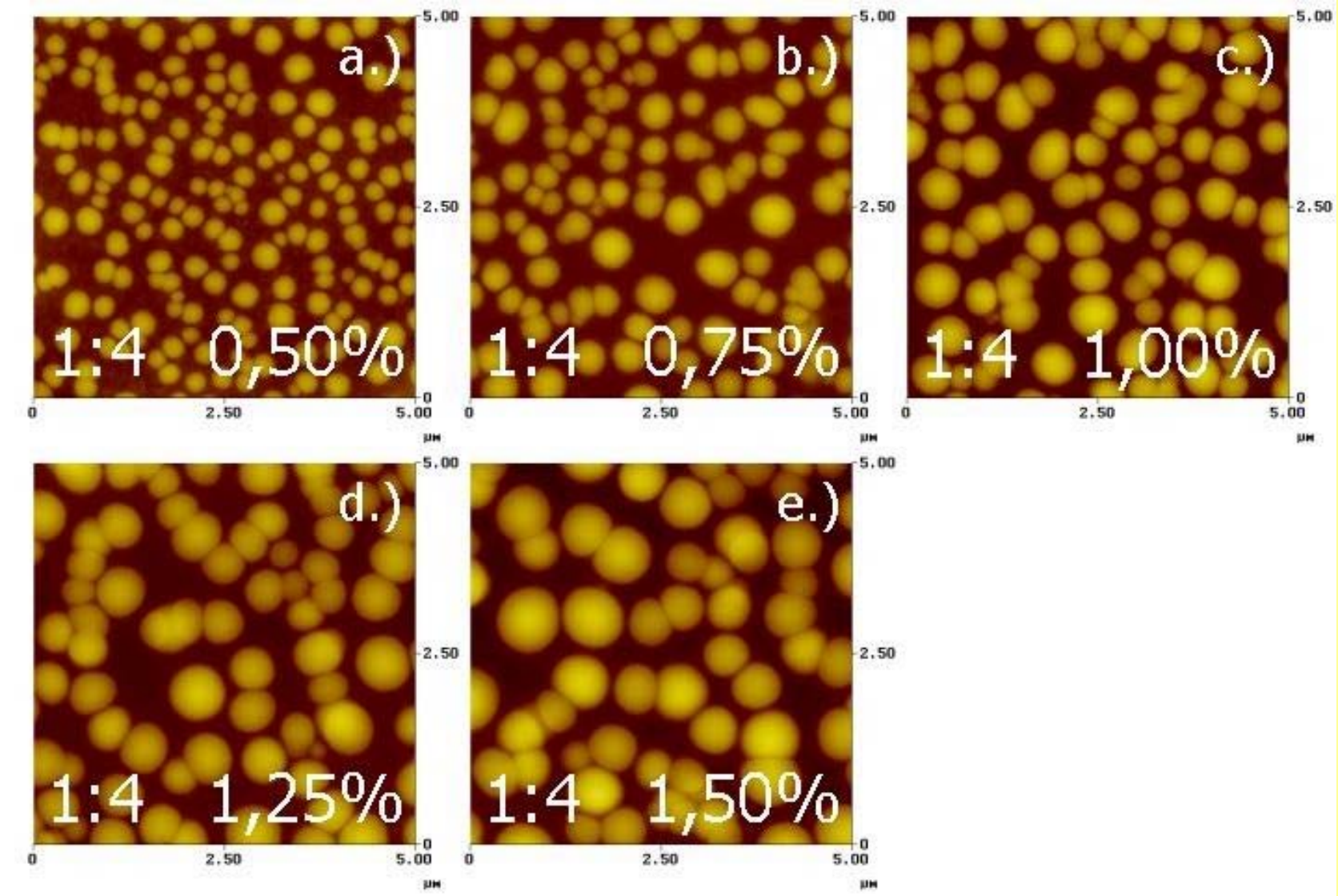

Harald Hoppe *et al. Adv. Func. Mater*. **14**, (2004) 1005

Kelvin Probe Force Microscopy (KPFM)

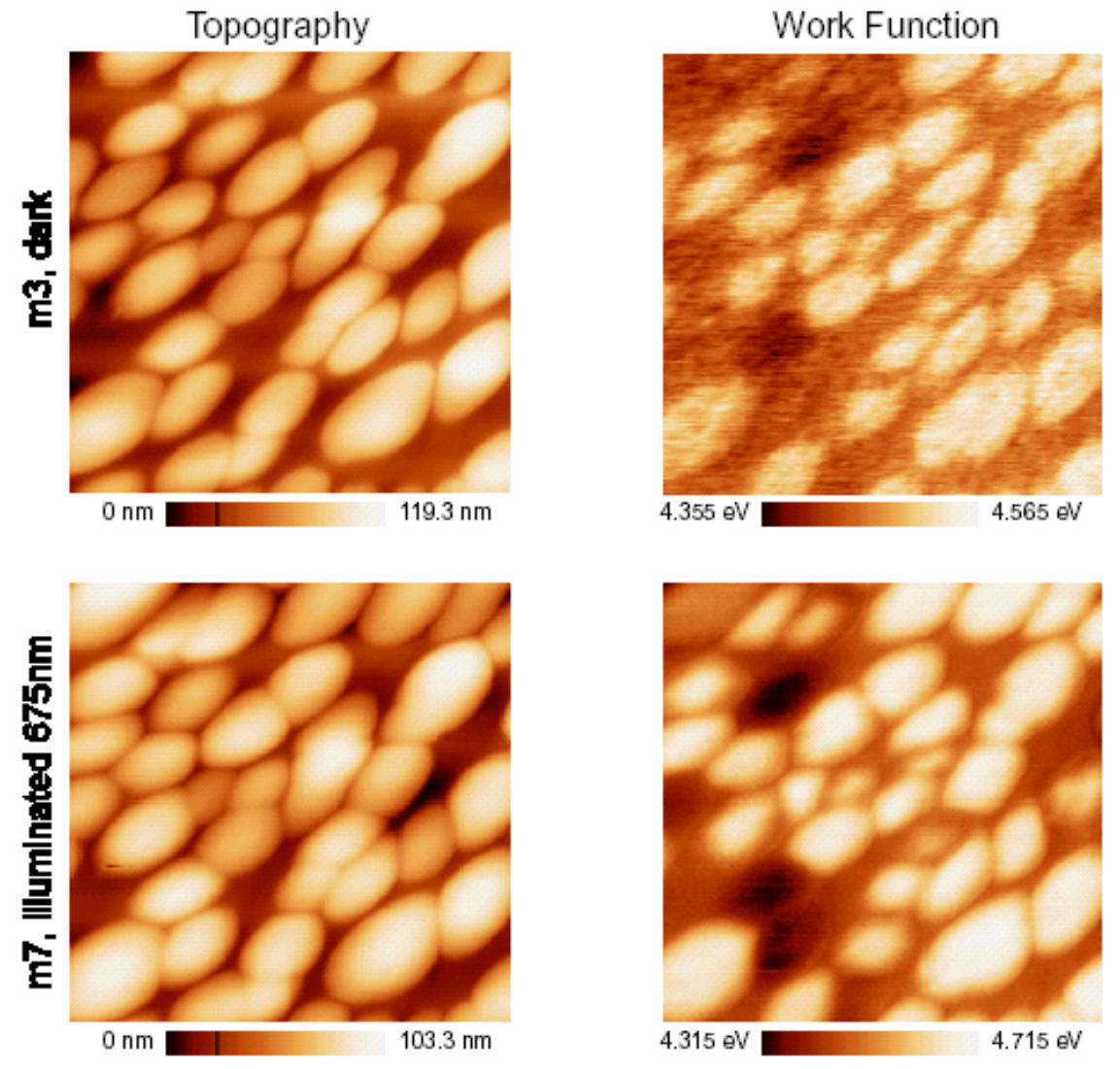

Harald Hoppe *et al. Nano Letters* **5** (2005) 269

AFM of an annealed film

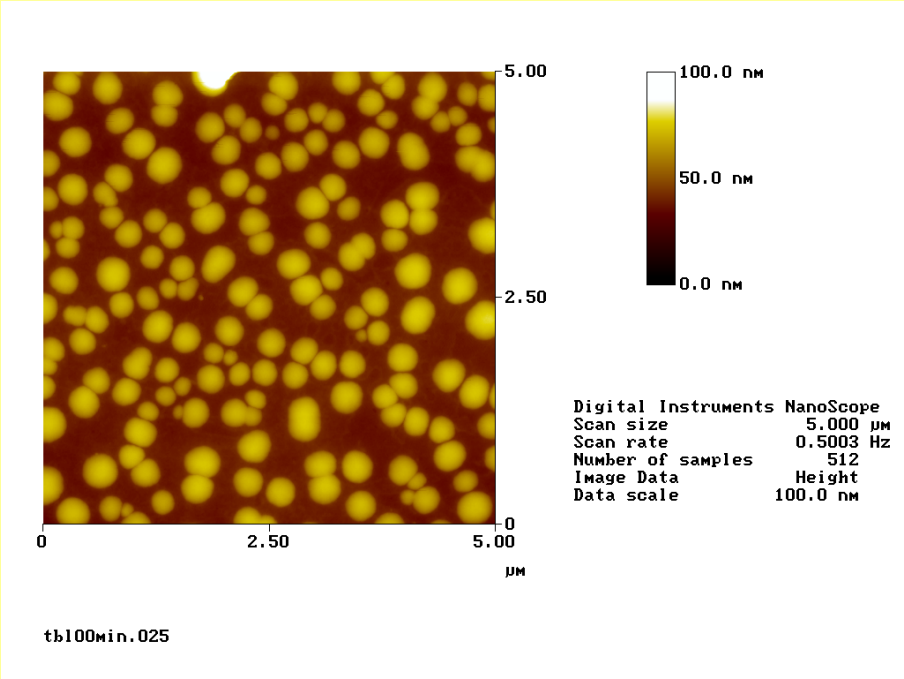

before annealing

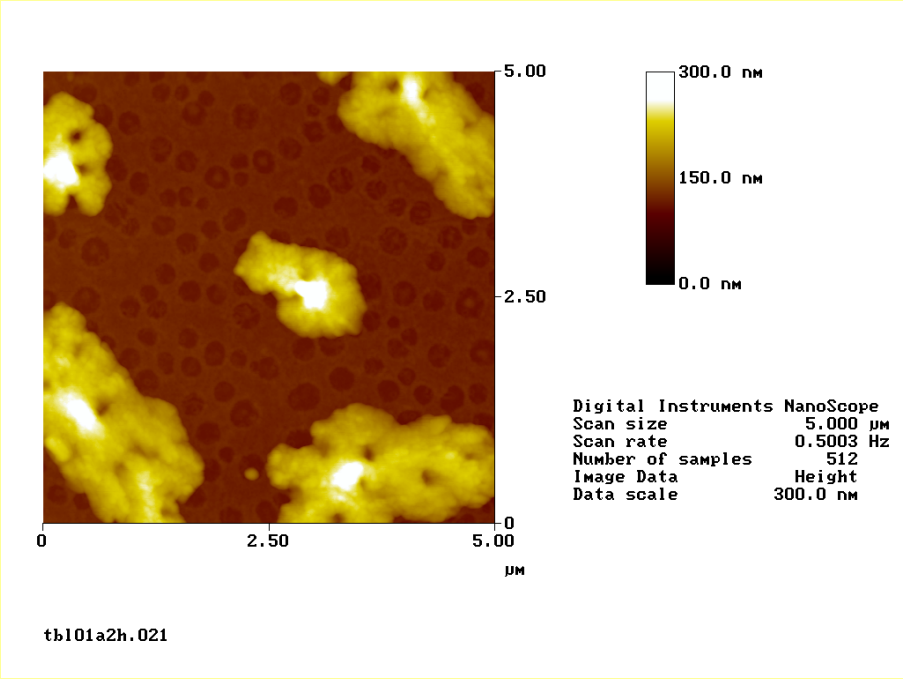

after annealing

from the clusters crystals are formed: PCBM

Nanomorphology Effects-TEM Studies

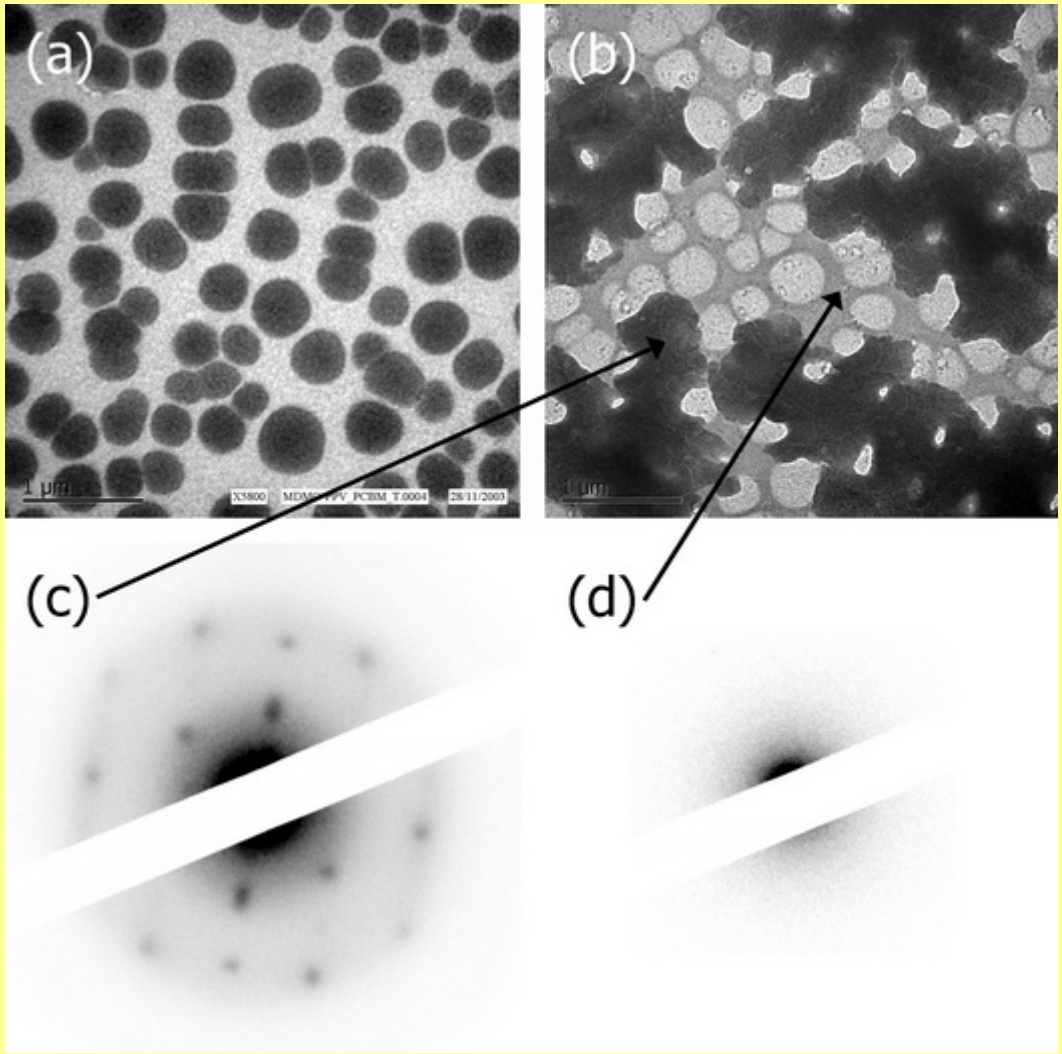

Annealing effects on MDMO-PPC/PCBM solar cells,
Harald Hoppe, PhD Thesis (2004)

...and from Chlorobenzene?

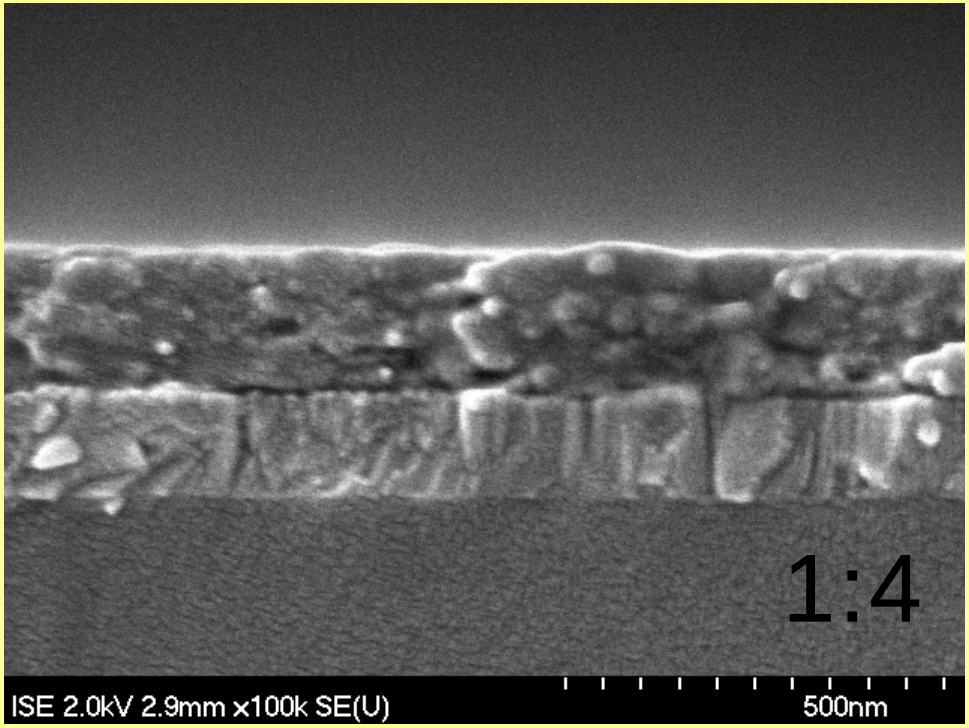

Harald Hoppe *et al*. *Adv. Func. Mater*. **14**, (2004) 1005,

Nanomorphology Effects-SEM Studies

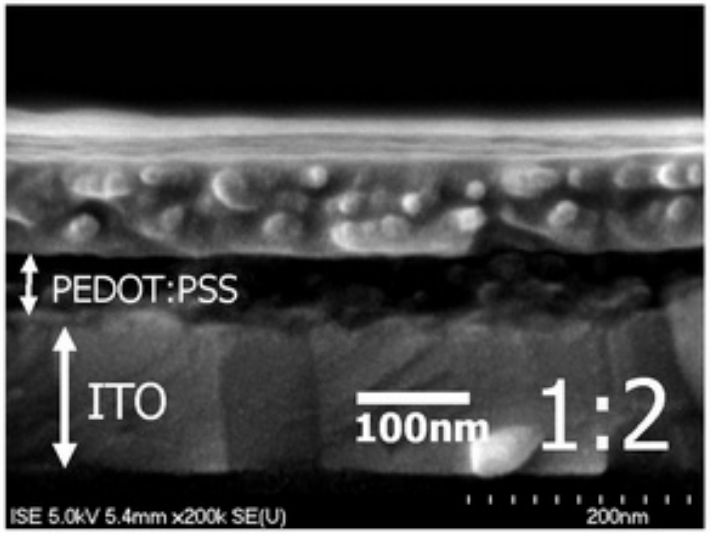

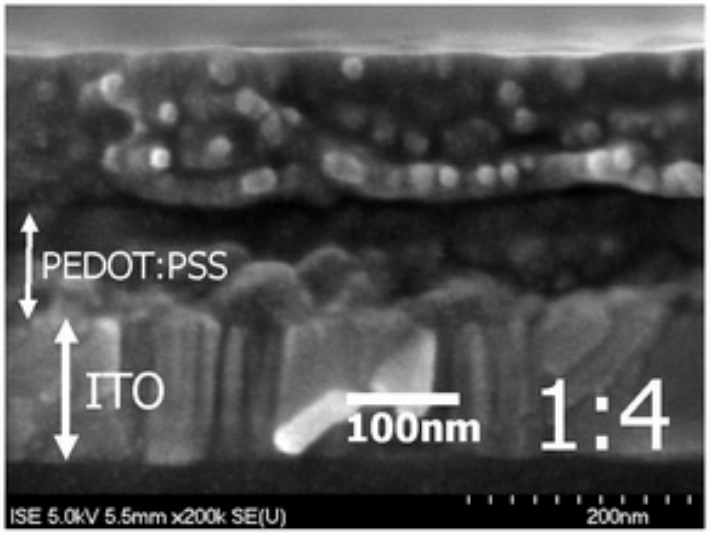

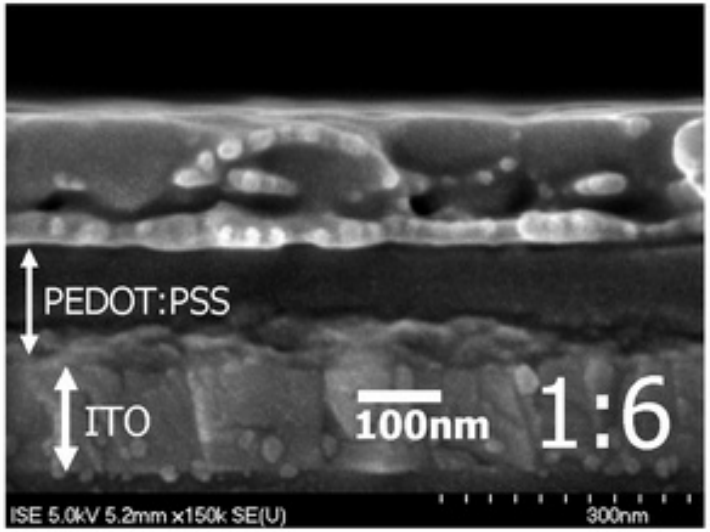

Chlorobenzene cast films have much smoother and more homogenous nanostrcuture

Harald Hoppe, et al. *Adv. Func. Mater*. **14**, 1005 (2004)

Wessling Nanospheres

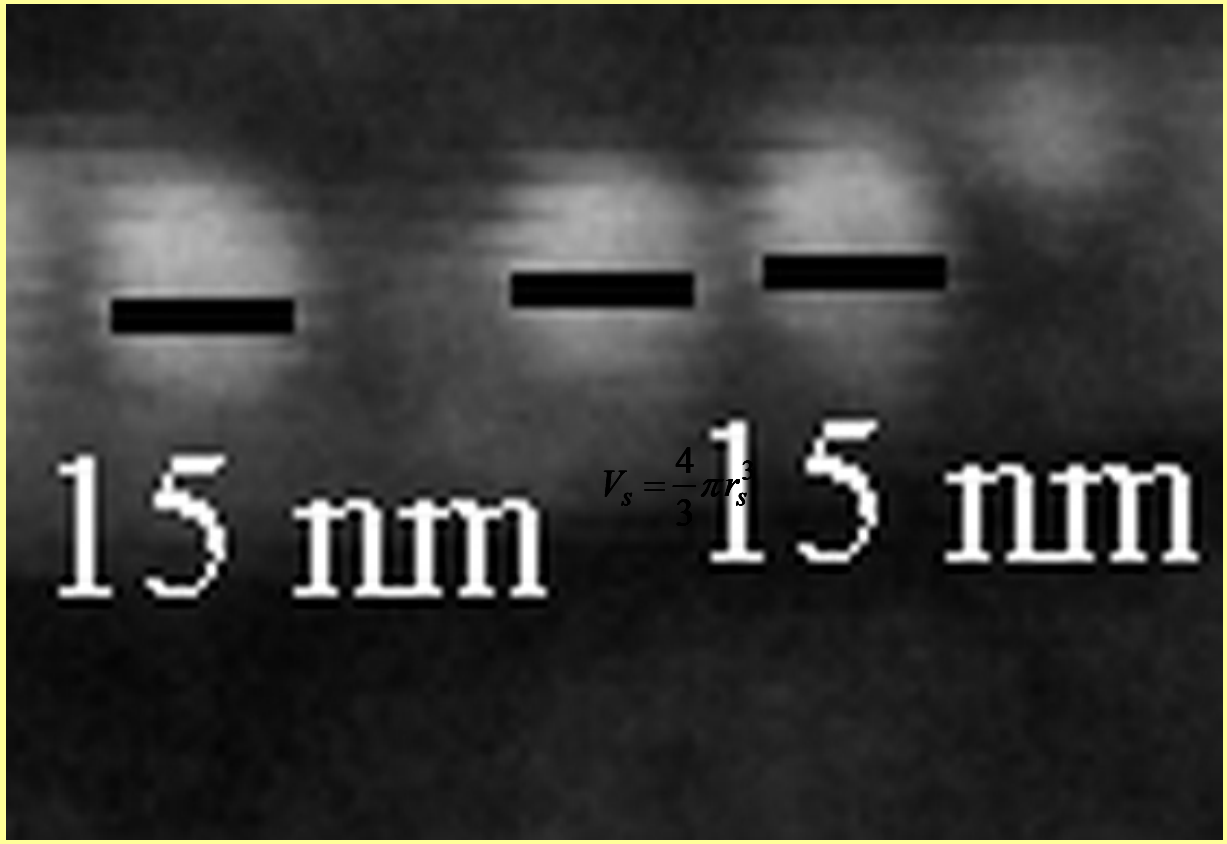

$$V_s = \frac{4}{3}\pi r_s^3$$

$\Rightarrow$ Diameter of MDMO-PPV Nanospheres $\approx$ 15-20 nm

Harald Hoppe, PhD Thesis (2004)

Bulk Heterojunctions: Revised

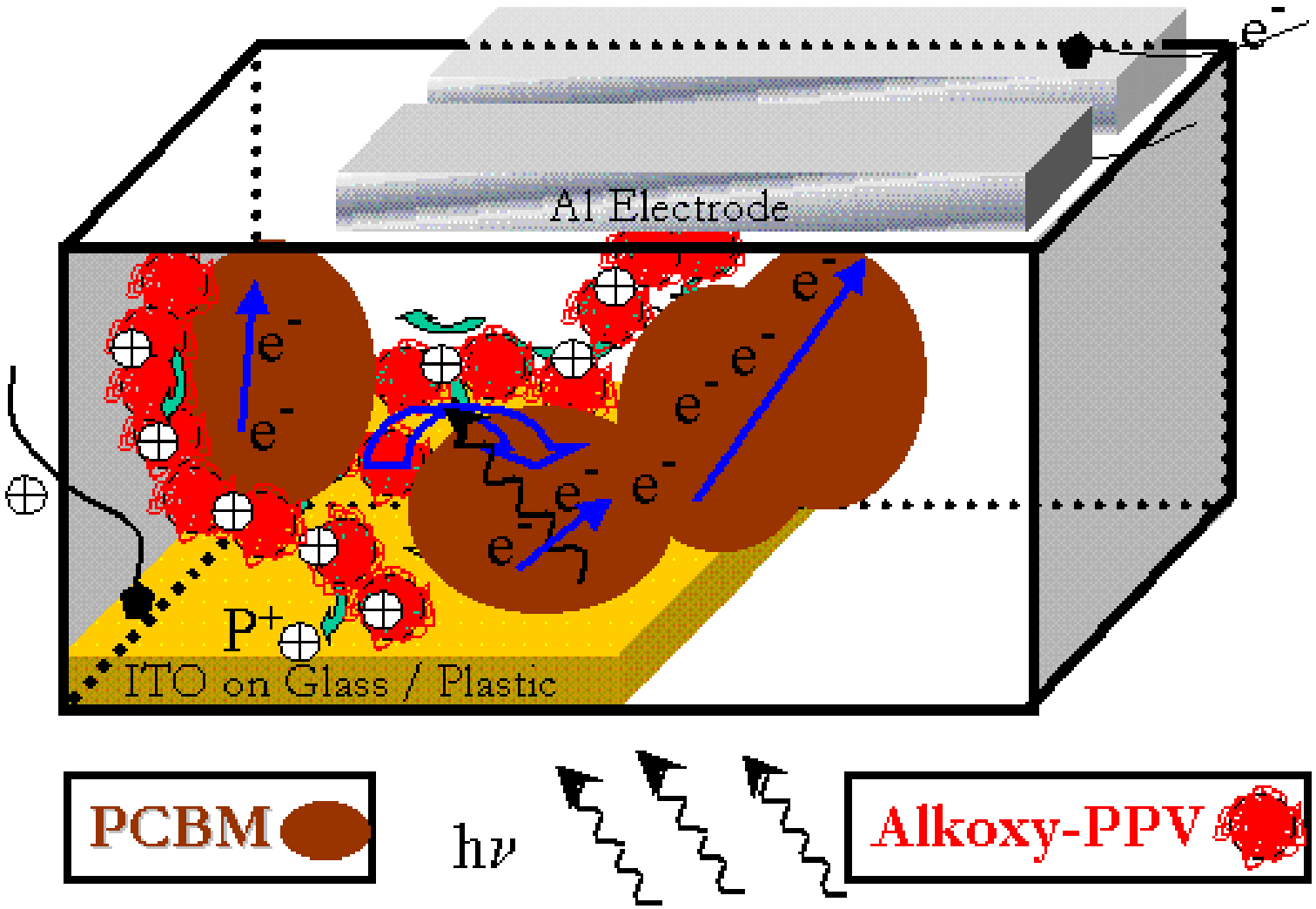

„Optimum“ Geometry for Organic and Hybrid Solar Cells

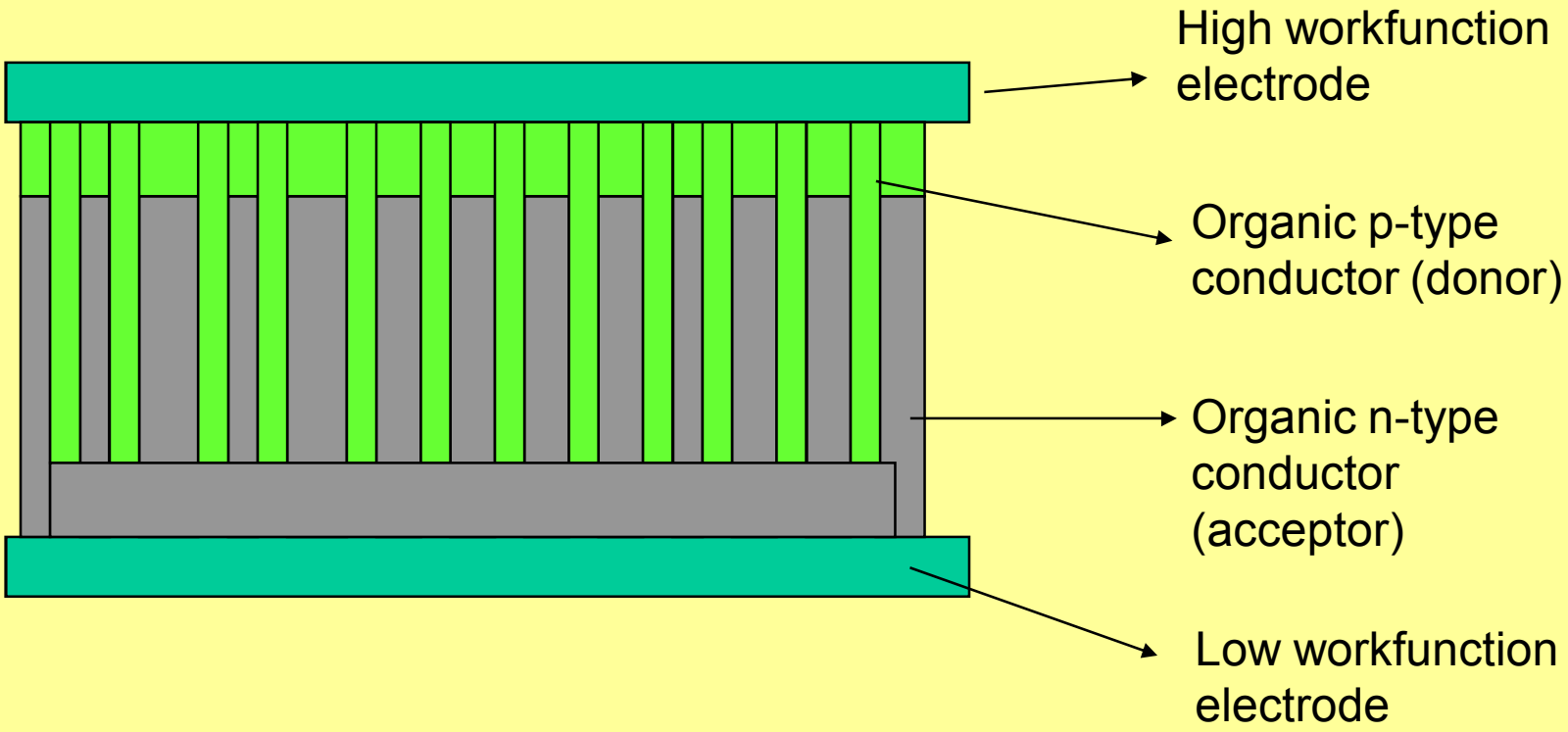

D-A block copolymers

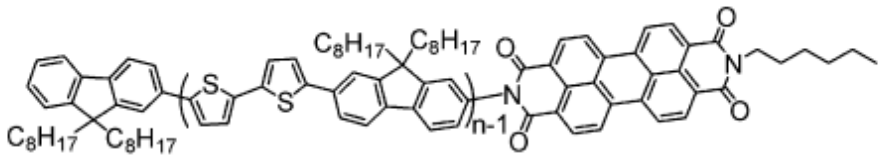

n = 3, **F3T4-hP** *G* 66.4 S_{X2} 212.3 S_{X1} 215.7 *I*
4, **F4T6-hP** *G* 83.4 S_{X3} 194.8 S_{X2} 204.7 S_{X1} 233.5 *I*
5, **F5T8-hP** *G* 90.4 S_X 189.5 *N* 248.5 *I*

[a] Symbols: *G*, glassy; *S*, smectic; *N*, nematic; *I*, isotropic.

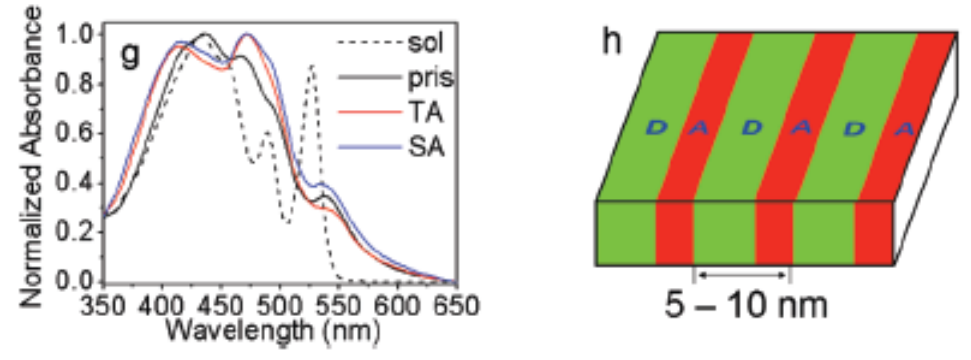

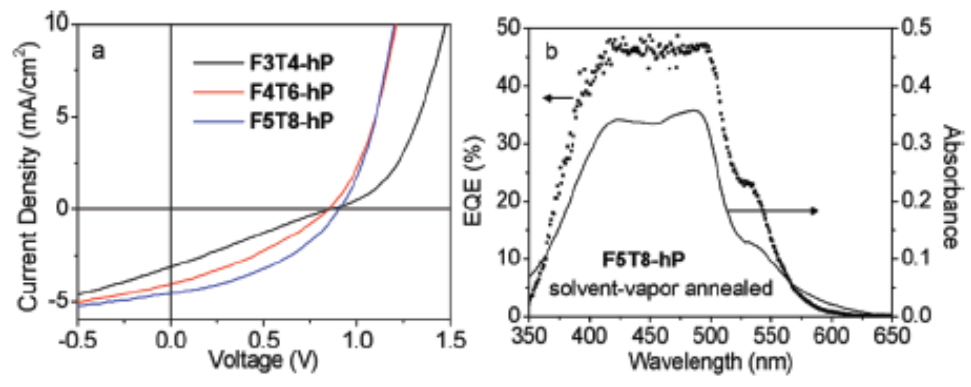

PCE = 1.50%
Voc = 0.87 V;
Isc = 4.49 mA/cm2;
FF = 0.38

[Y. H. Geng, et al., *J. Am. Chem. Soc.*, 2009, *131*, 13242–13243]

Supramolecular Ordering

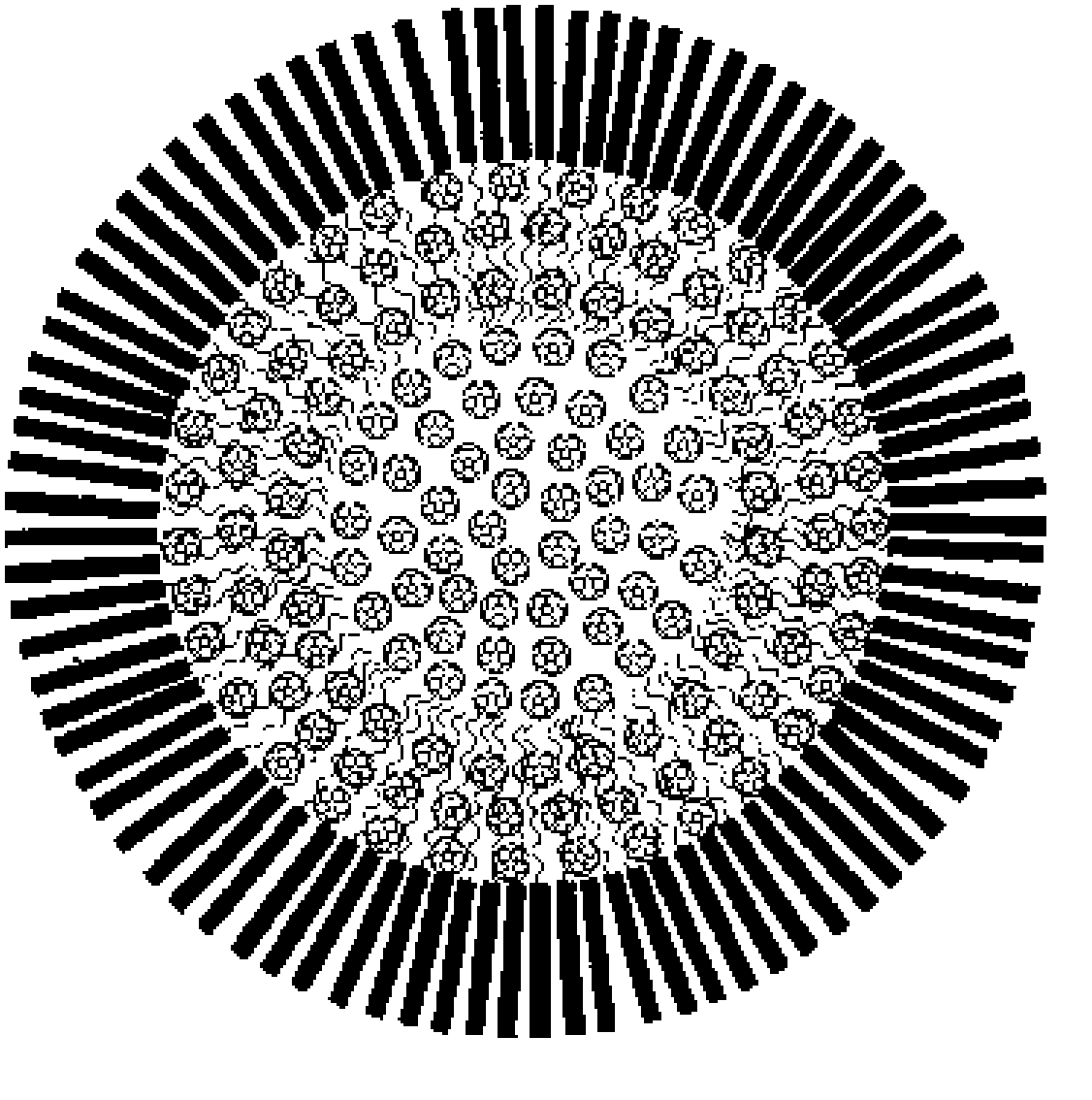

Di-block copolymer miscelle formation encapsulating fullerenes.

S. Jenekhe, & Chen, *Science* **279**, 1903 (1998)

„Double Cable“ Polymers

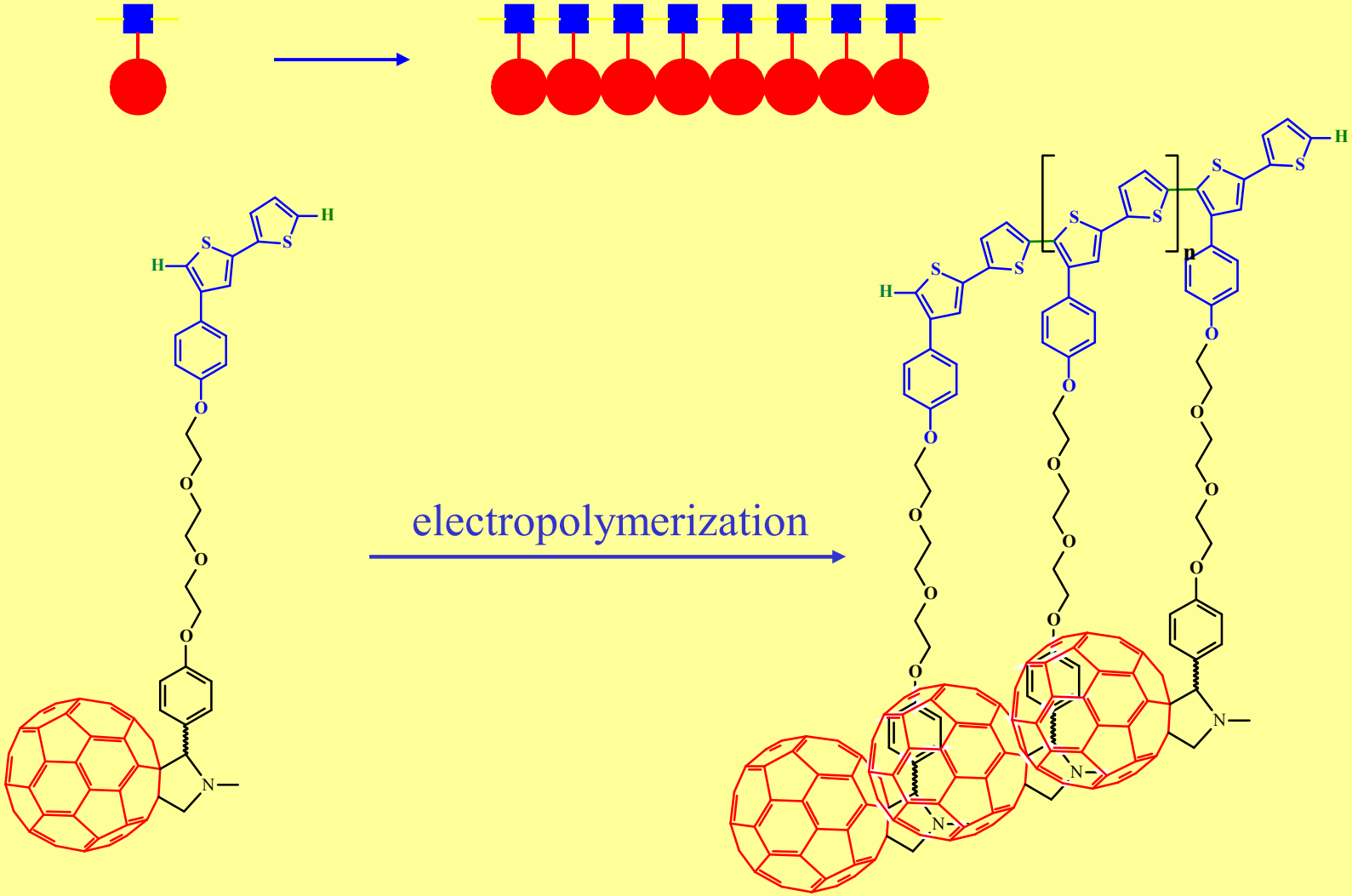

A. Cravino, G. Zerza, M. Maggini, S. Bucella, M. Svensson, M.R. Andersson, H. Neugebauer, N.S. Sariciftci, *Chem. Commun*. 2487 (2000)

The monomer

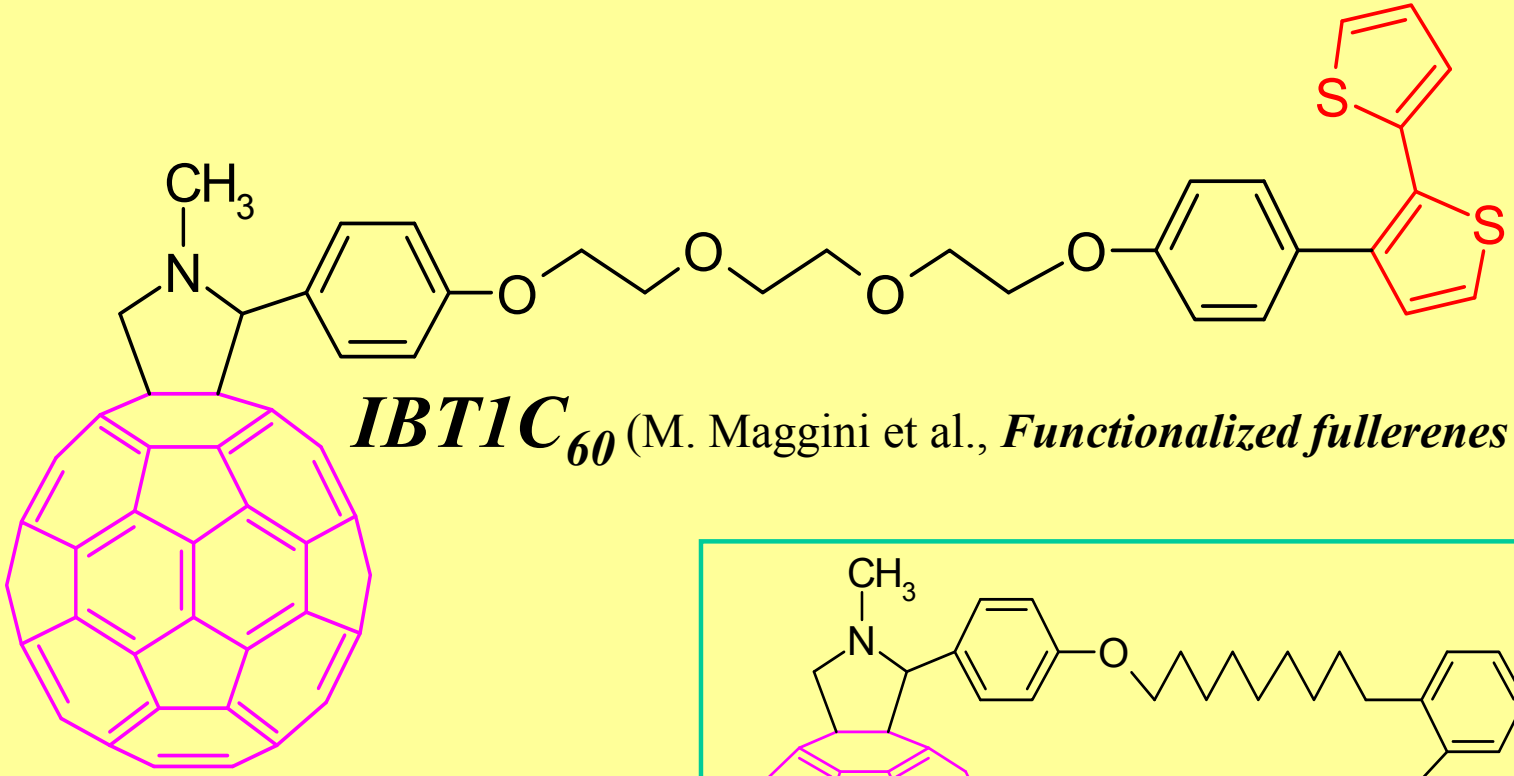

IBT1C$_{60}$ (M. Maggini et al., ***Functionalized fullerenes***

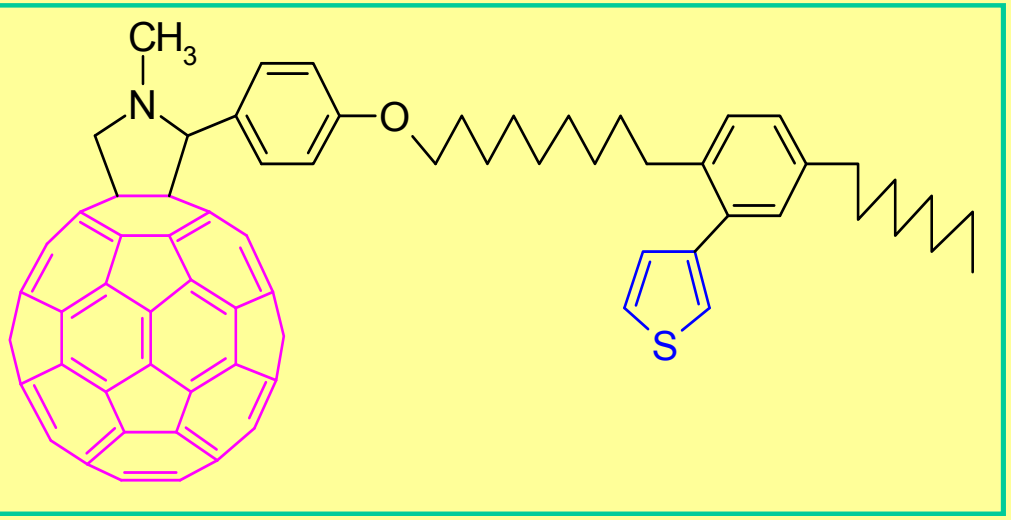

PolyUCM6: TCAQ type acceptor moieties

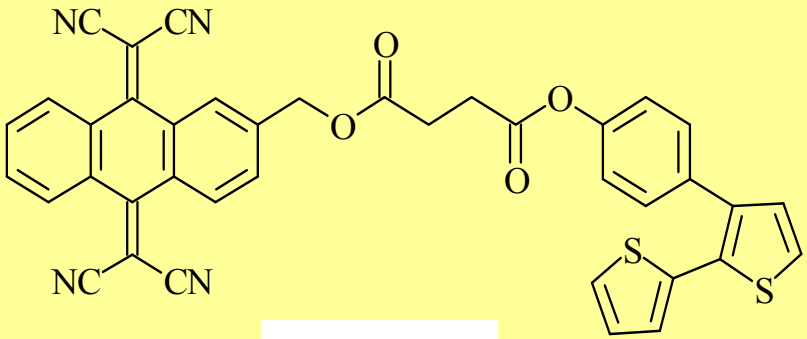

UCM6

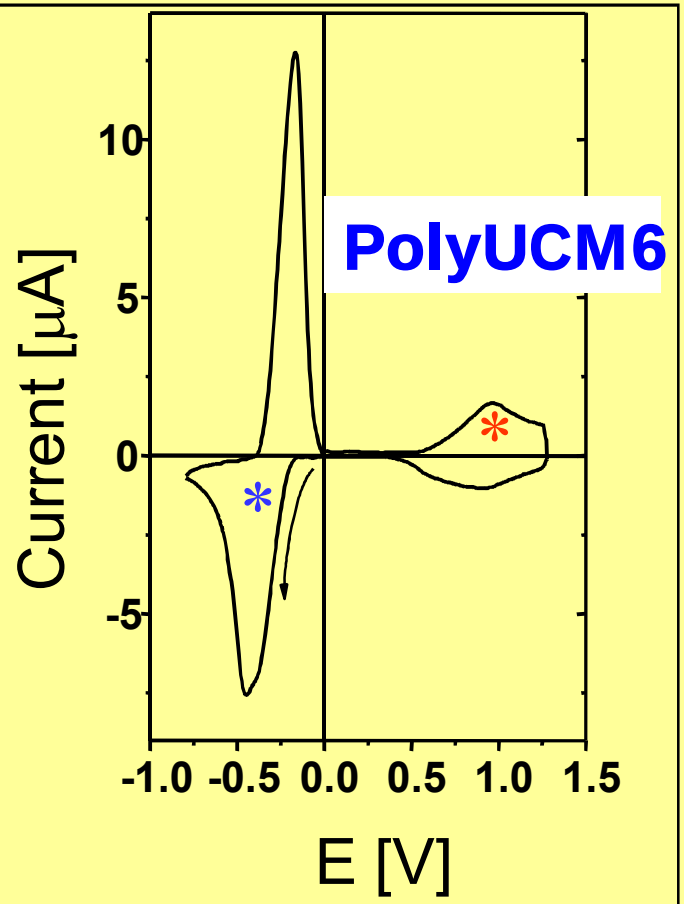

G. Zerza, A. Cravino, H. Neugebauer, N. S. Sariciftci, R. Gómez, J. L. Segura, N. Martín, M. Svensson, M. Andersson, *J. Phys. Chem. A*, 2000.

* Backbone ox./re-red.

* "TCAQ" red./re-ox.

Transport Theory

Free electron metallic conductivity

$$v_d = (e\tau/ m^*)E,$$

and the total current density is given by

$$j = Nev_{d.} = (Ne^2\tau/m^*)E.$$

From Ohm's Law, $j = \sigma E$, we identify the electrical conductivity, σ, of the metal,

$$\sigma = Ne^2\tau/m^*$$

Defining the carrier (electron) mobility by the relation $v_d \equiv \mu E$, this simple model of metallic transport yields

$$\mu = e\tau/m^* \qquad \sigma = Ne\mu.$$

Strong scattering: $\Delta k/k \sim 1$: The Ioffe-Regel inequality

$k_F l < 1$ Metallic wavefunction breaks down into $\psi_i \sim \exp(-\alpha|r - r_i|)$

LOCALIZATION OF ELECTRONIC STATES

Anderson localization: the problem

One-dimensional 'crystalline' system

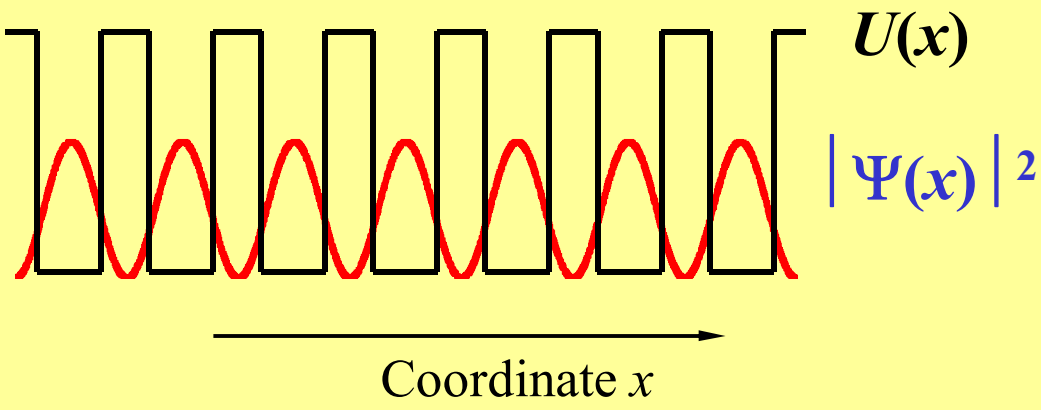

A periodic potential energy distribution yields an extended wave function

One-dimensional disordered system

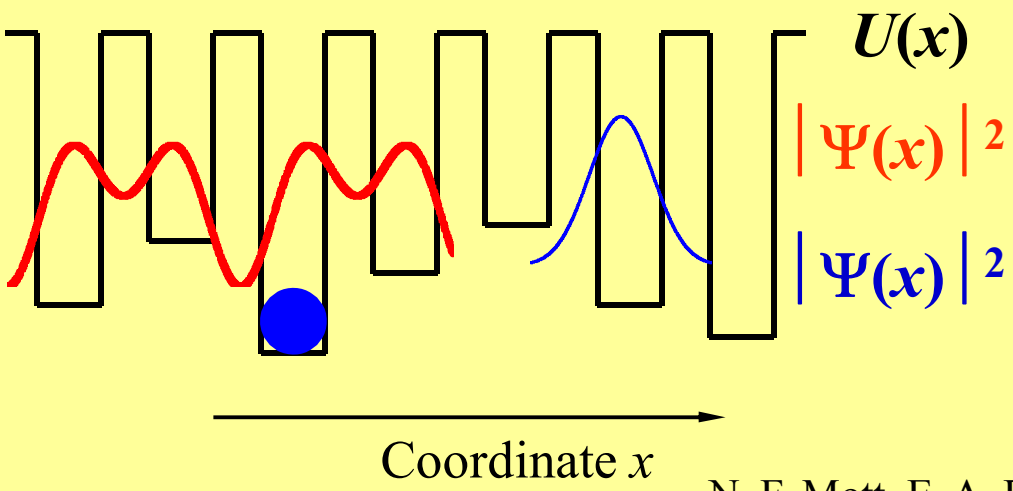

What will happen in an (energetically) disordered system? Can the wave function be still extended?

Or it will be localized within a single potential well?

N. F. Mott, E. A. Davis, Electronic processes in non-crystalline materials, 2ndEd., Oxford University Press, London (1979).

Anderson Localization

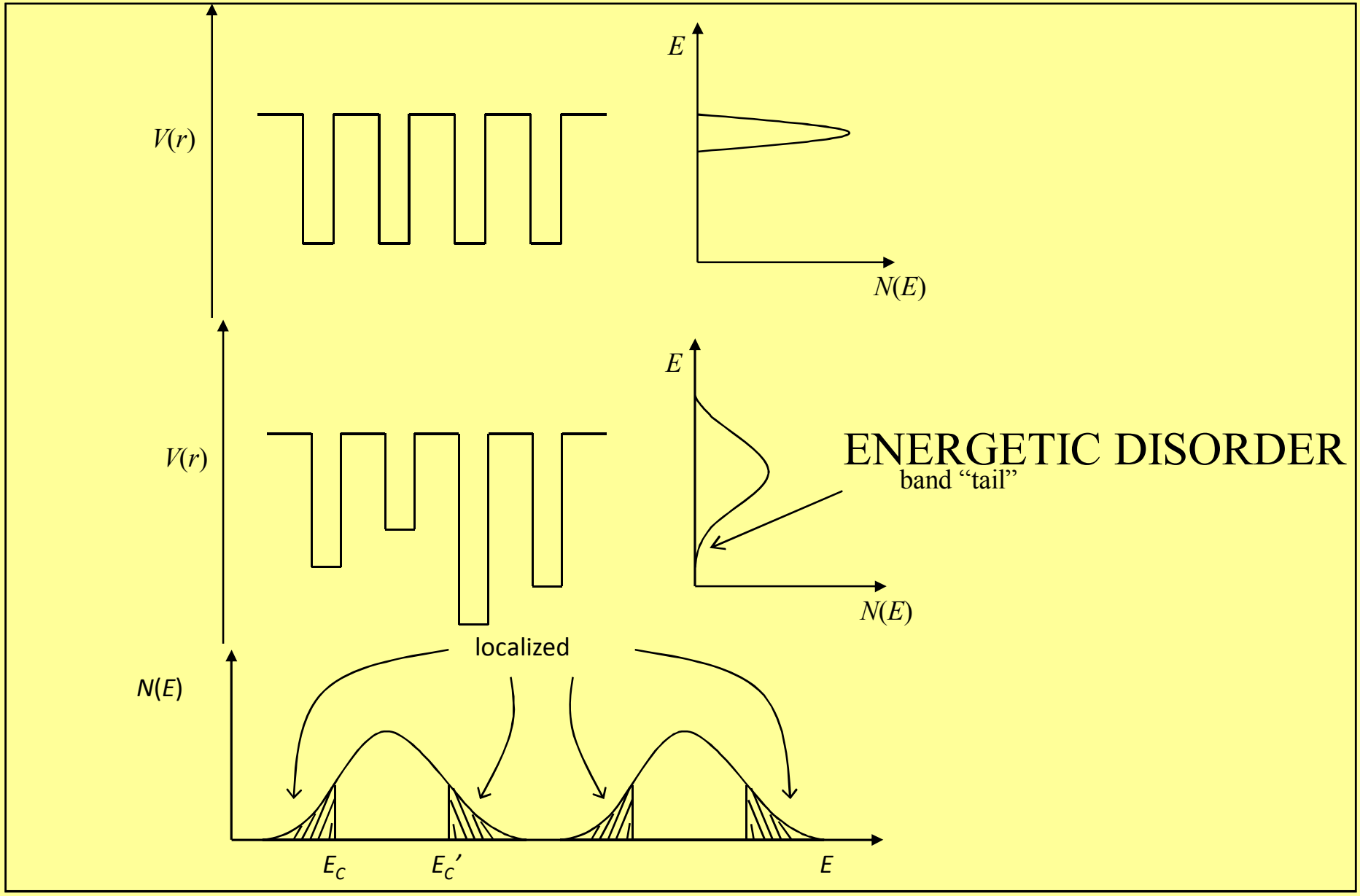

Hopping transport

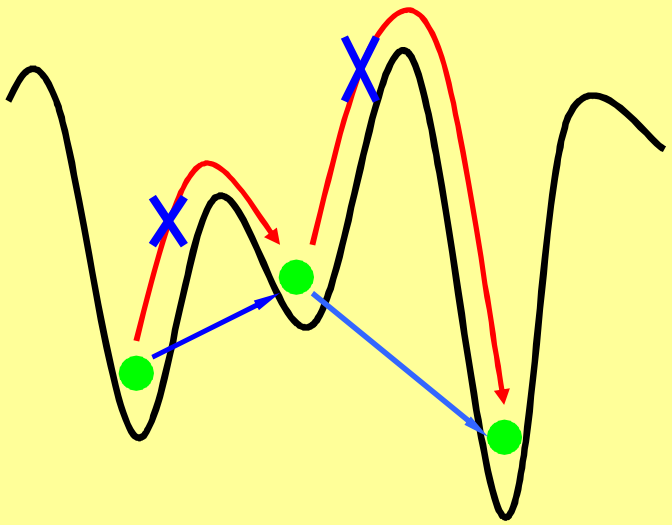

Over-barrier jumps dominate at higher temperatures

At lower temperatures, tunneling jumps take over

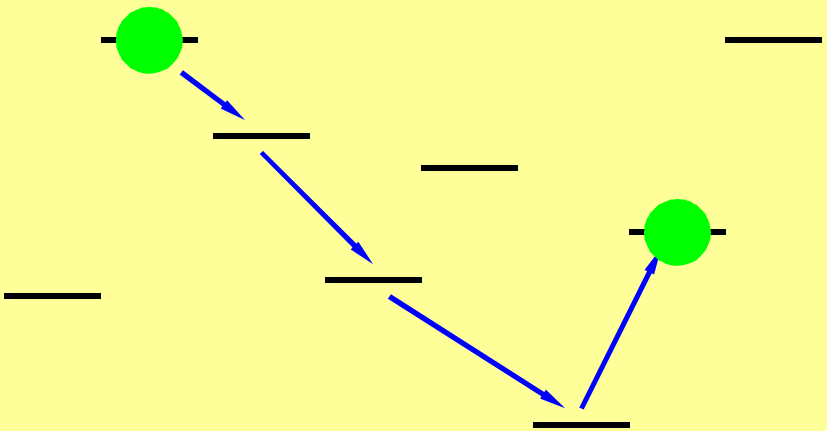

Most models of hopping transport assume that:

- positions of hopping sites are completely random

- positions and energies of hoping sites are uncorrelated

Transport in Disordered Media

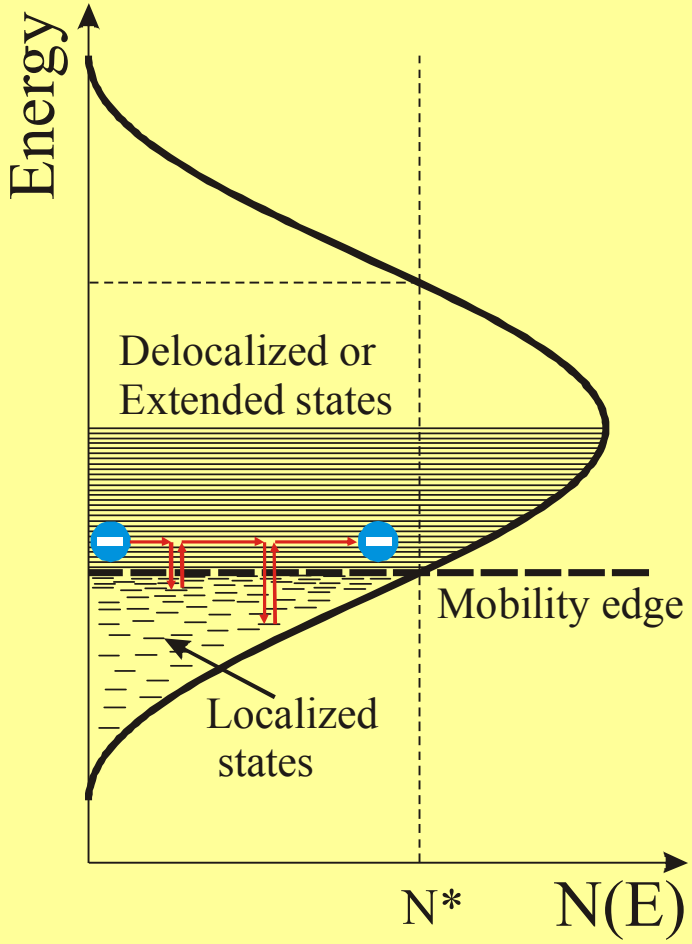

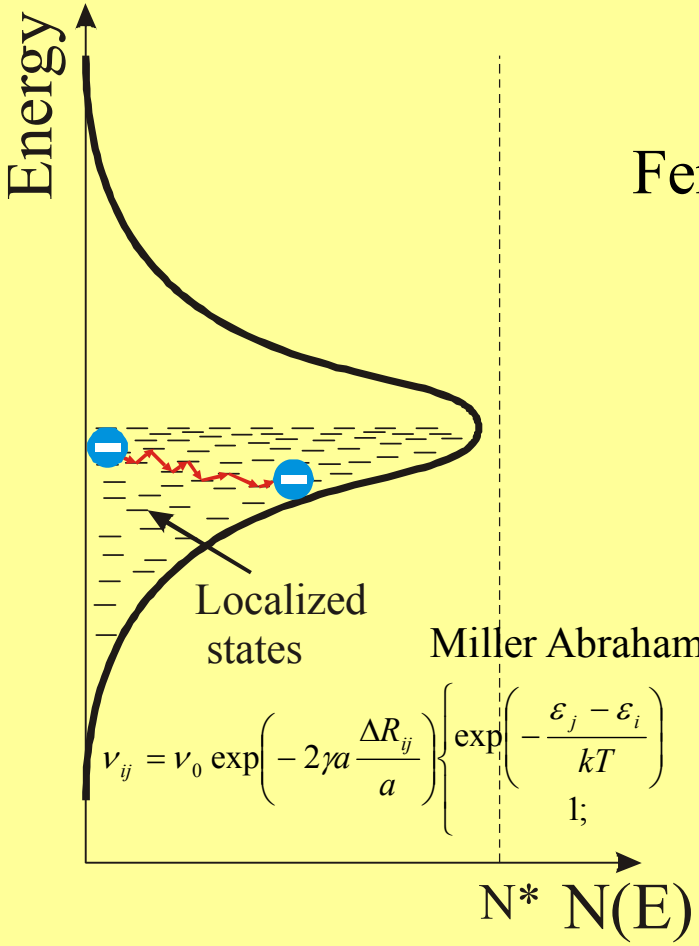

Fermi Glass

Miller Abrahams Jumping Rate

$$\nu_{ij} = \nu_0 \exp\left(-2\gamma a \frac{\Delta R_{ij}}{a}\right) \begin{cases} \exp\left(-\frac{\varepsilon_j - \varepsilon_i}{kT}\right) & \varepsilon_j > \varepsilon_i \\ 1; & \varepsilon_j < \varepsilon \end{cases}$$

Thermal activation over the Ec

$$\sigma = \sigma_{\min} e^{-(E_C - E_F)/kT}$$

Mott Variable Range Hopping

$$\sigma_{VRH}(T) = \sigma_o \exp[-\beta(T_o/T)^{1/(d+1)}]$$

Trap-controlled transport

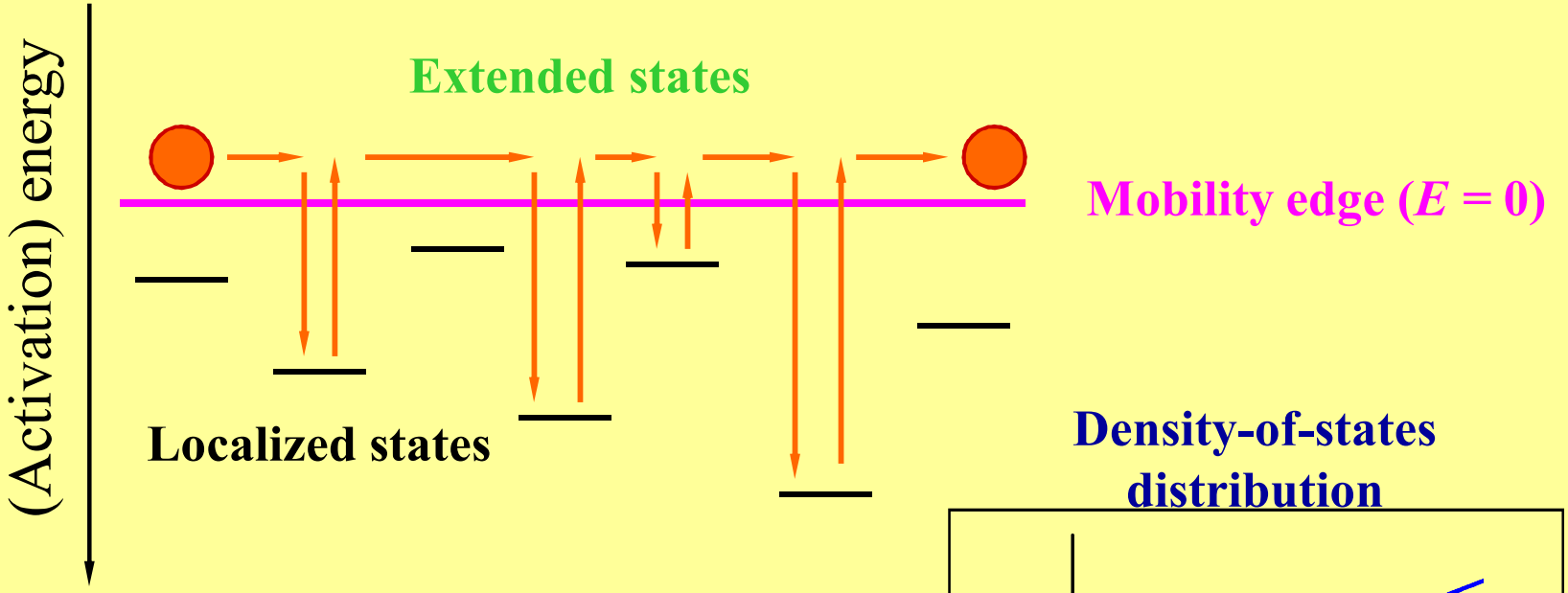

Density-of-states distribution

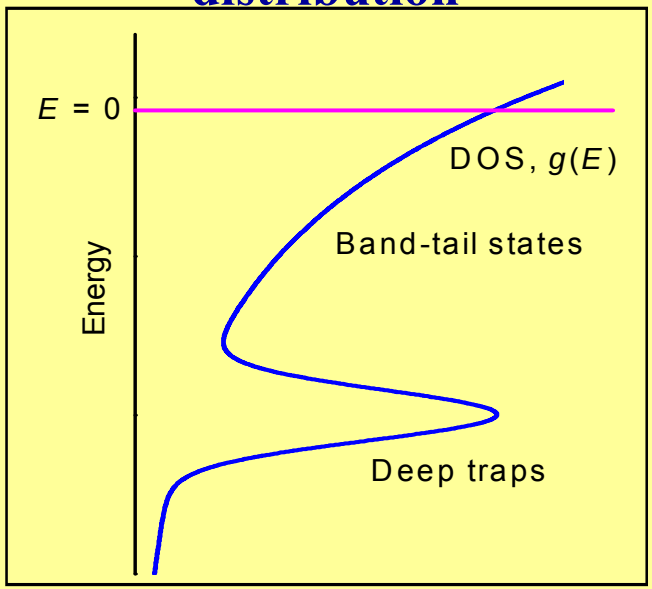

Important parameters:

μ_c - carrier mobility in extended states

τ_c - lifetime of carriers in extended states

ν_0 - attempt-to-escape frequency

Fermi glass

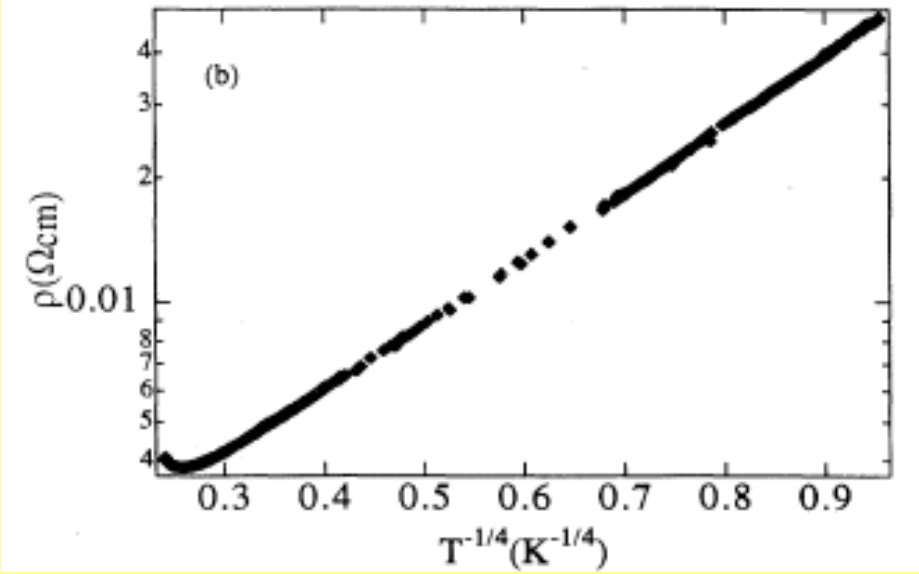

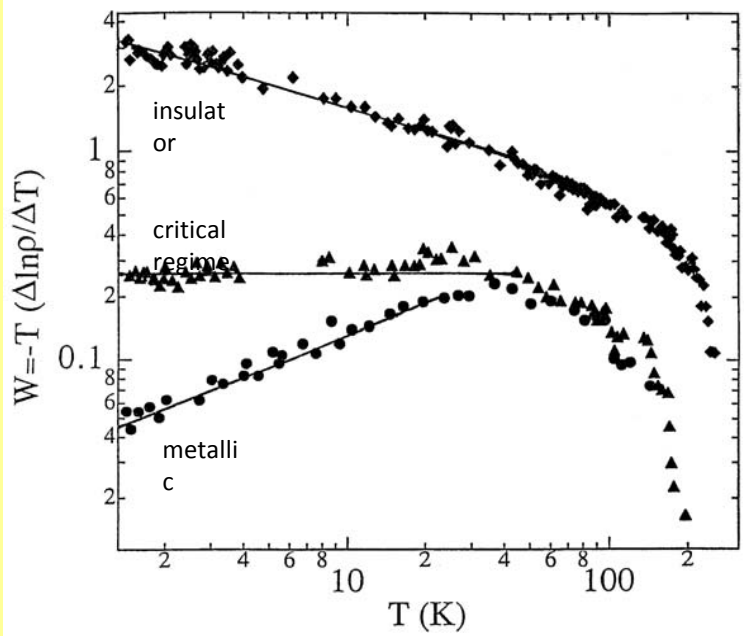

PANI-CSA , Zabrodski plots

R. Menon, C. O. Yoon, D. Moses, A. Heeger and Y. Cao, *Phys. Rev.* **B 48,** 17685 (1993)

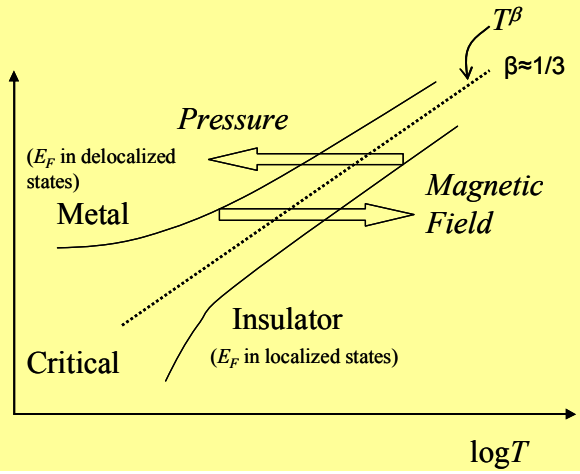

Metal-Insulator Transition by Pressure or Magnetic Field

Onsager Theory of Escape

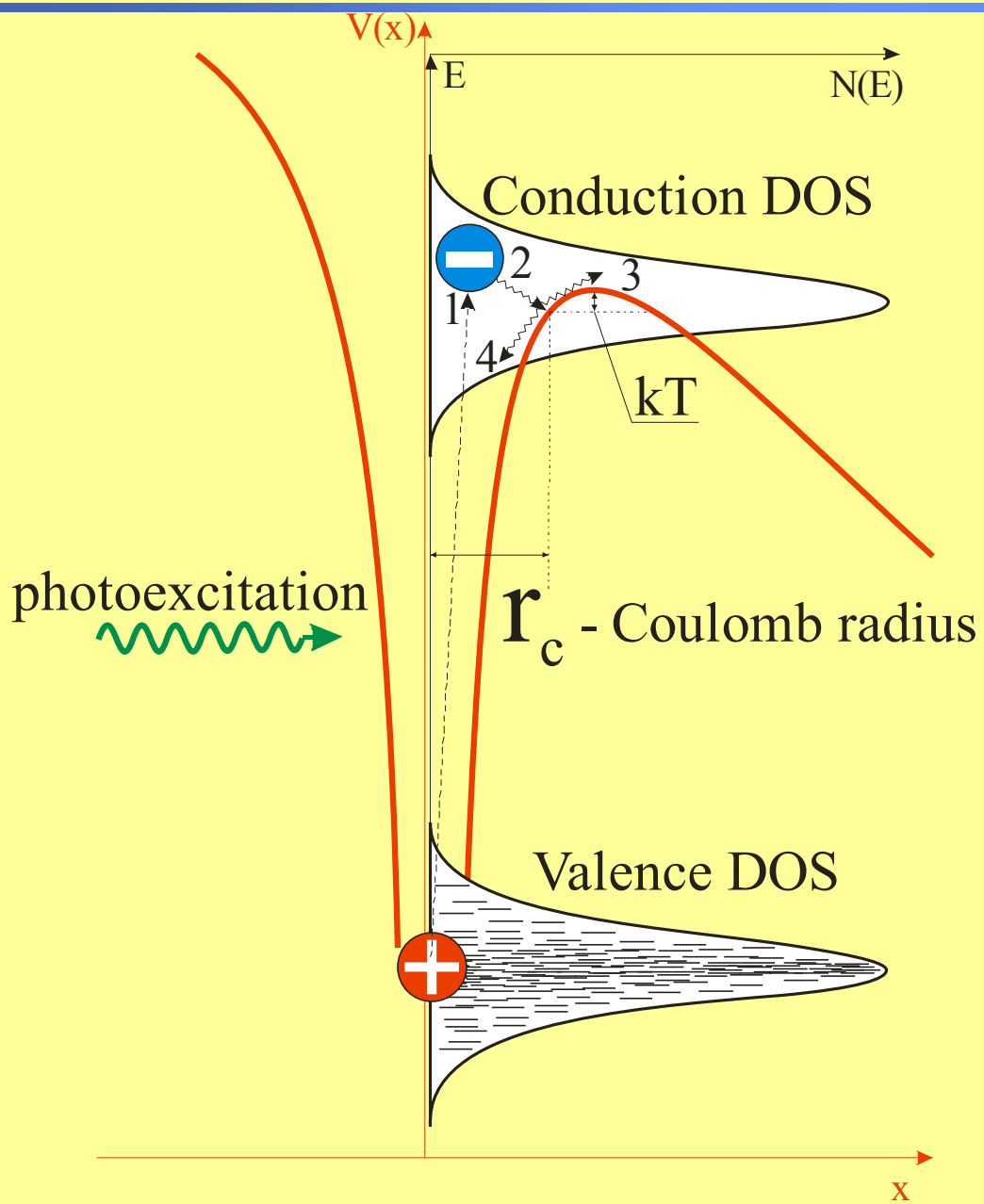

Electrical Field helps the Escape from the Coulomb Field of Partner

Poole-Frenkel Field Effect

The **field dependence of drift mobility** usually follows Poole-Frenkel law:

$$\mu = \mu_o \exp\left(-\frac{E_o - \gamma\sqrt{E_D}}{k_B T}\right)$$

where μ_o is zero field mobility, E_o is zero field activation energy, k_B is Boltzmann constant, γ is Poole-Frenkel constant and T is absolute temperature.

J. Frenkel, Phys. Rev., vol. 54, pp. 647-648, 1938.

Early models: **Poole-Frenkel Model**

The electric field dependence of the mobility is attributed to the lowering of the activation energy by tilting the coulomb barrier

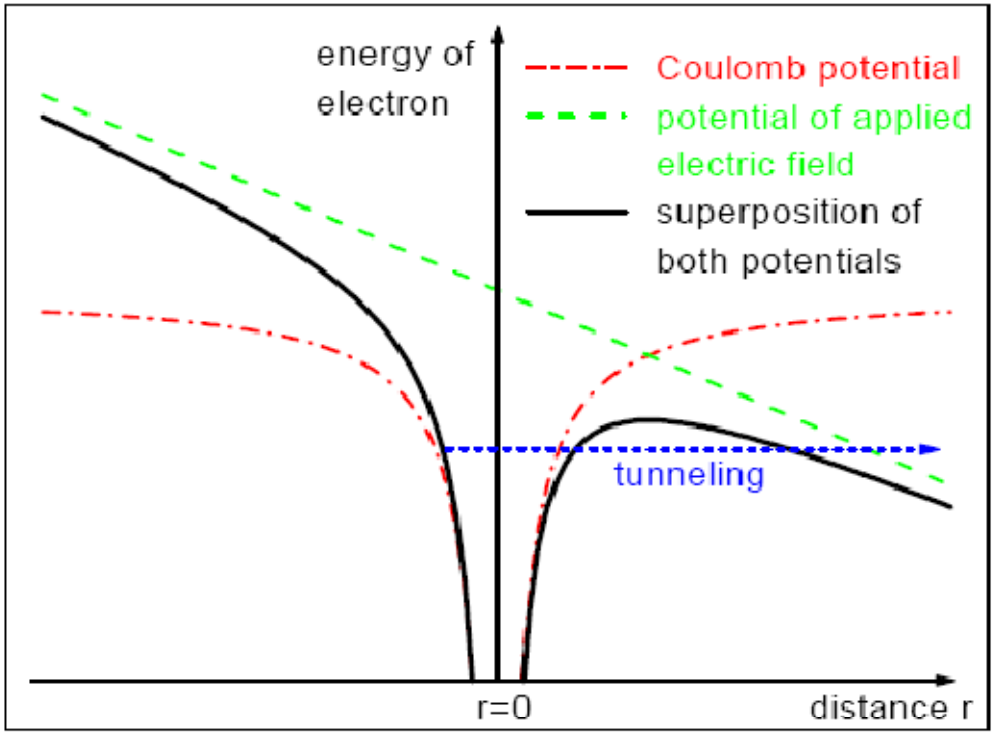

$$\mu = \mu_0 \exp\left(-\frac{\Delta E - \beta_{PF}\sqrt{F}}{k_B \cdot T_{\text{eff}}}\right)$$

$$\frac{1}{T_{\text{eff}}} = \frac{1}{T} - \frac{1}{T_0}$$

$$\beta_{PF} = \sqrt{\frac{q^3}{\pi \cdot \varepsilon_r \cdot \varepsilon_0}}$$

ΔE: activation energy

W.D. Gill, *J. Appl. Phys.* **43**, 5033 (1972)

For critical analysis see: L. B. Schein, et al. J. Appl. Phys. 66, 686 (1989).

Gaussian Disorder Model ("Bässler model")

Basic assumptions:

- Hopping transport described by Miller-Abrahams jump rates;
- Distribution of site energies and distances are Gaussian;
- Electron-phonon coupling is sufficiently weak that polaron effects can be neglected, yet strong enough to guarantee coupling to a heat bath;
- The process is incoherent, characterized by the loss of phase after each jump.
- Charge trapping is ignored → *trap-free transport".

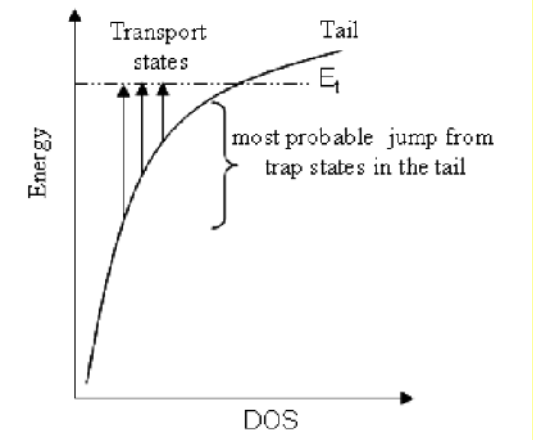

Solved by Monte-Carlo computer simulations

Gaussian DOS with width σ – "energy disorder parameter" ;

Σ – positional disorder parameter.

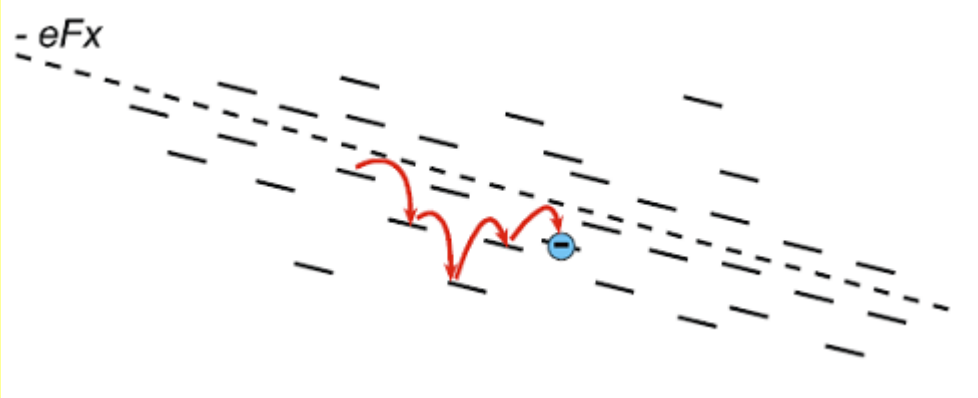

Review articles:
H. Bässler, *Phys.Status Solidi B.* **15**, 175 (1993).
more recent in: *ChemPhysChem*, **9**, 666 (2008)

Equilibrium carrier distribution

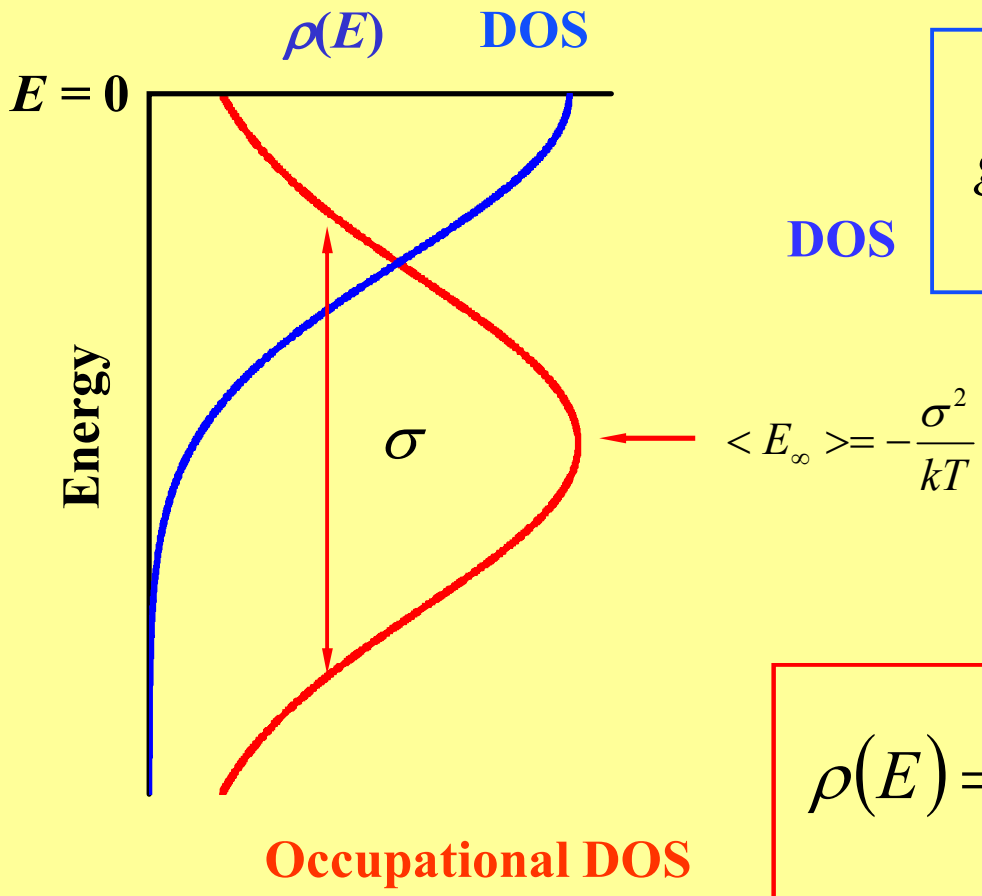

$$< E_\infty > = -\frac{\sigma^2}{kT}$$

DOS

$$g(E) = \sqrt{\frac{2}{\pi}}\frac{N_t}{\sigma}\exp\left(-\frac{E^2}{2\sigma^2}\right)$$

The width of the $\rho(E)$ distribution is the same as that of the Gaussian DOS !

$$\rho(E) = \frac{1}{\sqrt{2\pi}\sigma}\exp\left[-\frac{(E-E_\infty)^2}{2\sigma^2}\right]$$

The carrier at the long time limit are distributed as a Gaussian with mean value of $<E_\infty>=-\sigma^2/kT$ and energy width of σ.

Mobility Measurements

ORGANIC FIELD EFFECT MOBILITY

CELIV

TOF

HALL EFFECT

SPACE CHARGE LIMITED CURRENT MOBILITY

…….

Photo-CELIV Method

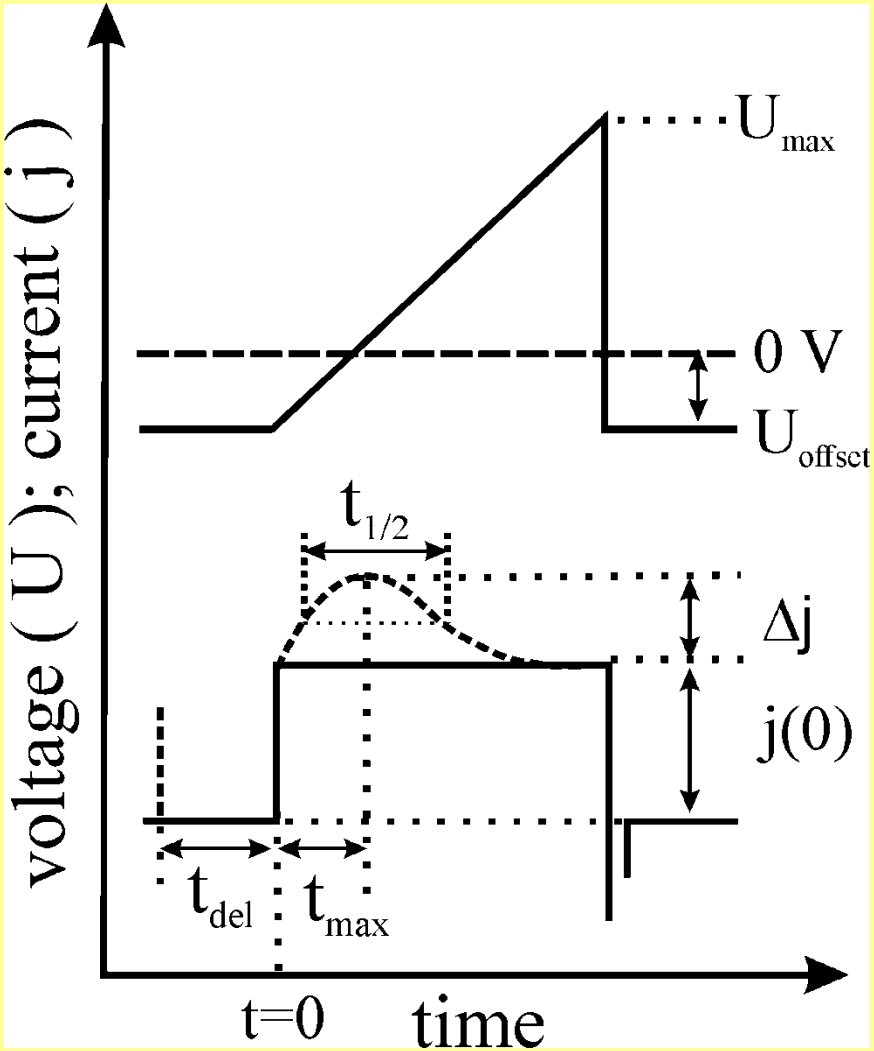

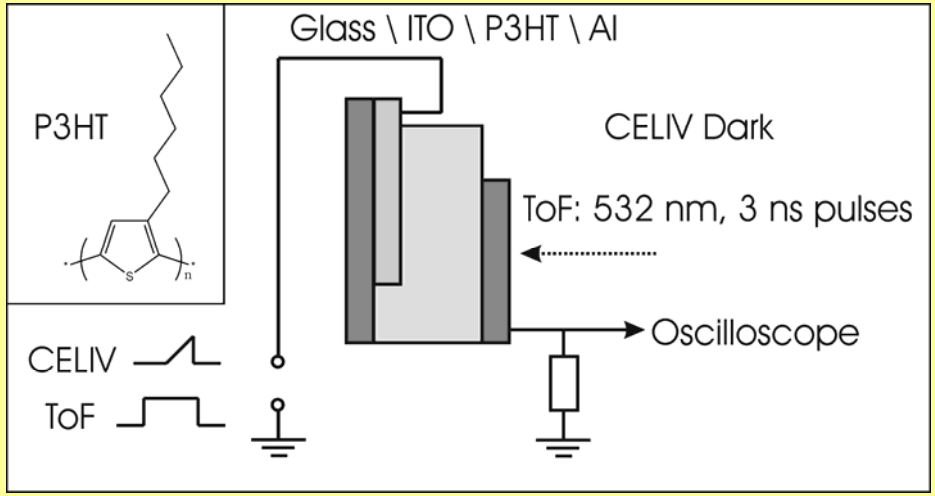

$$\mu = \frac{2d^2}{3At_{max}^2\left[1 + 0.36\frac{\Delta j}{j(0)}\right]}$$

Attila Mozer *et al*, *Phys. Rev.* **B 71**, (2005) 35214

Photo-CELIV Method

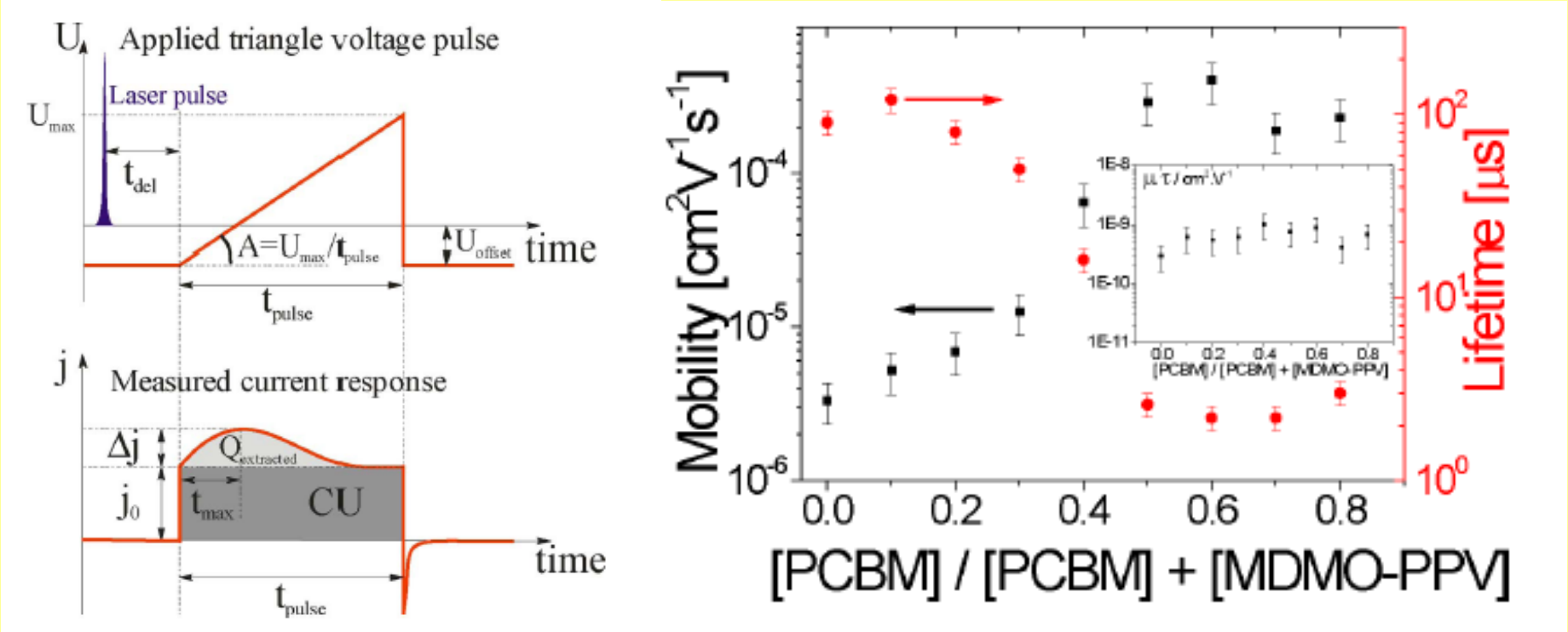

G. Dennler, A. Mozer, G. Juska, A. Pivrikas, R. Österbacka, A. Fuchsbauer, N.S. Sariciftci

***Organic Electronics* 7 (2006), 229-234**

Transport in Conjugated Polymers

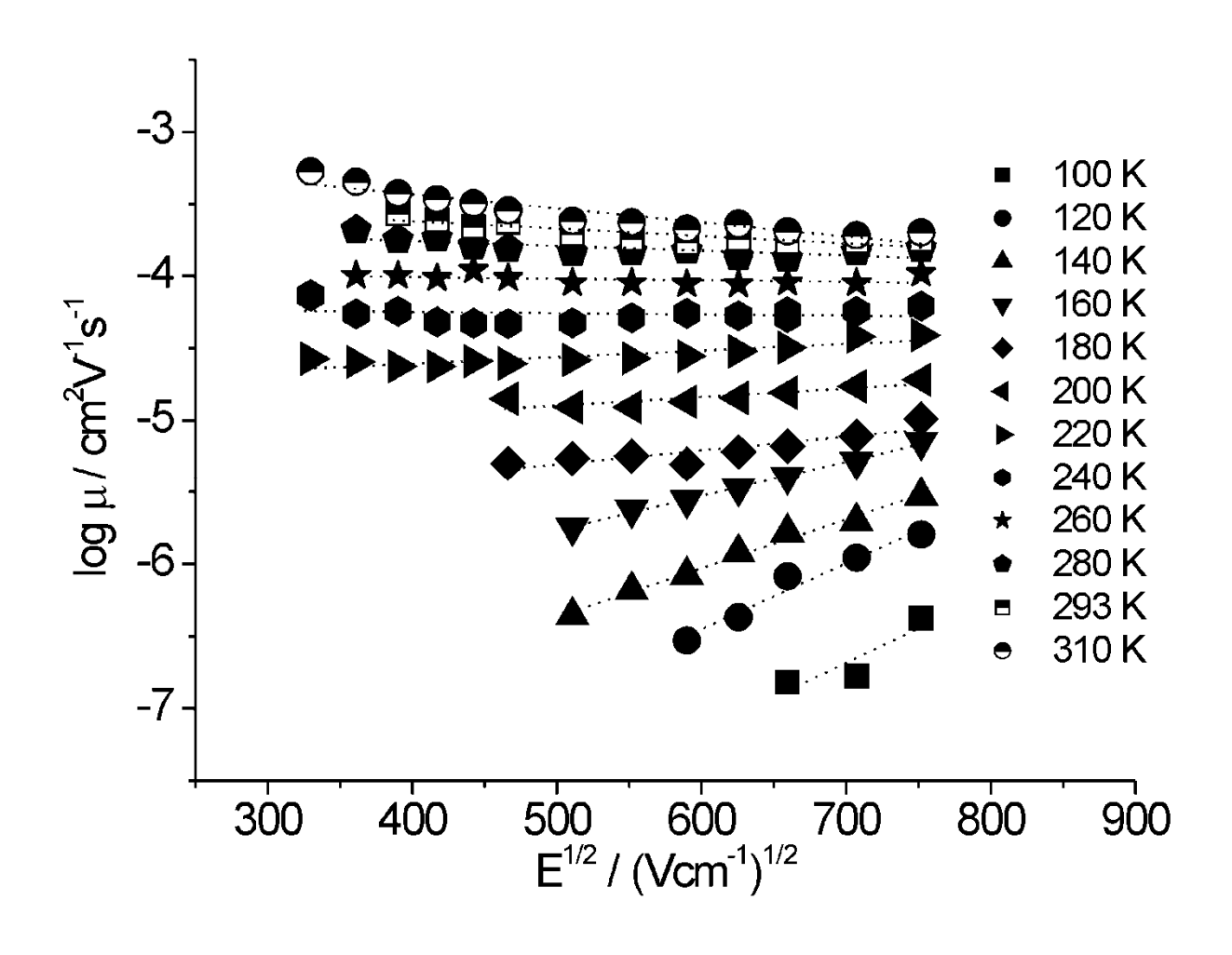

Negative Field Dependence in RR-P3HT

TOF STUDIES

Attila Mozer *et al, Chem. Phys. Lett.*, **389** (2004) 438

Transport in Conjugated Polymers

Bässler formalism, using Miller Abrahams hopping rate and a Gaussian density of localized states

$$\nu_{ij} = \nu_0 \exp\left(-2\gamma a \frac{\Delta R_{ij}}{a}\right) \begin{cases} \exp\left(-\frac{\varepsilon_j - \varepsilon_i}{kT}\right) & \varepsilon_j > \varepsilon_i \\ 1; & \varepsilon_j < \varepsilon \end{cases}$$

$$\mu(T,E) = \mu_0 \exp\left[-\frac{2}{3}\hat{\sigma}^2\right] \exp\left[-C\left(\hat{\sigma}^2 - \Sigma^2\right)E^{1/2}\right]$$

$\sigma = \sigma/(k_B T)$ and Σ are parameters characterizing energetic disorder and positional disorder,
σ [eV] is the width of the Gaussian density of states,
μ_0 [$cm^2V^{-1}s^{-1}$] is a prefactor mobility in the disorder-free system,
E [Vcm^{-1}] is the electric field, and C is a fit parameter.

H. Bässler; Phys. Stat. Sol (b) 175 (1993) 15

ToF-Photo-CELIV Comparisons

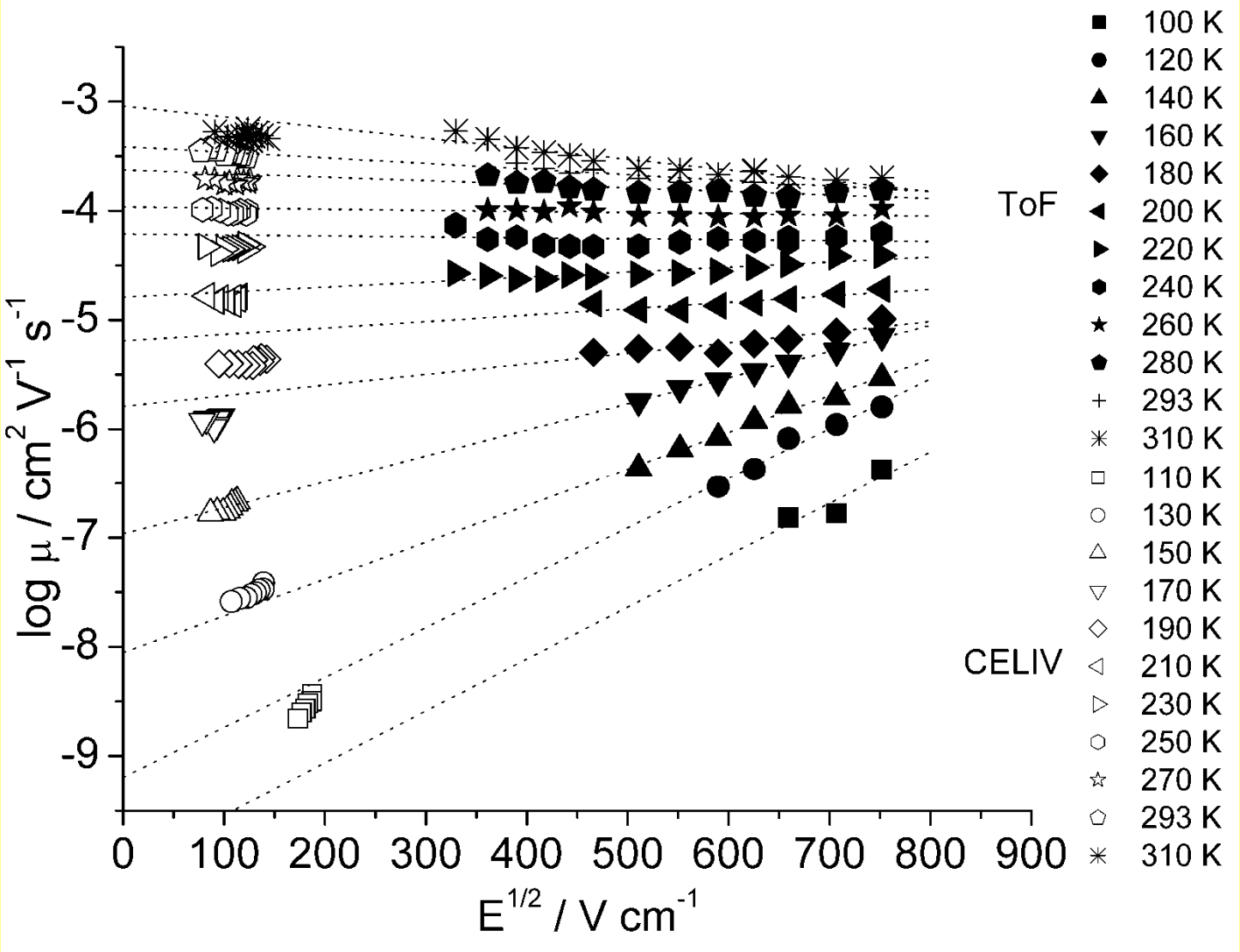

Attila Mozer *et al, Phys. Rev.* **B 71**, (2005) 35214

Mobility of Fullerene OFETs

Meyer –Neldel rule (1937):

$$\mu_{F.E} = \mu_{MN} \exp\left[-E_A \left(\frac{1}{k_B T} - \frac{1}{k_B T_{MN}} \right) \right] \qquad (3)$$

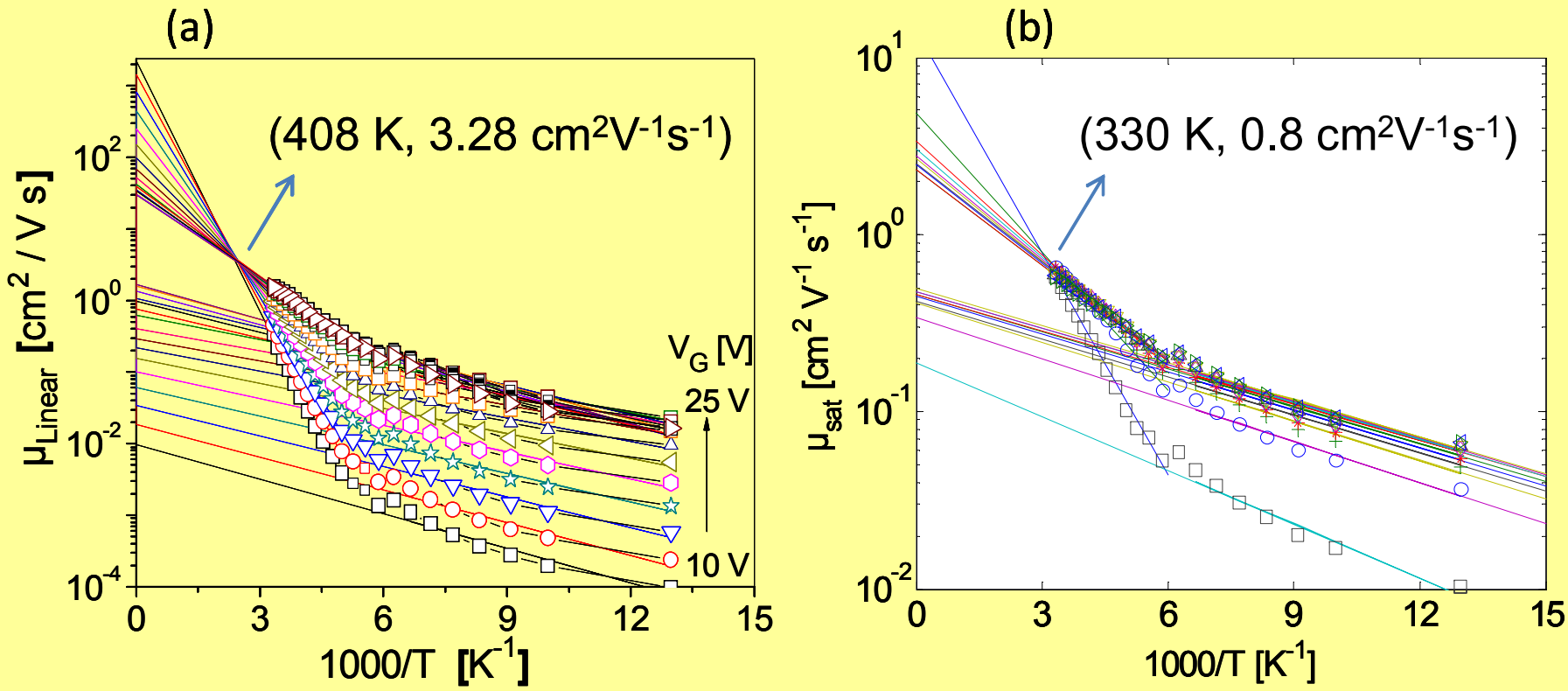

Mujeeb Ullah *et al. Applied Physics* ***A*** **97,** 521(2009)

Meyer-Neldel rule

"A phenomenon that can occur in any situation which involves an thermally activated process"

The Arrhenius dependence:

$$\mu = \mu_o \exp\left(-\frac{E_A}{k_B T}\right)$$

$$\mu_o = \mu_{MN} \exp\left(\frac{E_A}{k_B T_{MN}}\right)$$

μ_{MN} - constant pre-factor, E_{MN} - Meyer-Neldel energy

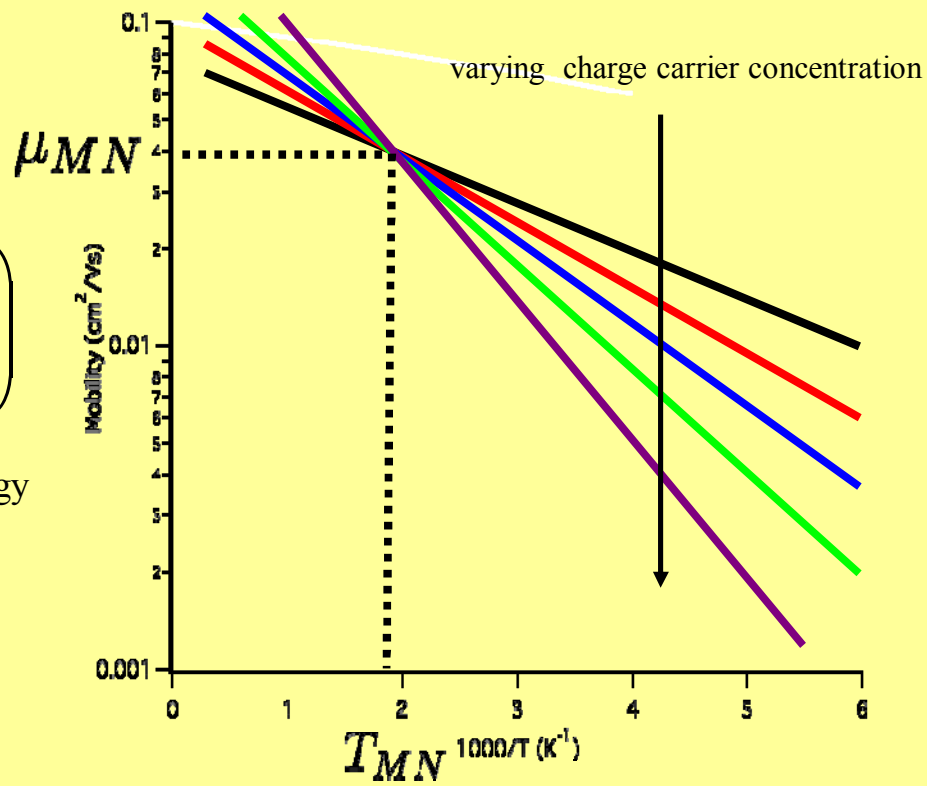

W. Meyer and H. Neldel, *Z. Tech*. **18**, 588 (1937).

CELIV vs OFET Comparison

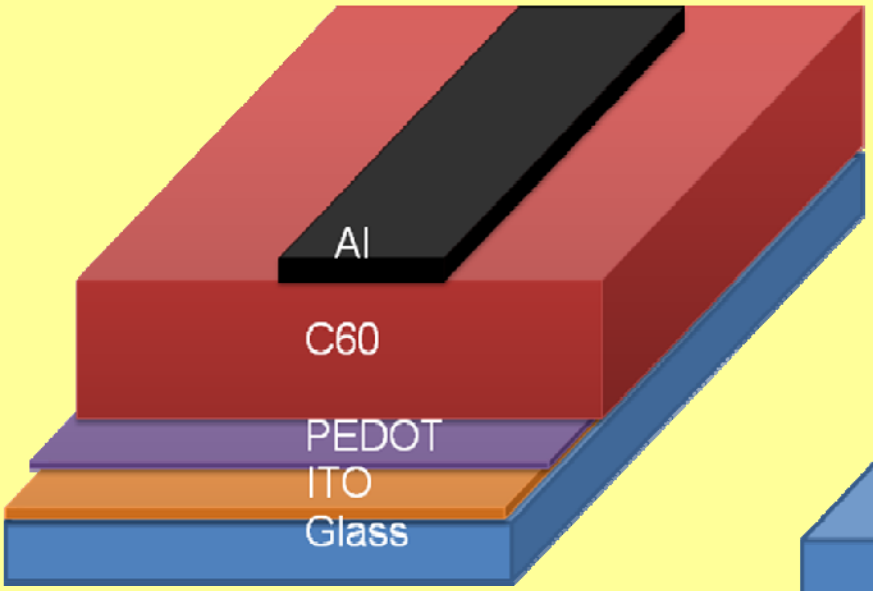

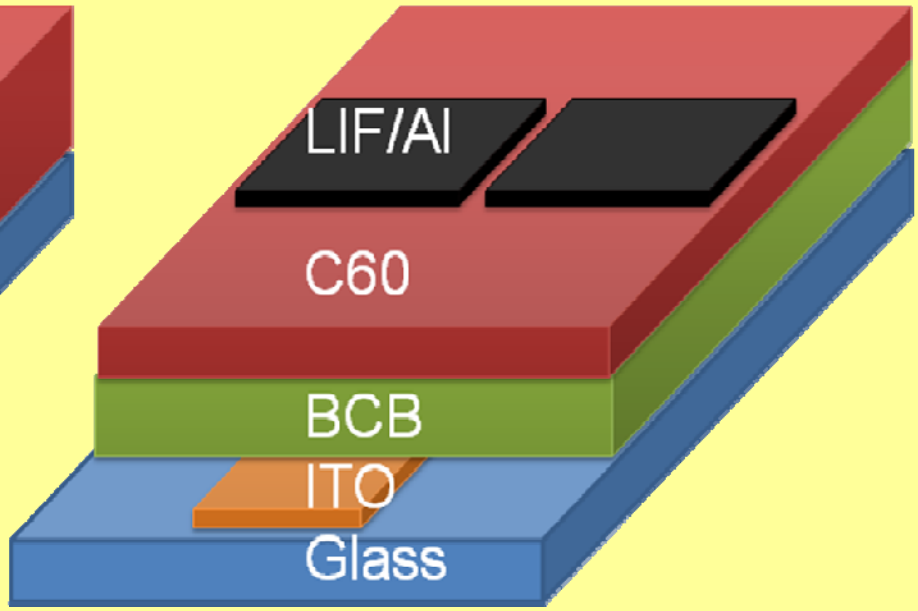

$$\mu = \frac{2d^2}{3At_{\max}^2\left[1+0.36\frac{\Delta j}{j(0)}\right]}$$

$$I_D\Big|_{V_{DS} << V_G.} = \frac{W}{L}\ \mu\, C_i\, V_{DS}\,(V_G - V_{th.})$$

- Carrier concentration are different in CELIV and OFET experiment

CELIV vs OFET Comparison

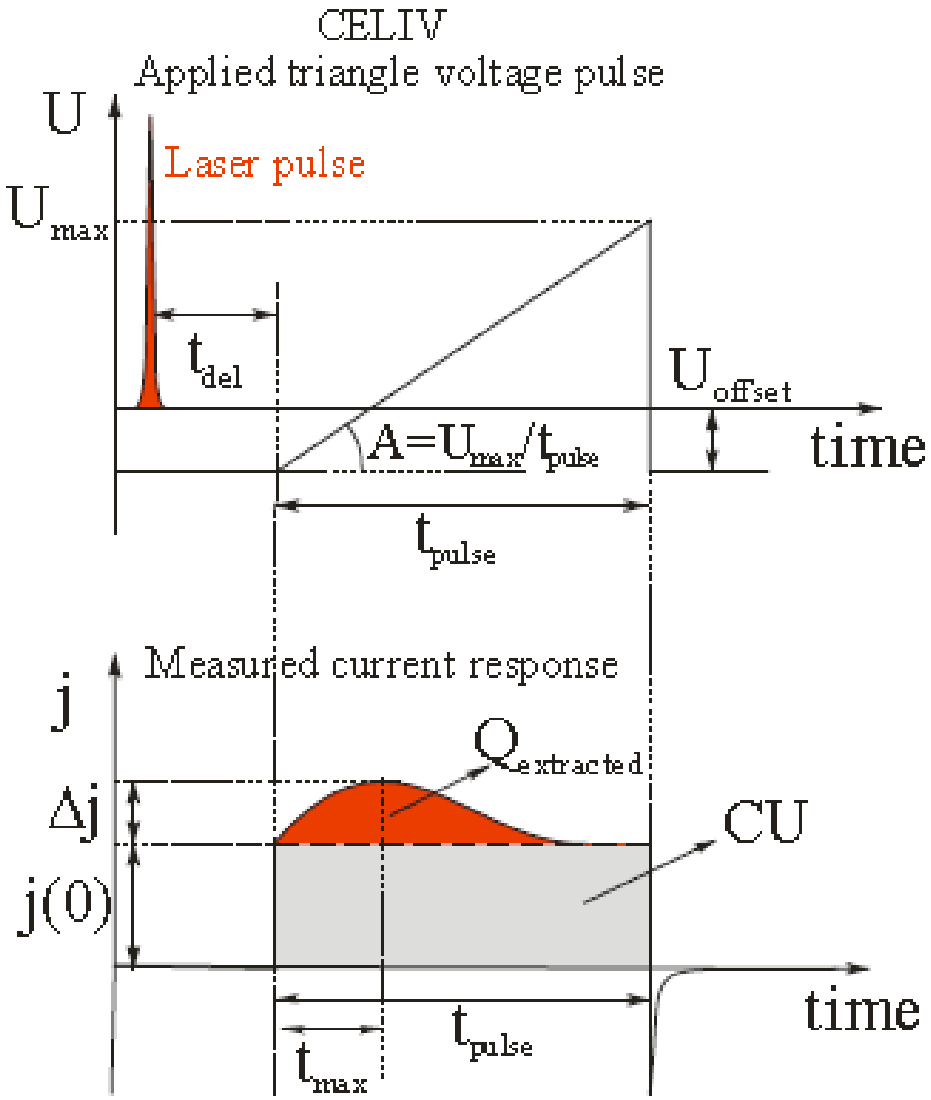

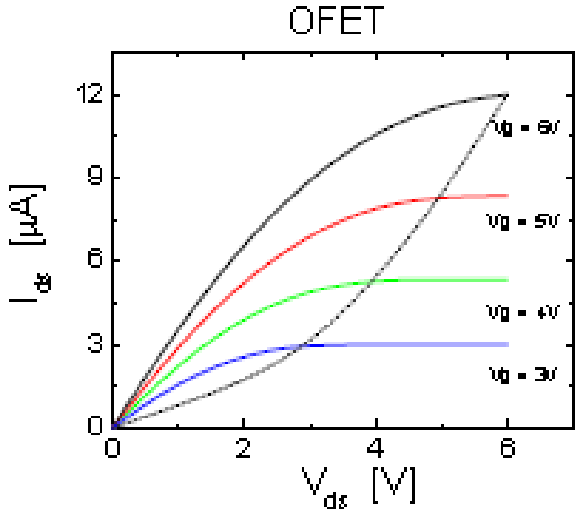

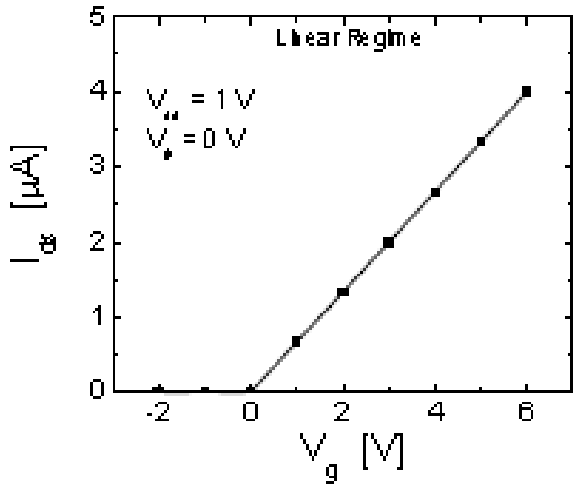

CELIV vs OFET Comparison

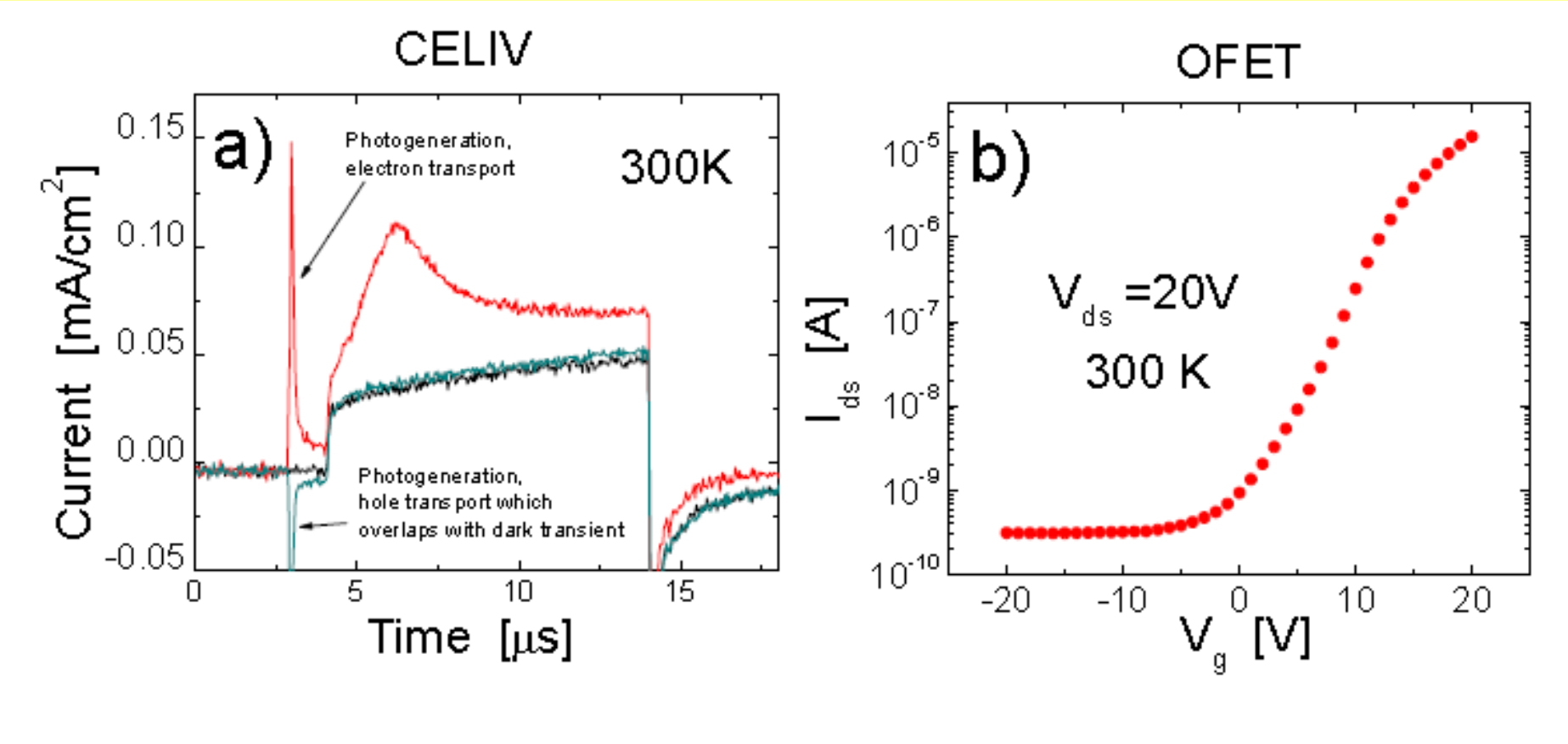

Almantas Pivrikas *et al.* (2010)

CELIV vs OFET Comparison

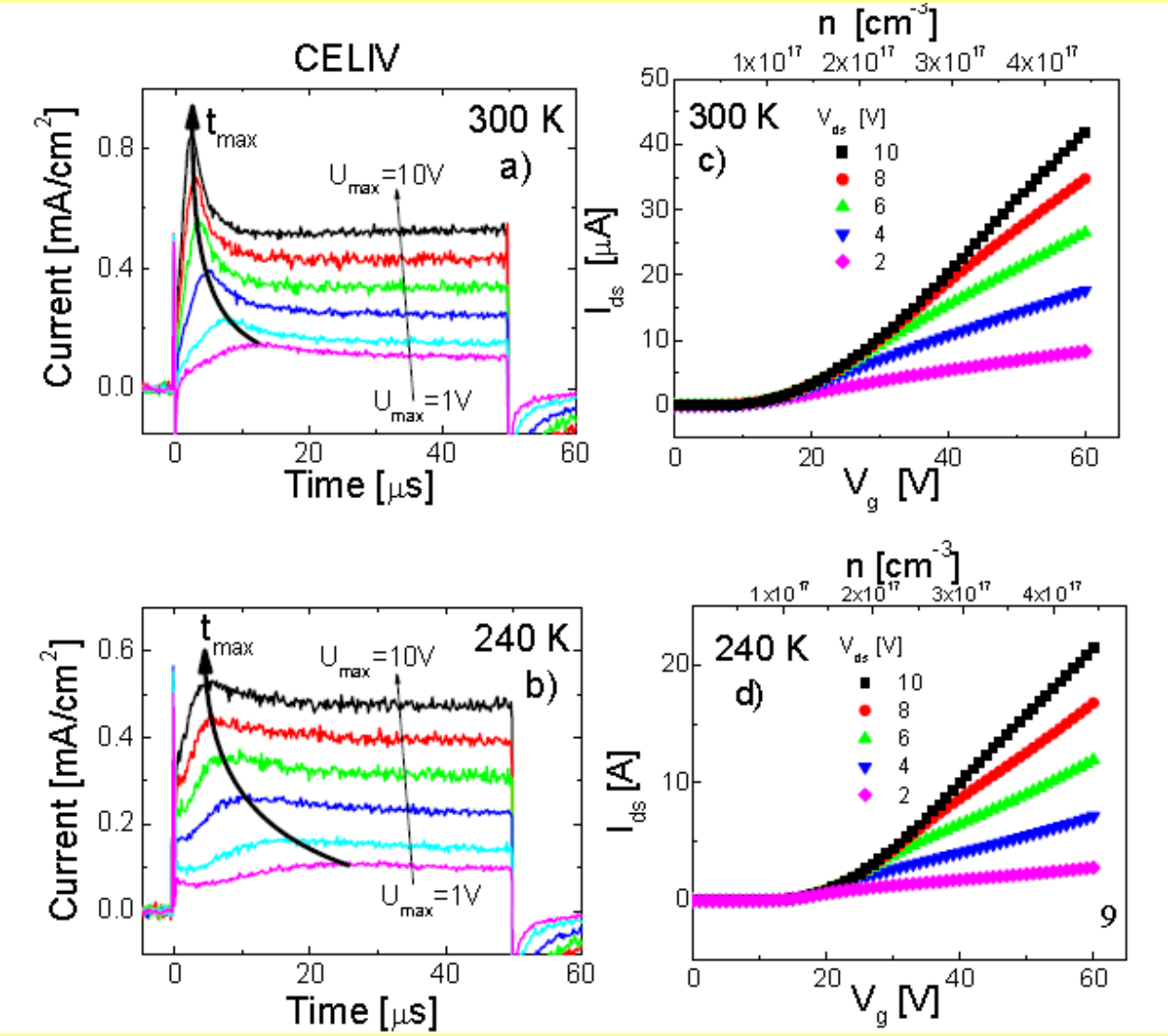

Almantas Pivrikas *et al.* (2010)

Poole-Frenkel law

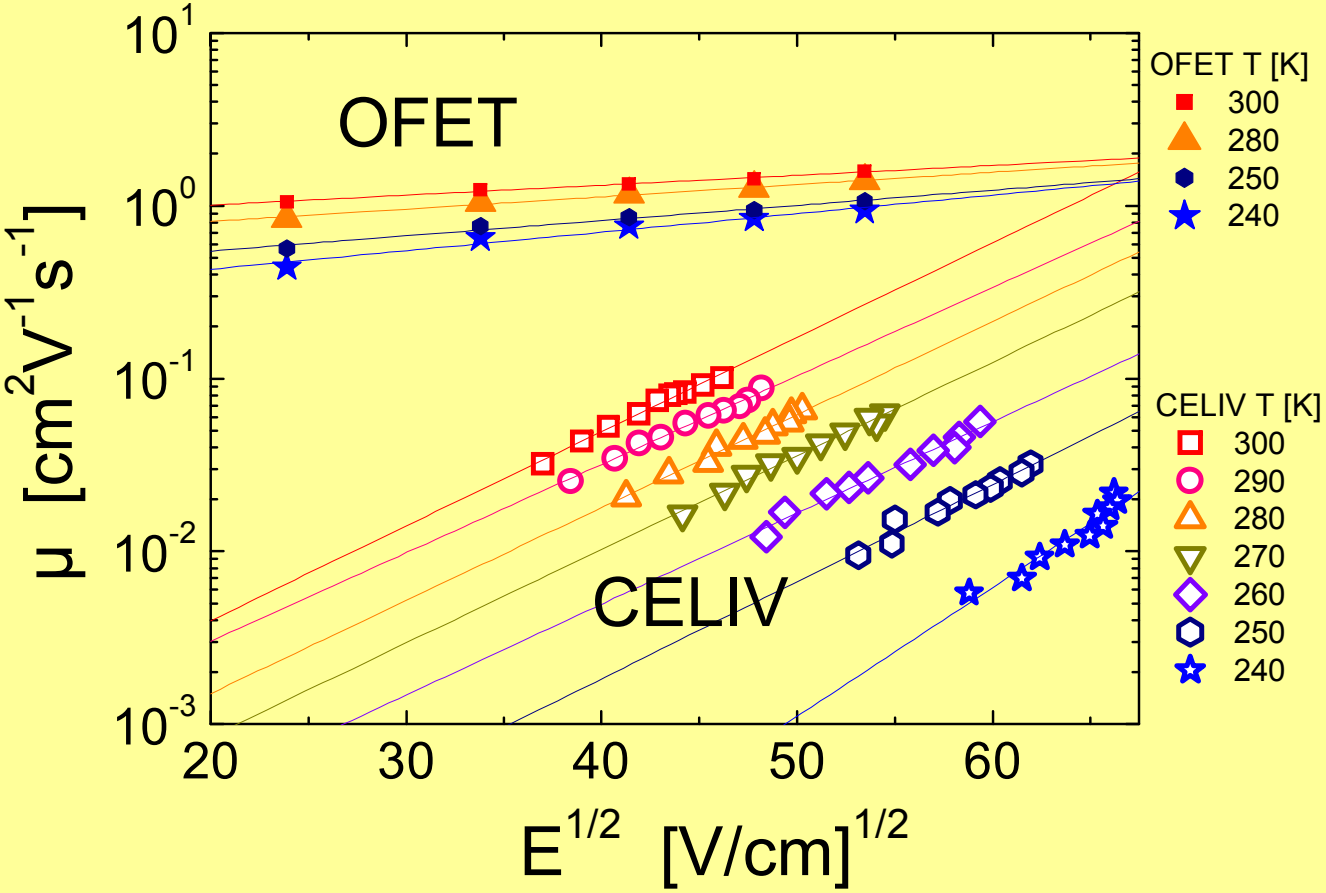

Almantas Pivrikas *et al.* (2010)

Mobility versus time in CELIV

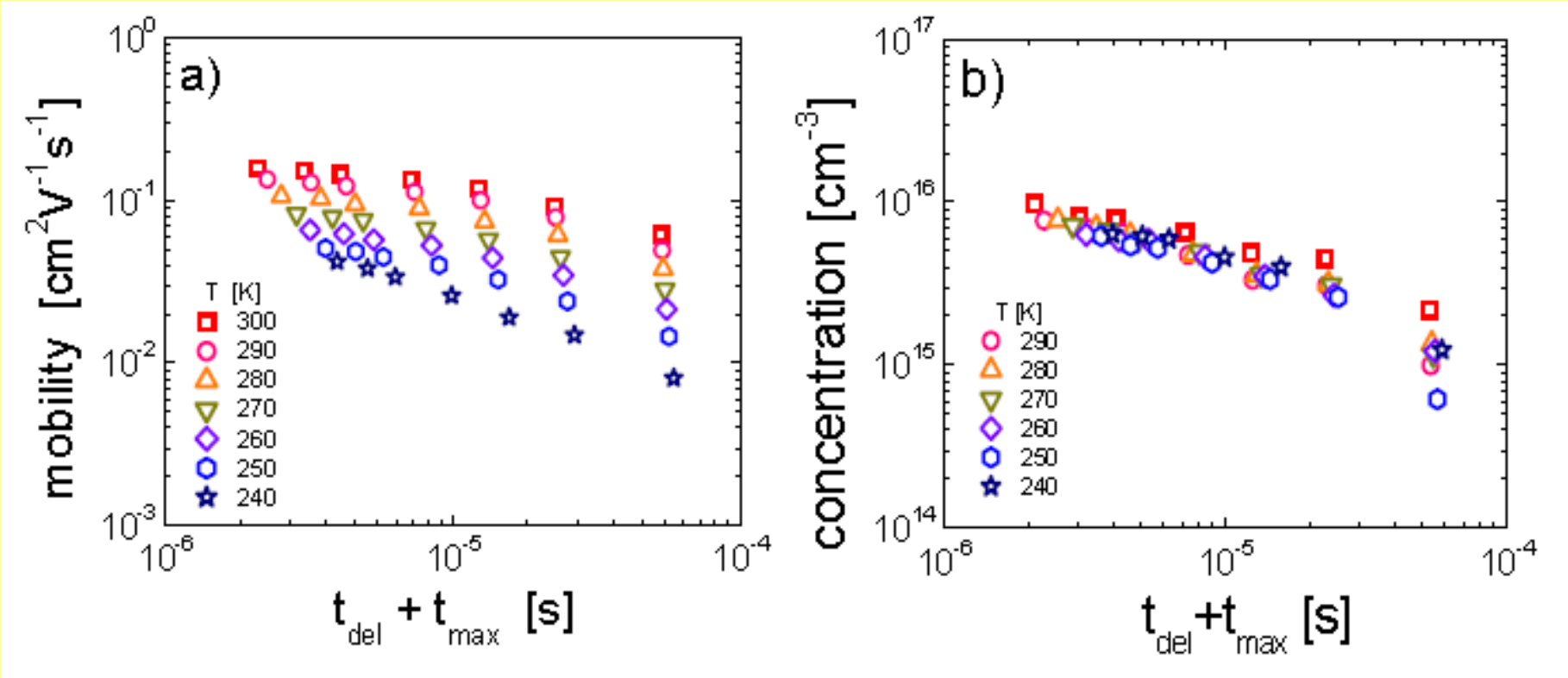

Almantas Pivrikas *et al.* (2010)

Mobility versus Concentration

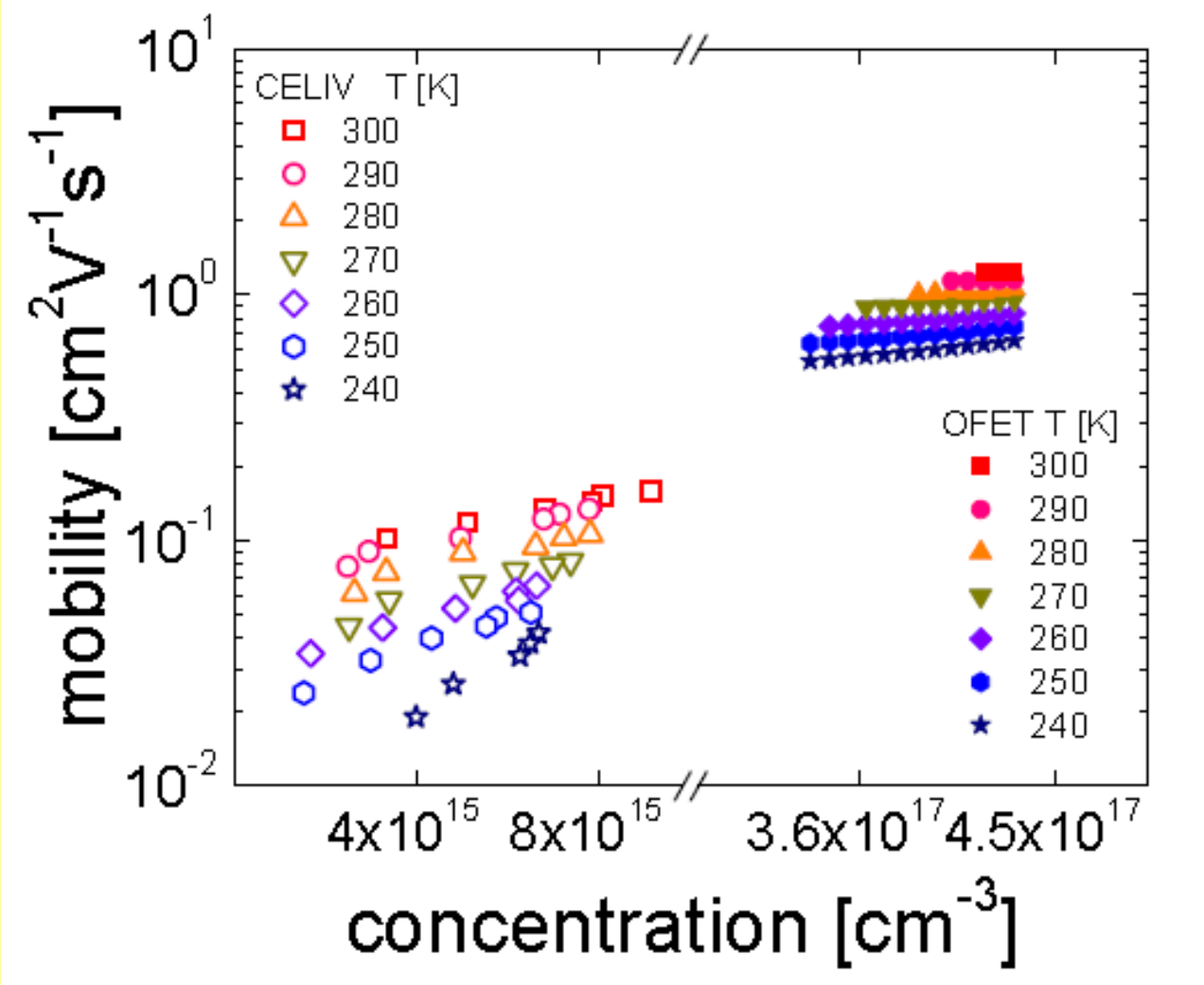

For OFETs assuming 10nm channel thickness

$$n = C_i V_G \frac{1}{e} \left(\frac{1}{1 \times 10^{-8}} \right)$$

Almantas Pivrikas *et al.* (2010)

Meyer-Neldel rule

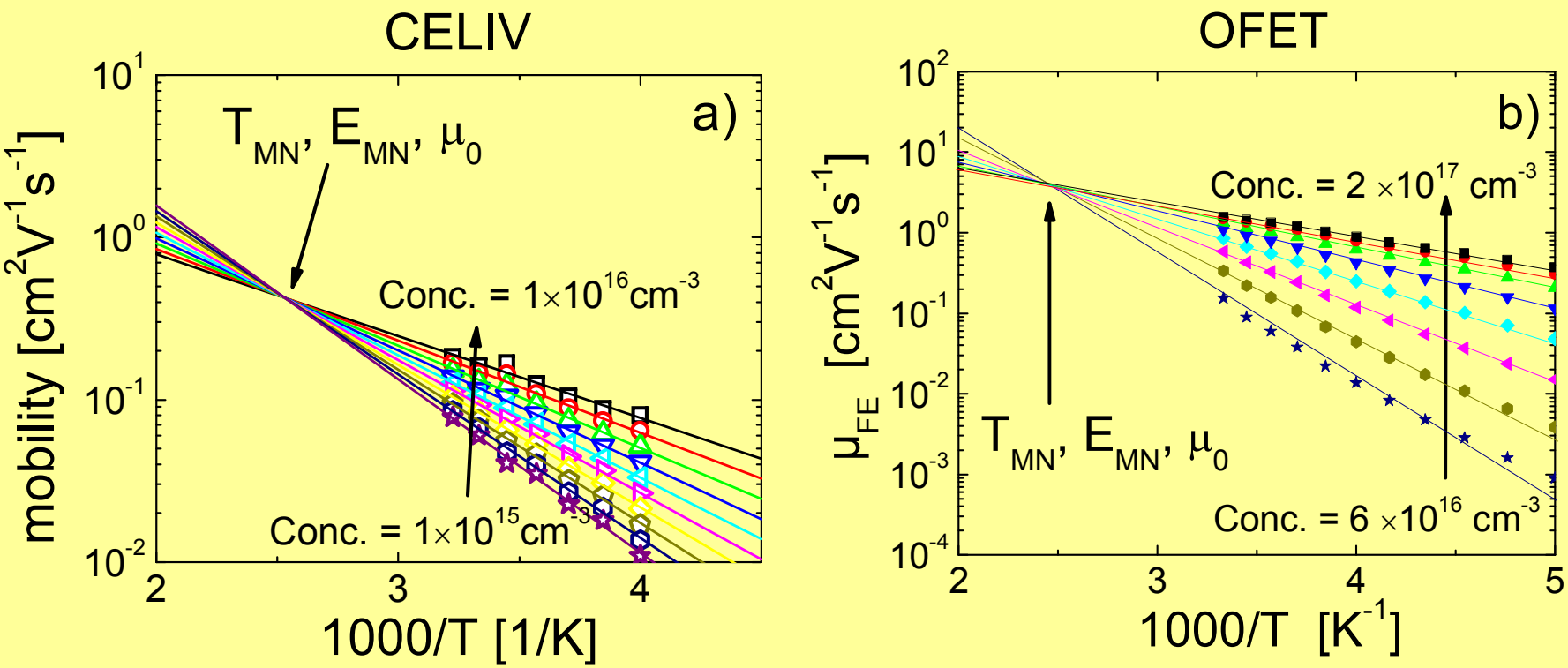

- CELIV and OFET in C60 devices shows E_{MN} = 35 meV,.

μ_{MN}= 0.4 cm^{2}V^{-1}s^{-1} from CELIV

μ_{MN}= 4 cm^{2}V^{-1}s^{-1} from OFET.

Almantas Pivrikas *et al.* (2010)

Meyer-Neldel rule : Theory

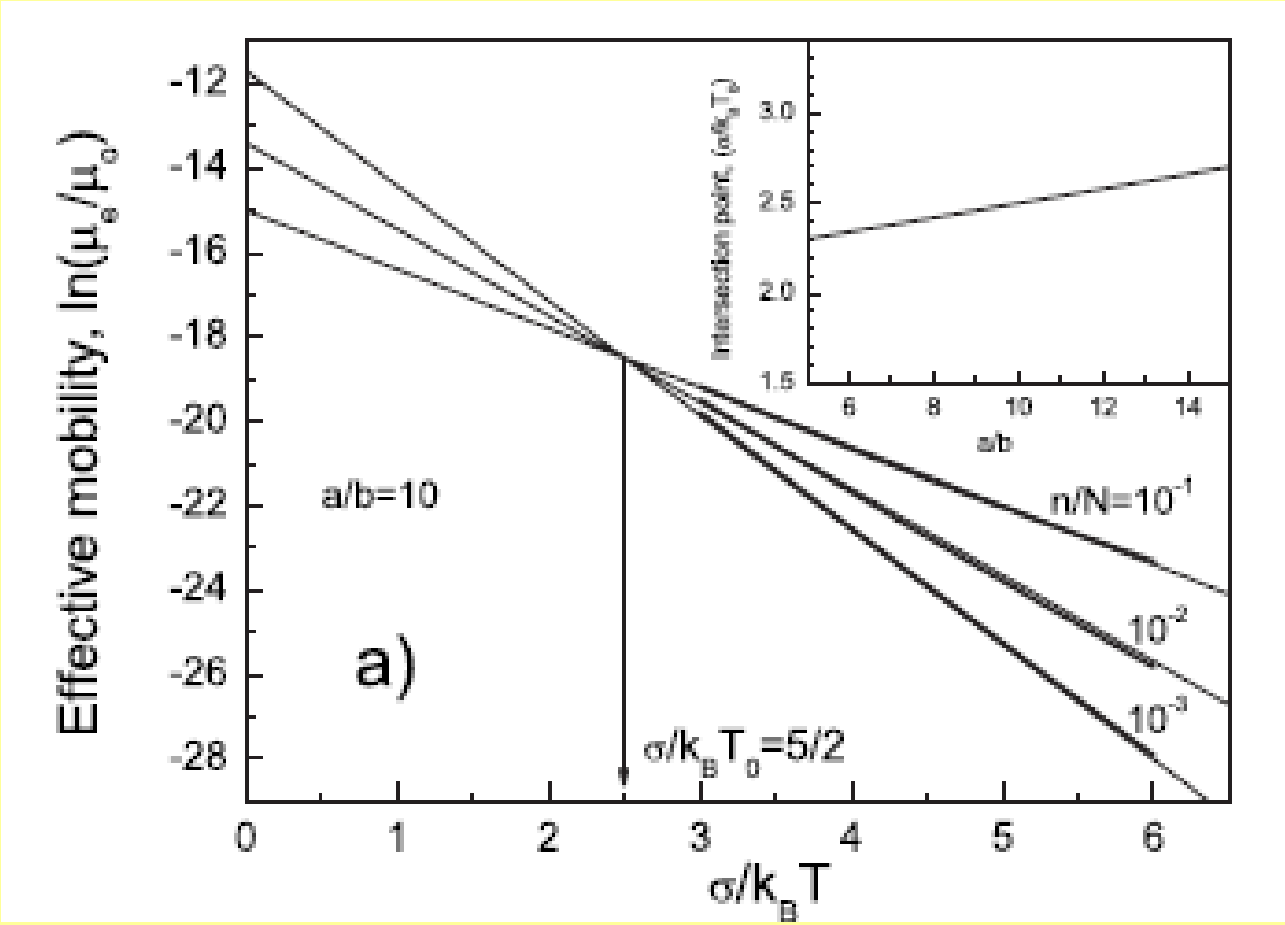

Fishchuk, A. Kadashchuk, J. Genoe, M. Ullah, H. Sitter, B. Singh, N.S. Sariciftci, H. Bässler
***Physical Review* B 81 (2010), 045202**

What about recombination?

$$R_{recombination} = \beta np = \beta n^2 = \frac{n}{1/\beta p} = \frac{n}{\tau_\beta}$$

Langevin Recombination

$$\beta_L = \frac{e(\mu_{faster} + \mu_{slower})}{\varepsilon\varepsilon_0}$$

Langevin recombination

$Q_{injected} \approx CU$

a)

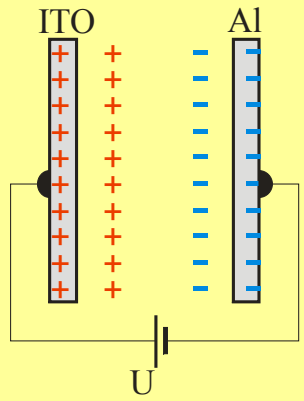

In MDMO-PPV/PCBM solar cells Langevin Rec.

Charge carrier must reach the electrodes prior to recombination

Recombination time >> transit time

Non-Langevin recombination

$Q_{injected} >> CU$

b)

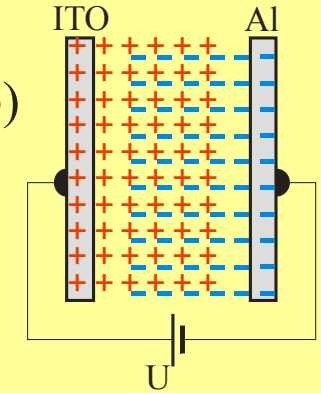

In P3HT/PCBM solar cells non-Langevin Rec.

Mozer and Pivrikas et al.

Diffusion versus Drift Effects

JOURNAL OF APPLIED PHYSICS VOLUME 93, NUMBER 6 15 MARCH 2003

Comparing organic to inorganic photovoltaic cells: Theory, experiment, and simulation

Brian A. Gregg[a)] and Mark C. Hanna
National Renewable Energy Laboratory, 1617 Cole Boulevard, Golden, Colorado 80401

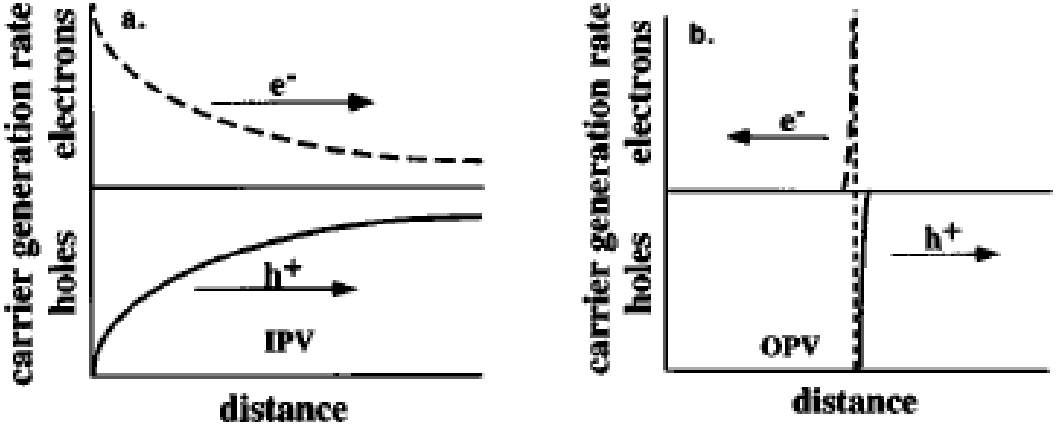

FIG. 3. A cartoon illustrating the difference in charge-carrier generation mechanisms in conventional (a) and excitonic (b) solar cells. In conventional solar cells (a), electrons and holes are photogenerated together wherever light is absorbed. Therefore, the photoinduced chemical-potential-energy gradient $\nabla \mu_{h\nu}$ (represented by arrows) drives both carrier types in the same direction. In the excitonic cell (b), however, electrons are photogenerated in one phase while holes are generated in the other via interfacial exciton dissociation. Carrier generation is simultaneous to, and identical with, carrier separation across the interface in OPV cells; $\nabla \mu_{h\nu}$ therefore drives electrons and holes in opposite directions.

The general kinetic expression for the one-dimensional current density of electrons $J_n(x)$ through any device is usually expressed as[1]

$$J_n(x) = n(x)\mu_n \nabla U(x) + kT\mu_n \nabla n(x), \quad (1)$$

where $n(x)$ is the concentration of electrons, μ_n is the electron mobility (not to be confused with the chemical potential energy μ), and k and T are Boltzmann's constant and the

ing force. Thus, ∇U can be ≈ 0, for example, and a highly efficient solar cell can be made based wholly on $\nabla \mu_{h\nu}$. This is how dye-sensitized solar cells (DSSCs) function,[19,32] in which the mobile electrolyte permeating the cell eliminates the internal electric fields (see below). In solid-state OPV cells without mobile electrolyte, both ∇U and $\nabla \mu$ must be taken into account.

Schematic Band Diagram

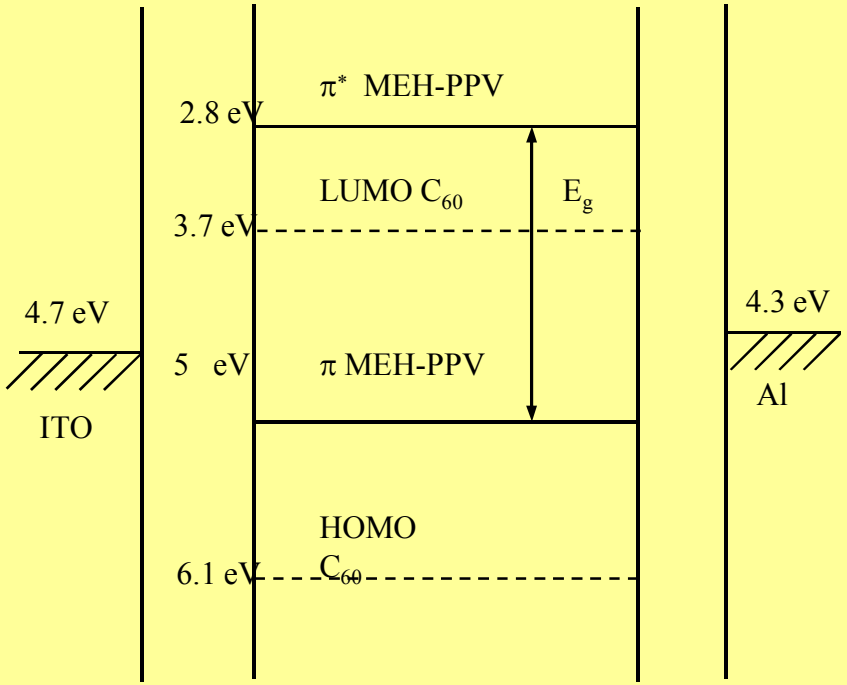

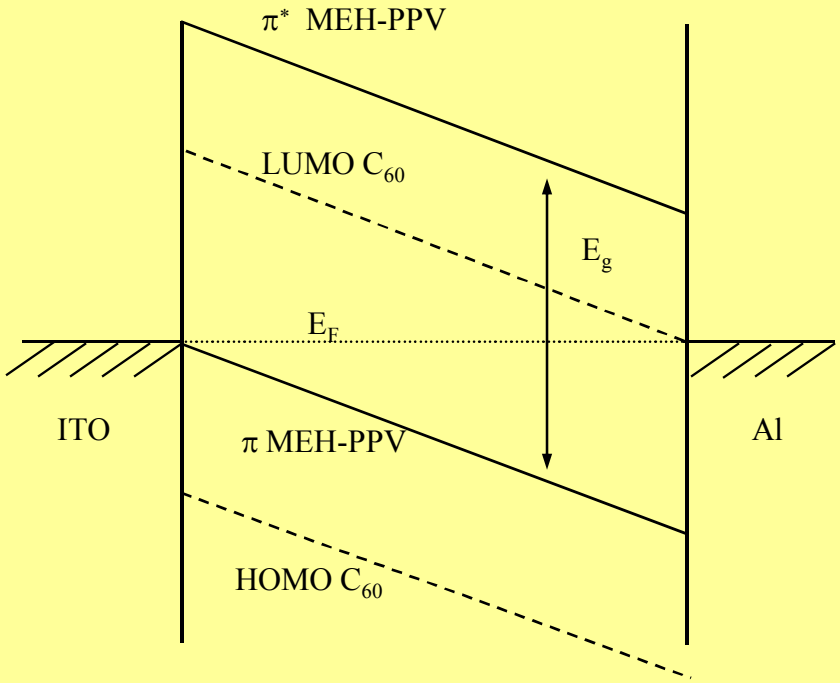

Metal-Insulator-Metal (MIM) picture
implies the field of assymetric metal electrodes
(All interface effects neglected!)

Schematic Band Diagram

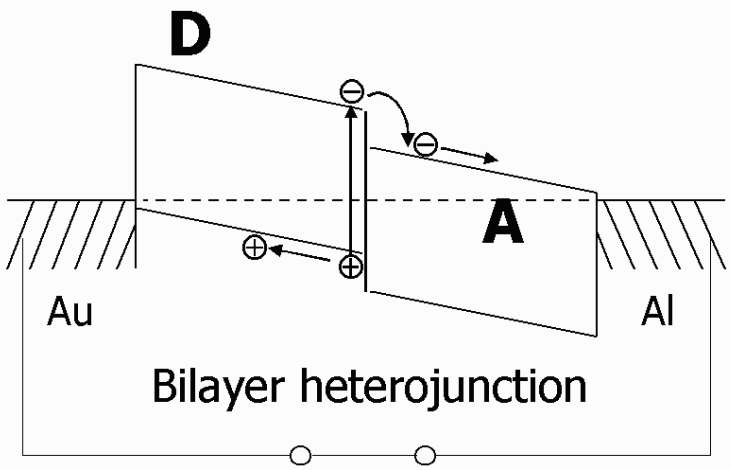

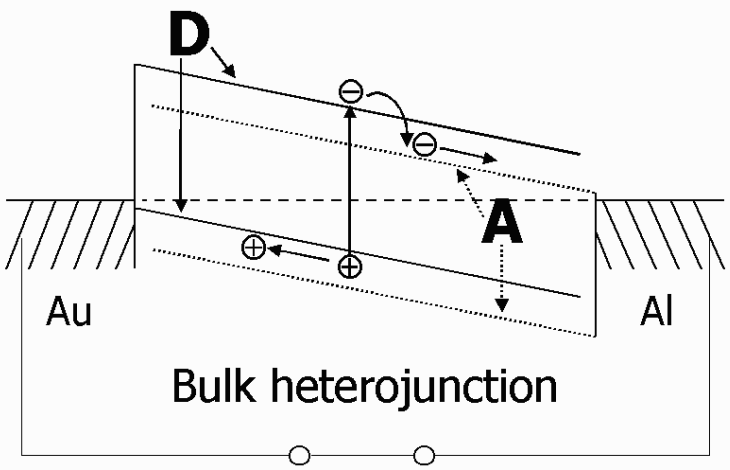

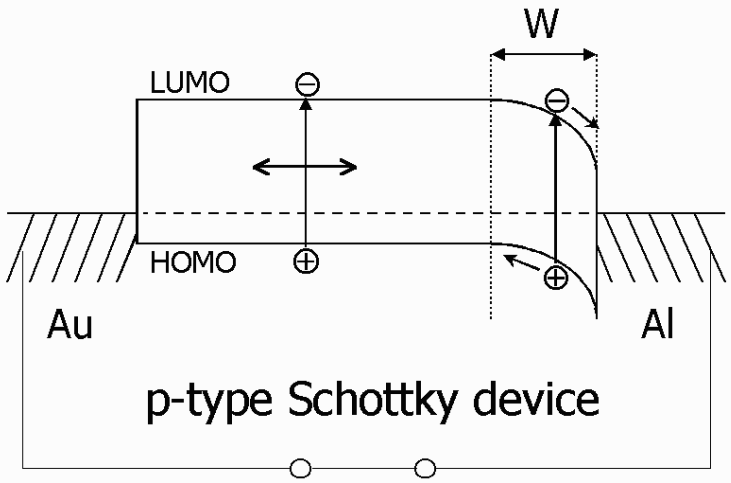

Under heavy illumination
a Schottky barrier formation ?

Fowler-Nordheim Tunneldiodes

Carrier tunneling and device characteristics in polymer light-emitting diodes

J. Appl. Phys. 75 (3), 1 February 1994

I. D. Parker
UNIAX Corporation, 5375 Overpass Road, Santa Barbara, California 93111

(Received 19 August 1993; accepted for publication 15 October 1993)

Fowler–Nordheim tunneling theory

$$I \propto F^2 \exp\left(\frac{-\kappa}{F}\right),$$

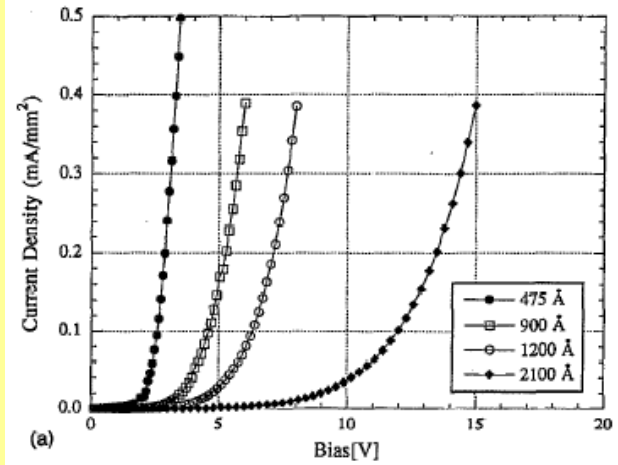

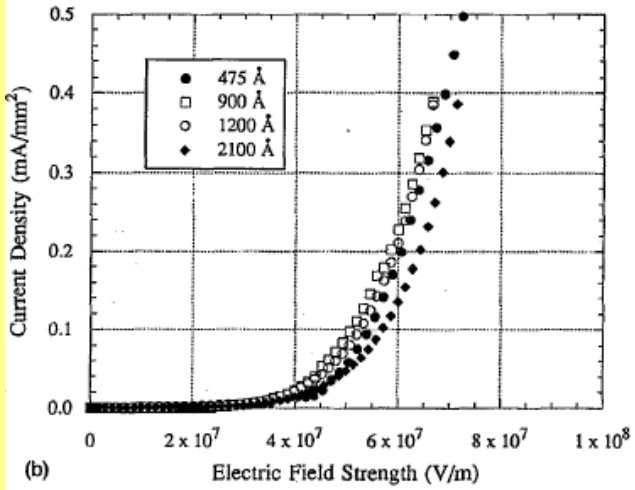

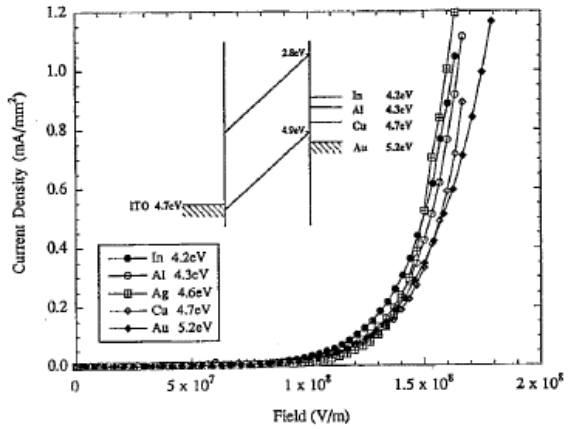

FIG. 3. *I-V* characteristics of 1200 Å thick "hole-only" devices. Inset shows band models indicating the relative position of the Fermi energies of the various materials.

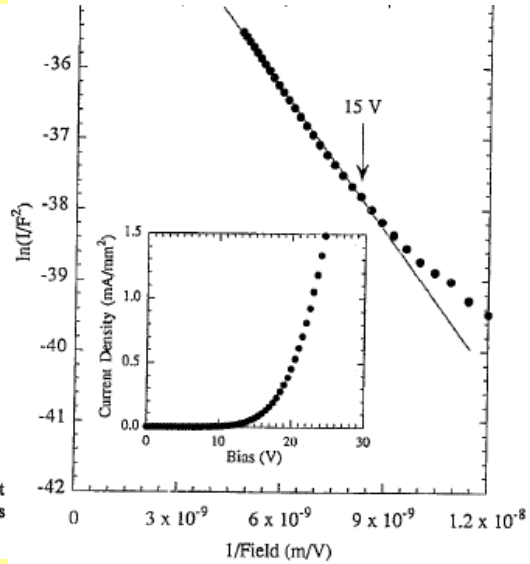

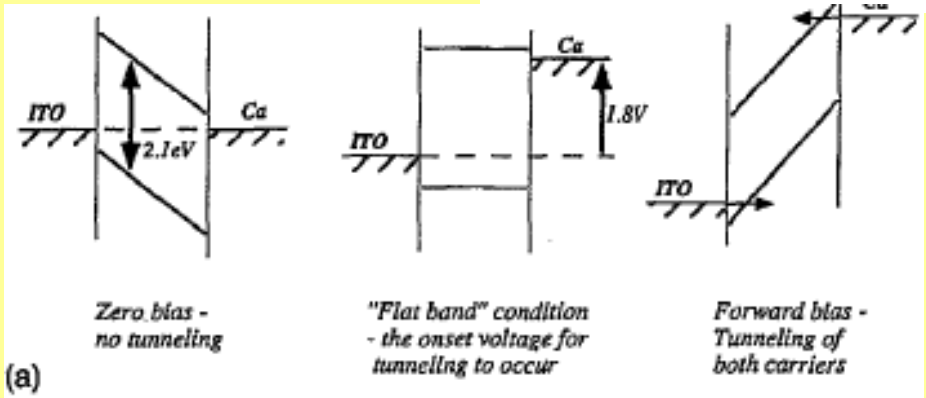

Band Models

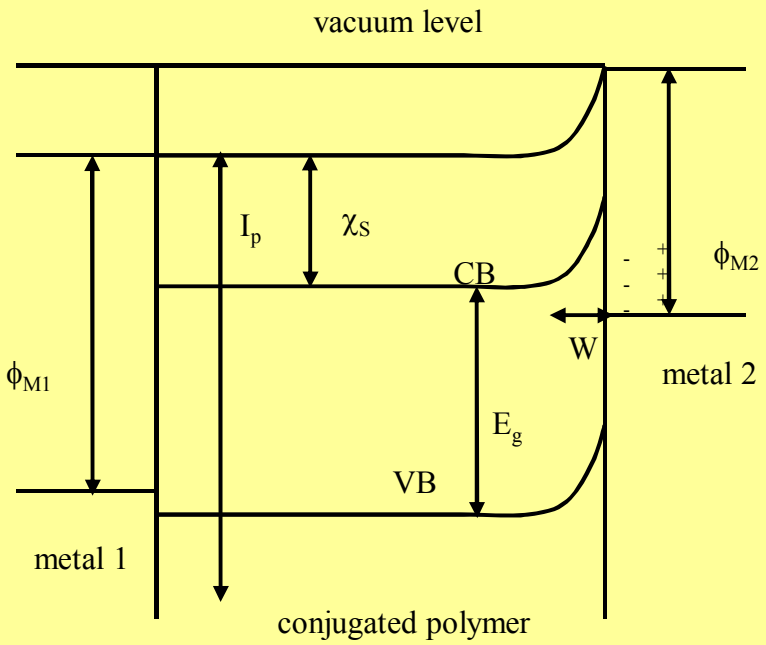

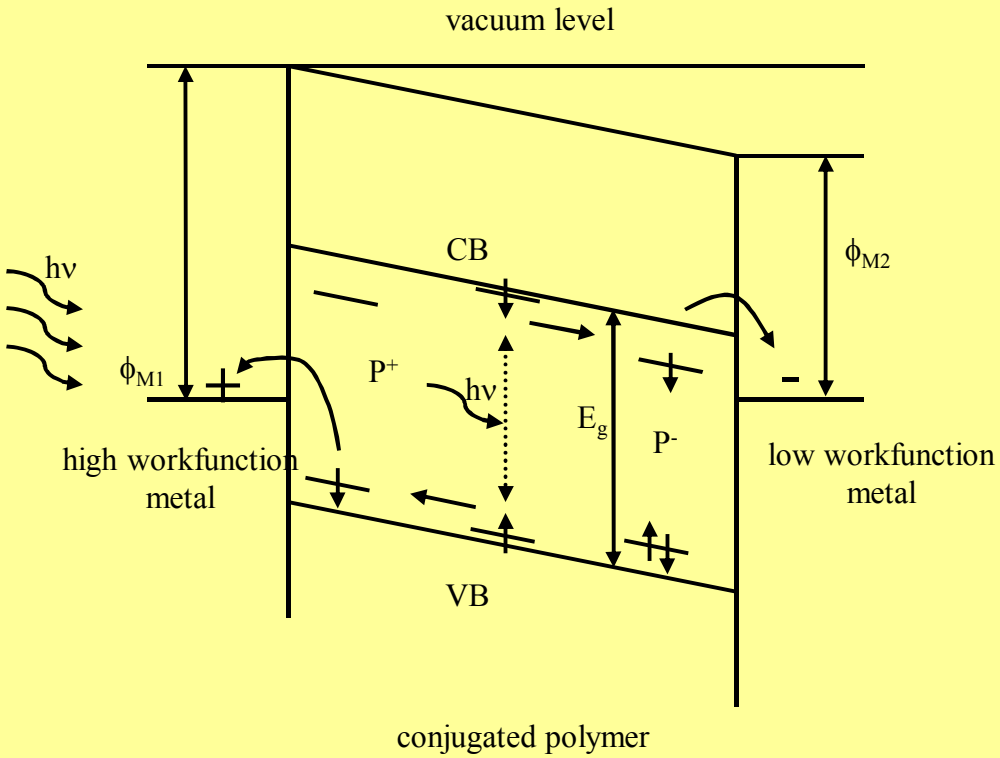

Schottky Contacts for high Impurities
$n >> 10^{16} cm^{-3}$

MIM Picture for low Impurities
$n << 10^{16} cm^{-3}$

Electroabsorption Studies

A measure of the internal electric field in the device

$$\frac{|\Delta T|}{T}(h\nu) \propto (V_{dc} - V_{int}) \cdot V_{ac}$$

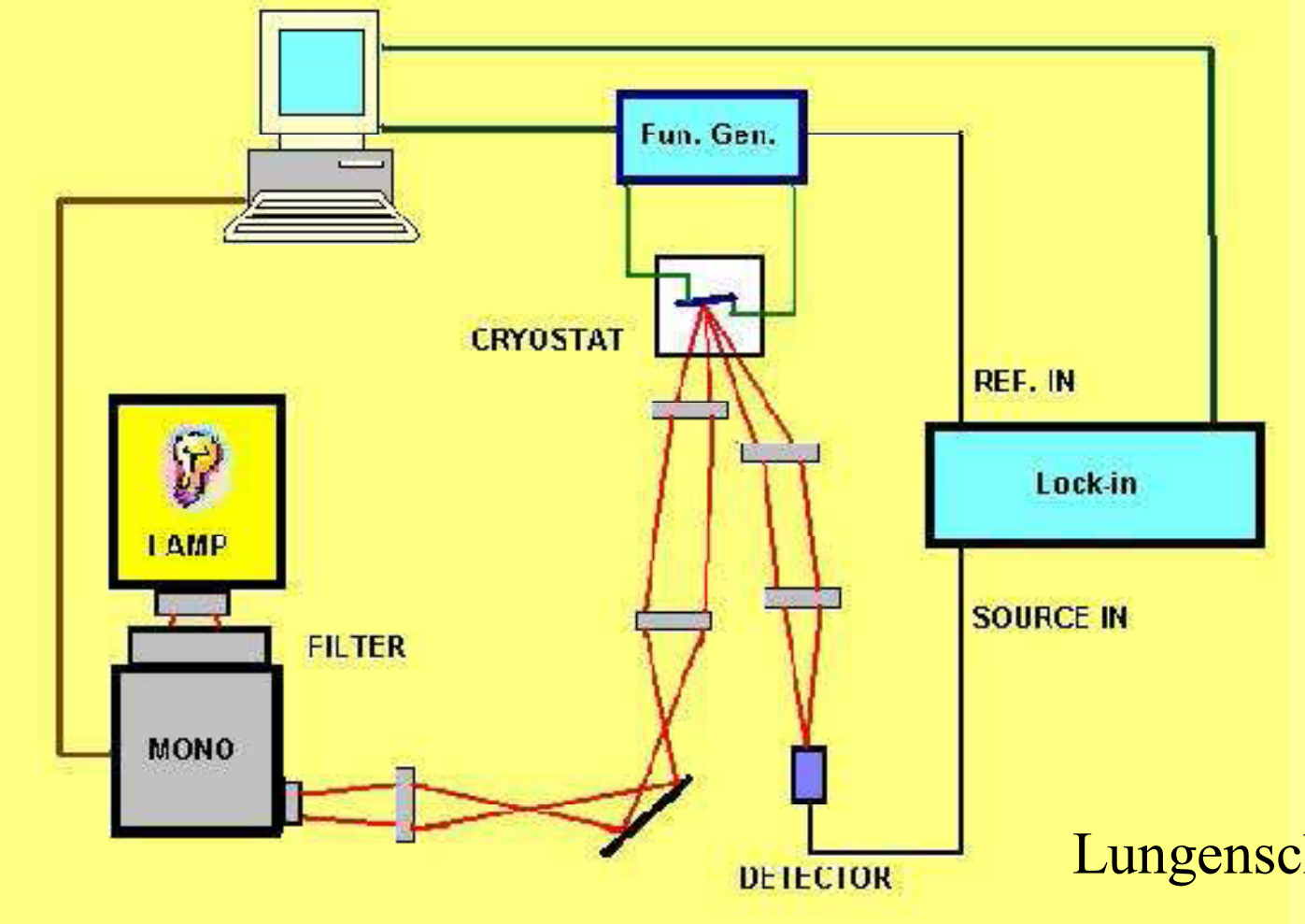

Lungenschmied et al., 2006

Electroabsorption Studies

A measure of the internal electric field in the device

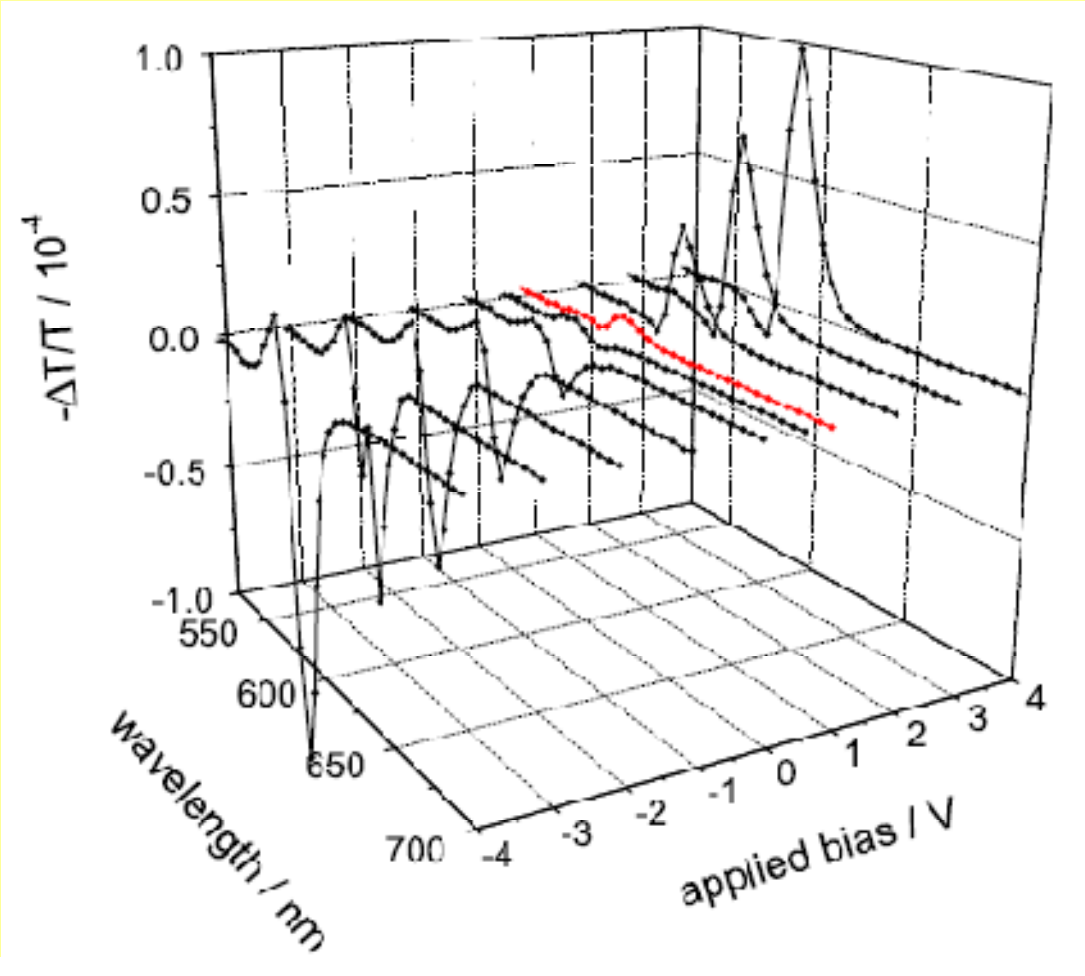

$$\frac{|\Delta T|}{T}(h\nu) \propto (V_{dc} - V_{int}) \cdot V_{ac}$$

Lungenschmied et al., 2006

Electroabsorption Studies

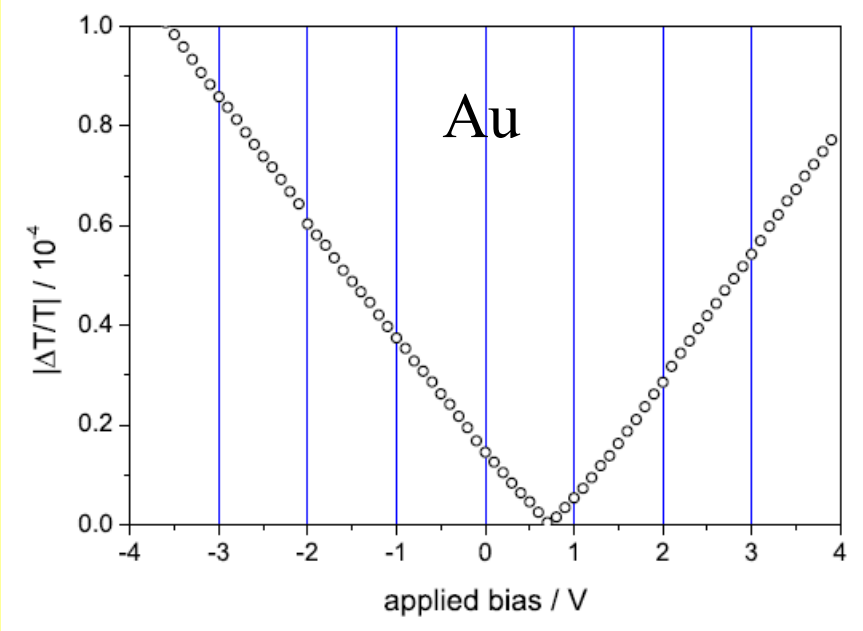

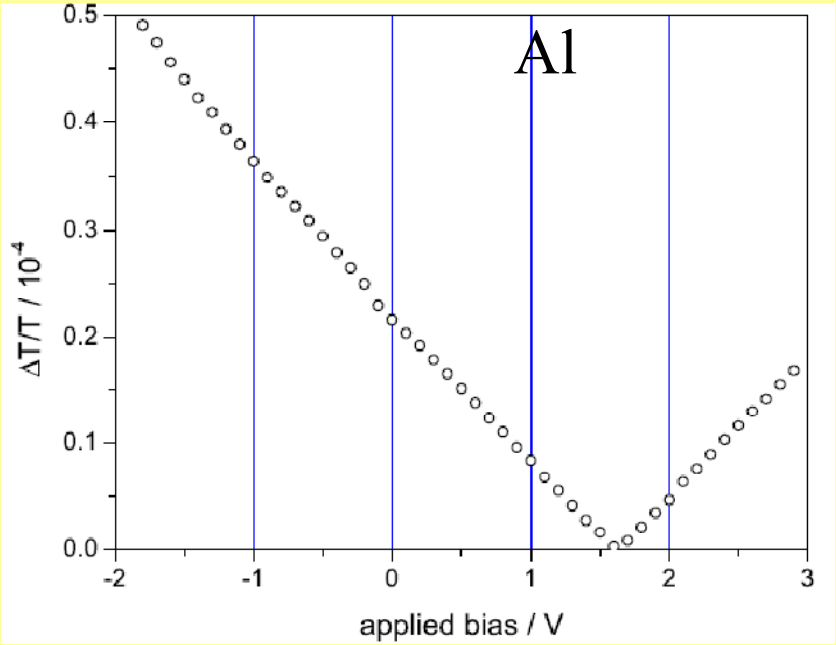

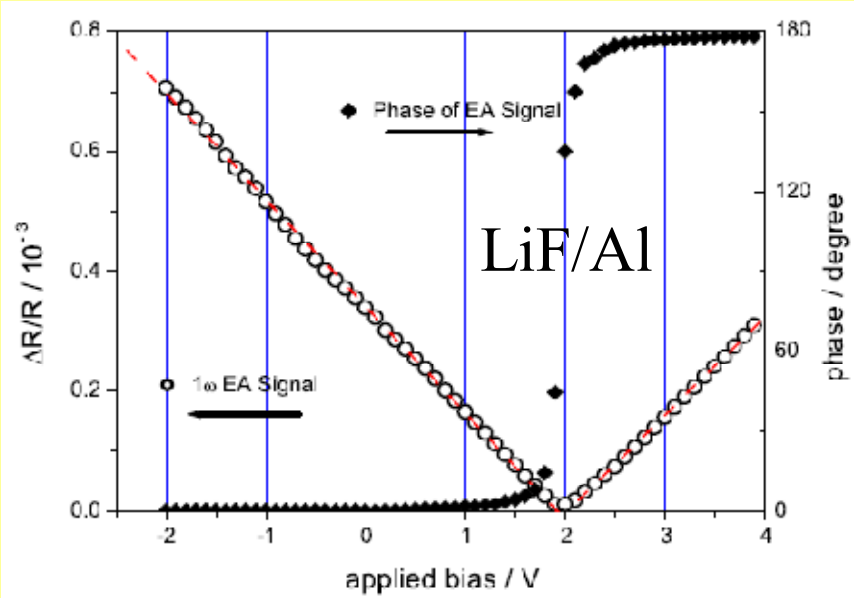

ITO/PEDOT-PSS/MDMO-PPV/Metal

100 K Electroabsorption Vac = 1V
@590nm probed

Lungenschmied et al., 2006

Summary for MDMO-PPV

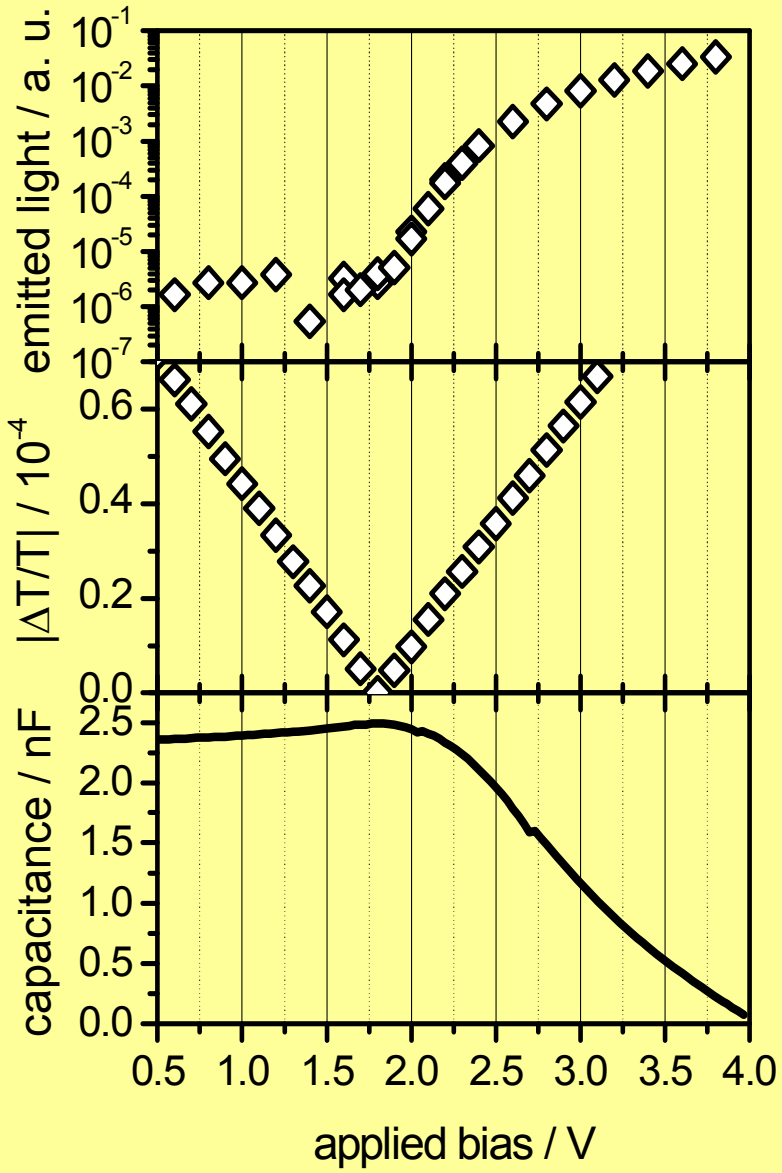

Lungenschmied et al., 2006

ITO/PEDOT-PSS/MDMO-PPV/LiF/Al

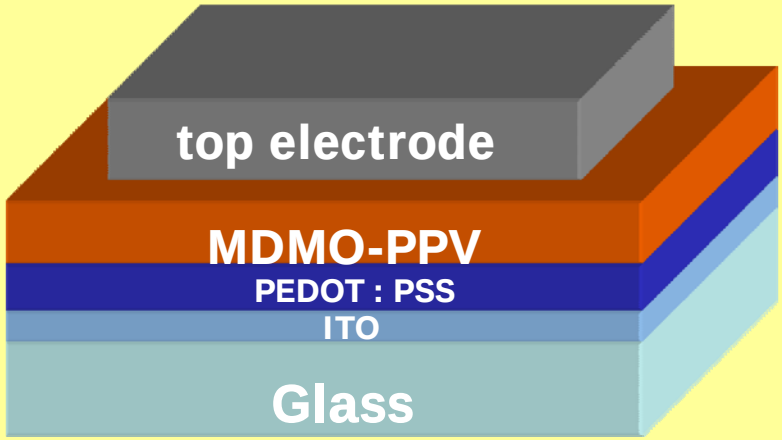

Below the built-in field the MDMO-PPV diodes behave like field driven devices but built-in field is higher than MIM model prediction

Summary for MDMO-PPV

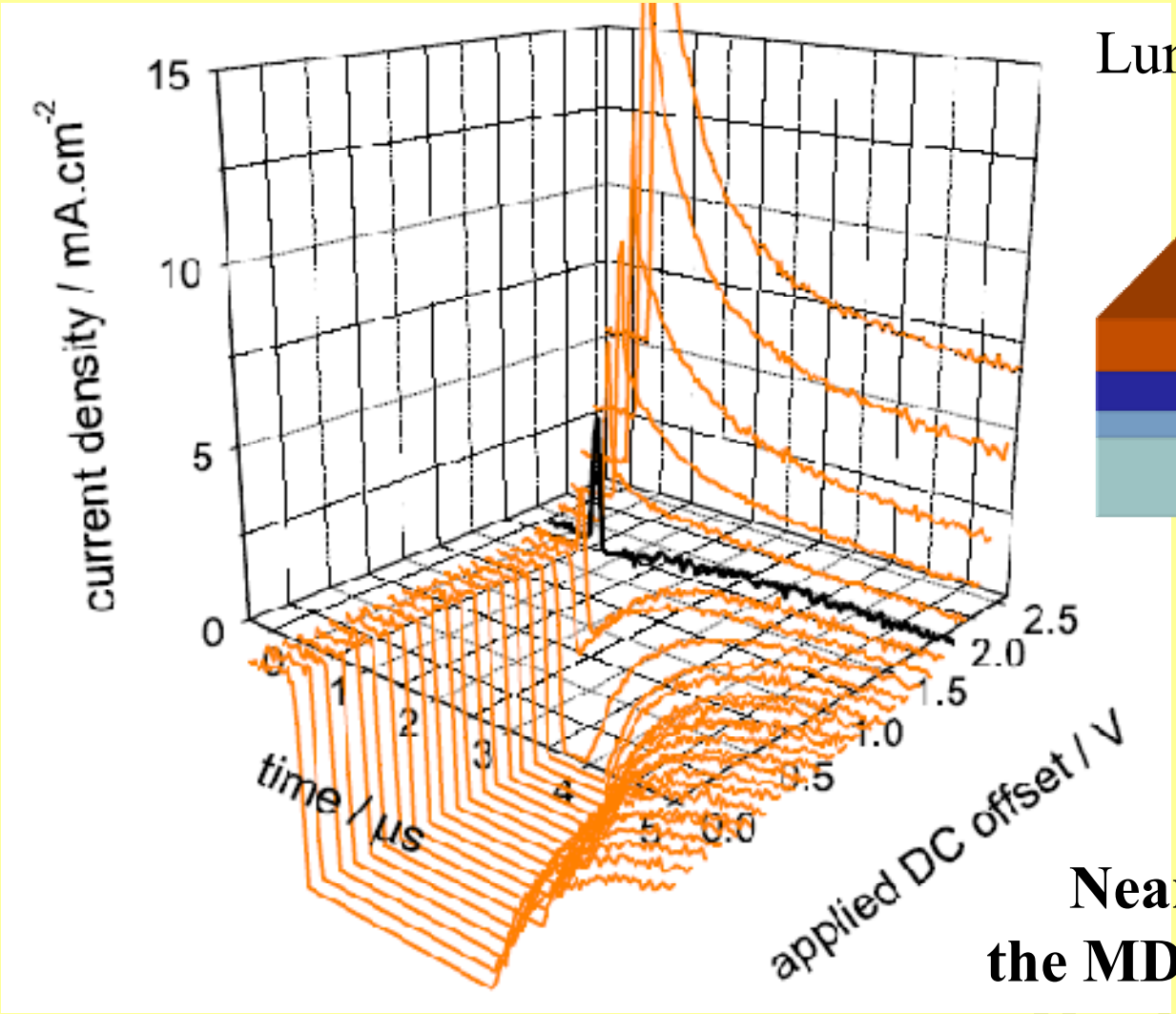

Lungenschmied et al., 2006

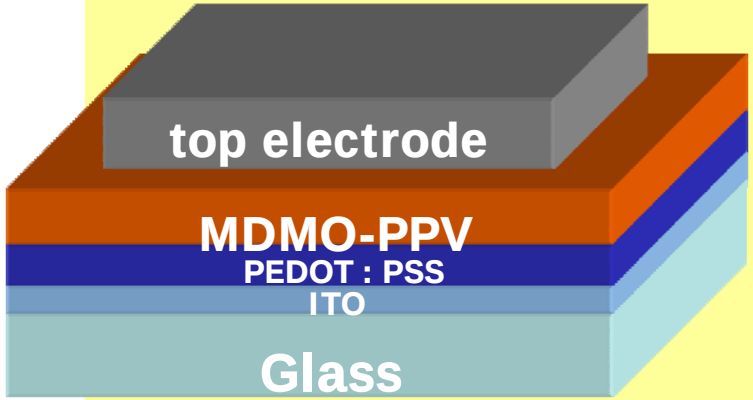

Near the built-in voltage the MDMO-PPV diodes show No photocurrent transients

ITO/PEDOT-PSS/MDMO-PPV/LiF/Al

MDMO-PPV mixed with 1% C60

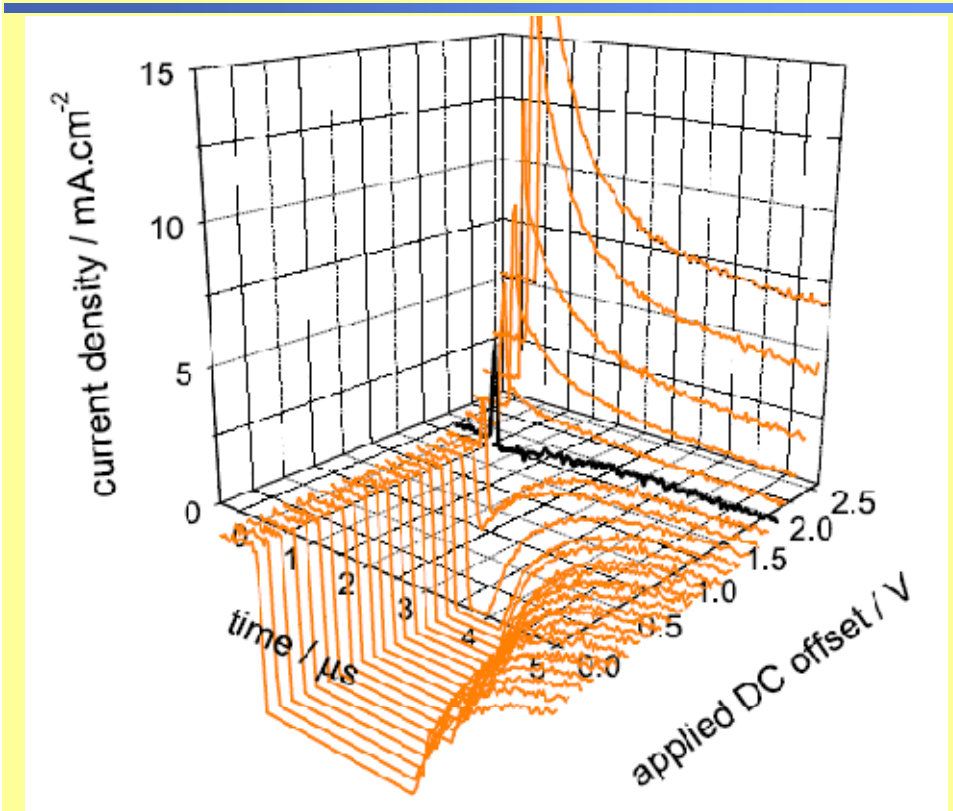

ITO/PEDOT-PSS/MDMO-PPV/LiF/Al

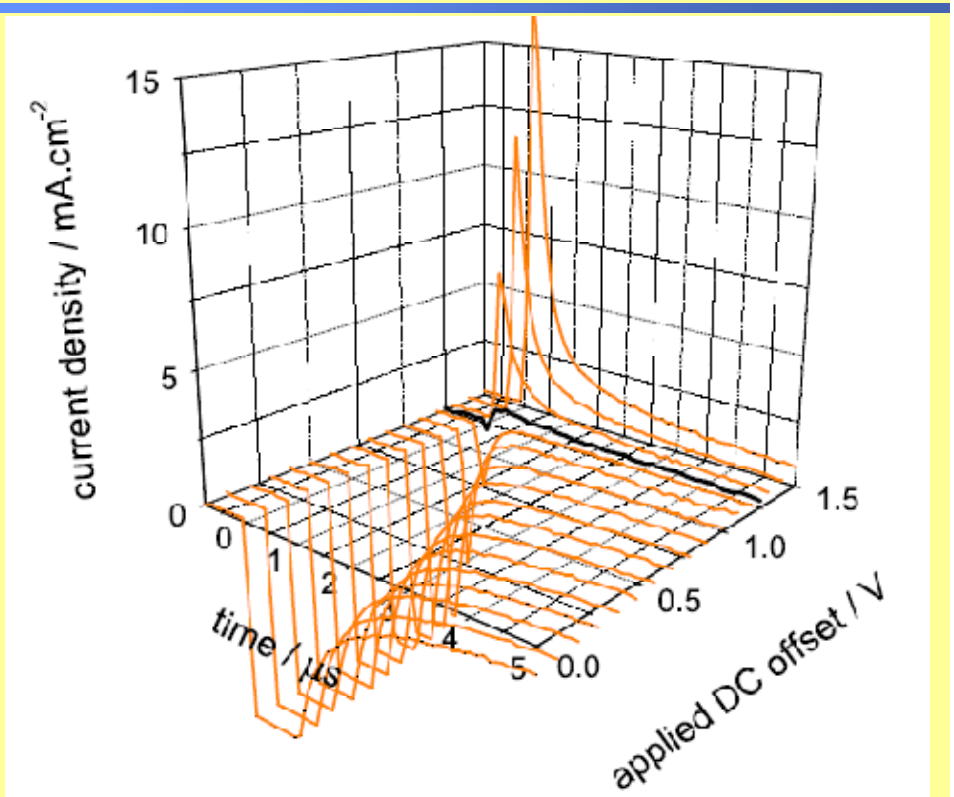

ITO/PEDOT-PSS/MDMO-PPV+1% PCBM/LiF/Al

Built-in field is reduced by nearly 0.8 V
upon addition of 1% PCBM into MDMO-PPV

C. Lungenschmied, G. Dennler, H. Neugebauer, N.S. Sariciftci, E. Ehrenfreund
Applied Physics Letters 89 (2006), 223519

MDMO-PPV mixed with 1% C60

Internal field is reduced by nearly 1 V
upon addition of 1% PCBM into MDMO-PPV

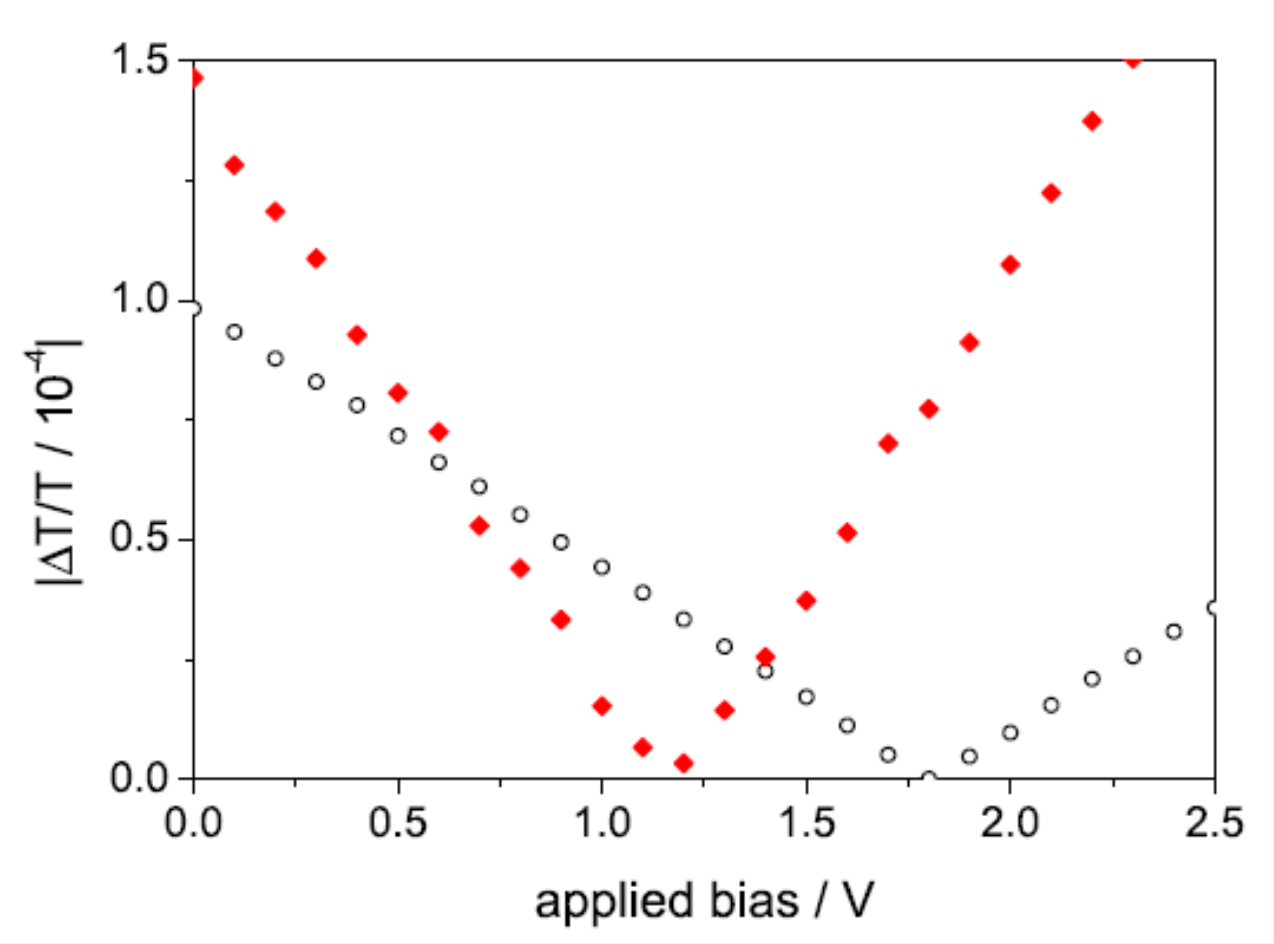

C. Lungenschmied, G. Dennler, H. Neugebauer, N.S. Sariciftci, E. Ehrenfreund
Applied Physics Letters 89 (2006), 223519

What about P3HT ?

Internal field in P3HT diodes is nearly independent to LiF insertion

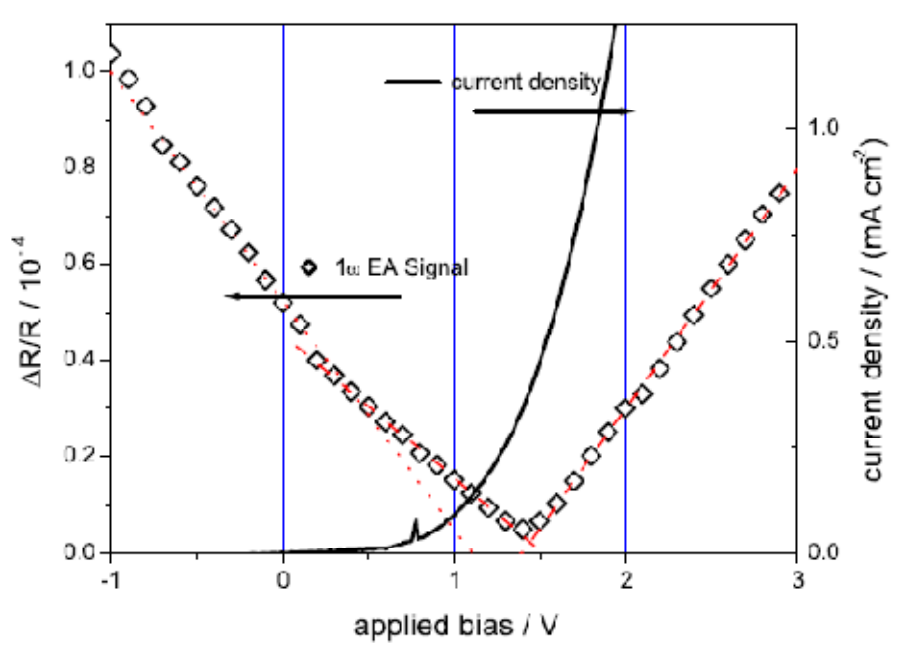

ITO/PEDOT-PSS/P3HT/Al

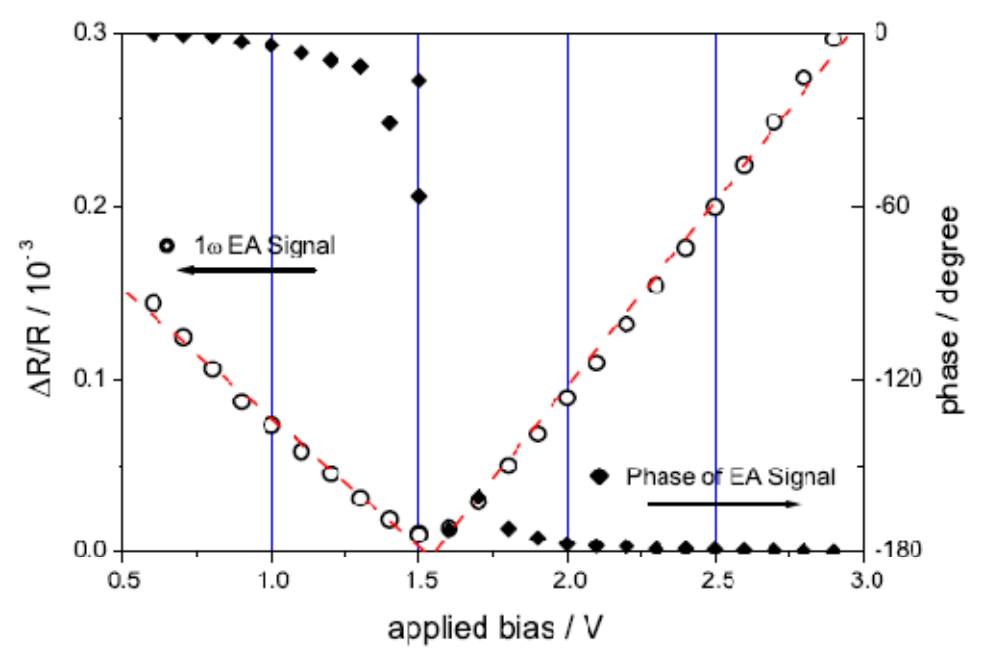

ITO/PEDOT-PSS/P3HT/LiF/Al

Measured @ 640nm and 77 K

SCHOTTKY JUNCTION FORMATION IS PROBABLE IN P3HT DIODES !

C. Lungenschmied (2006)

Schottky Junction in P3HT Devices ?

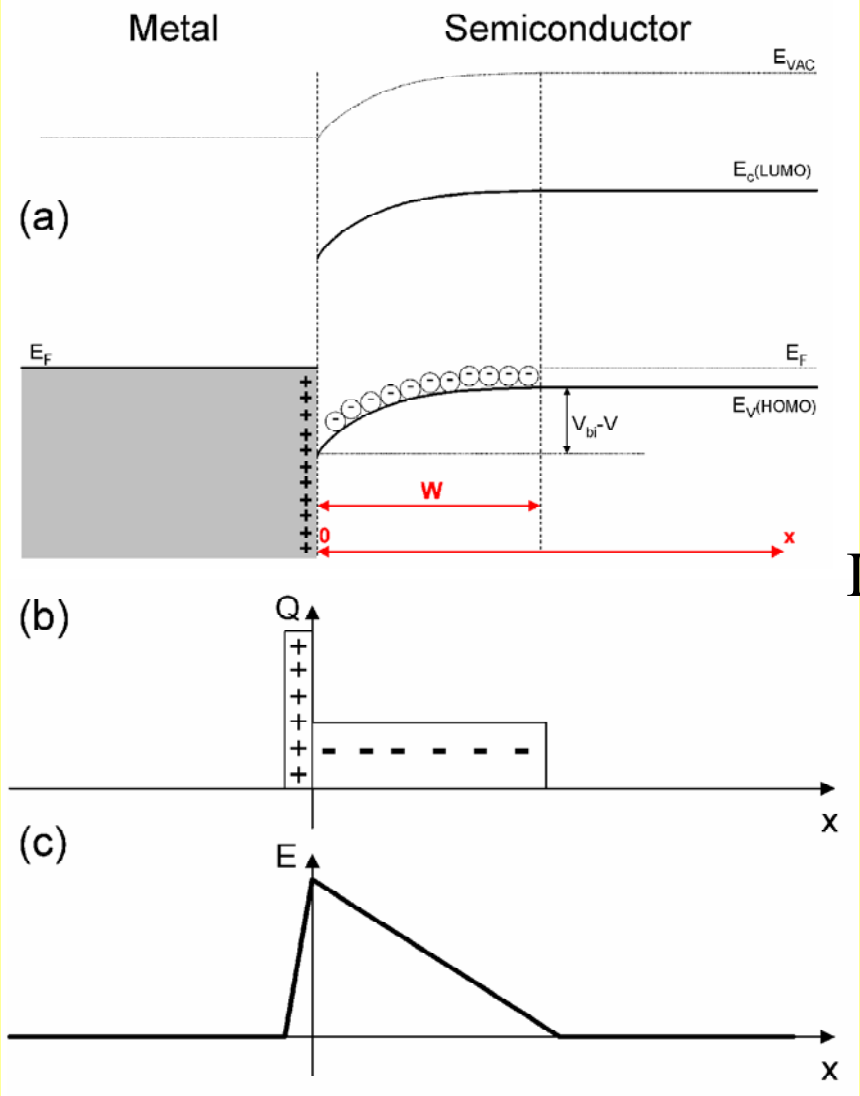

In the dark:
YES !

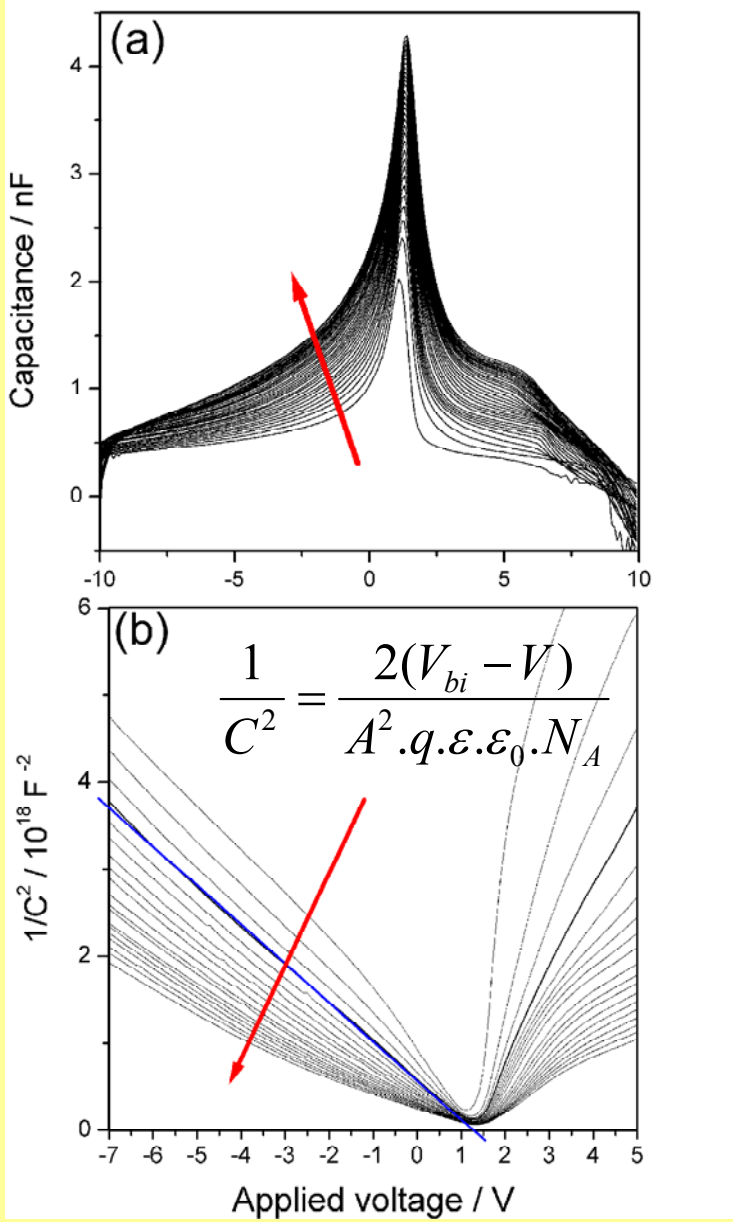

G. Dennler, C. Lungenschmied, N.S. Sariciftci, R. Schwoediauer, S. Bauer, H. Reiss
Applied Physics Letters 87 (2005), 163501

Band Models

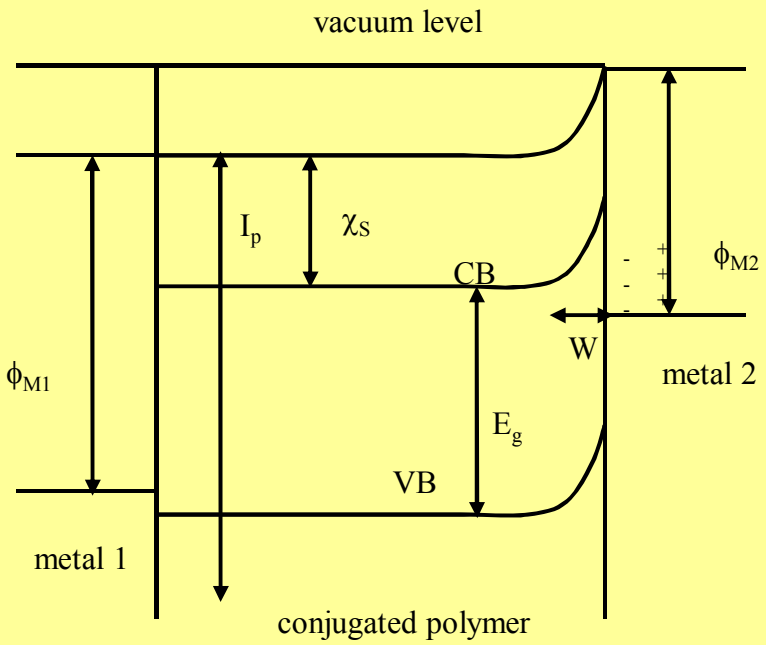

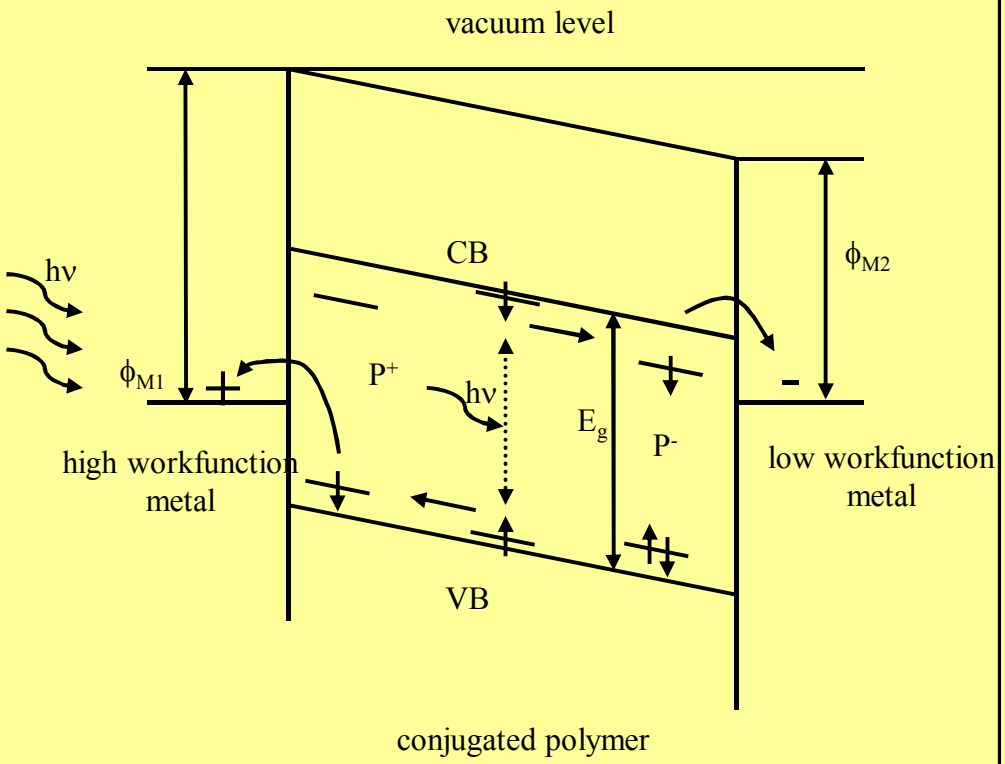

Schottky Contacts for high Impurities
$n >> 10^{16} cm^{-3}$

MIM Picture for low Impurities
$n << 10^{16} cm^{-3}$

Voc of Organic Solar Cells

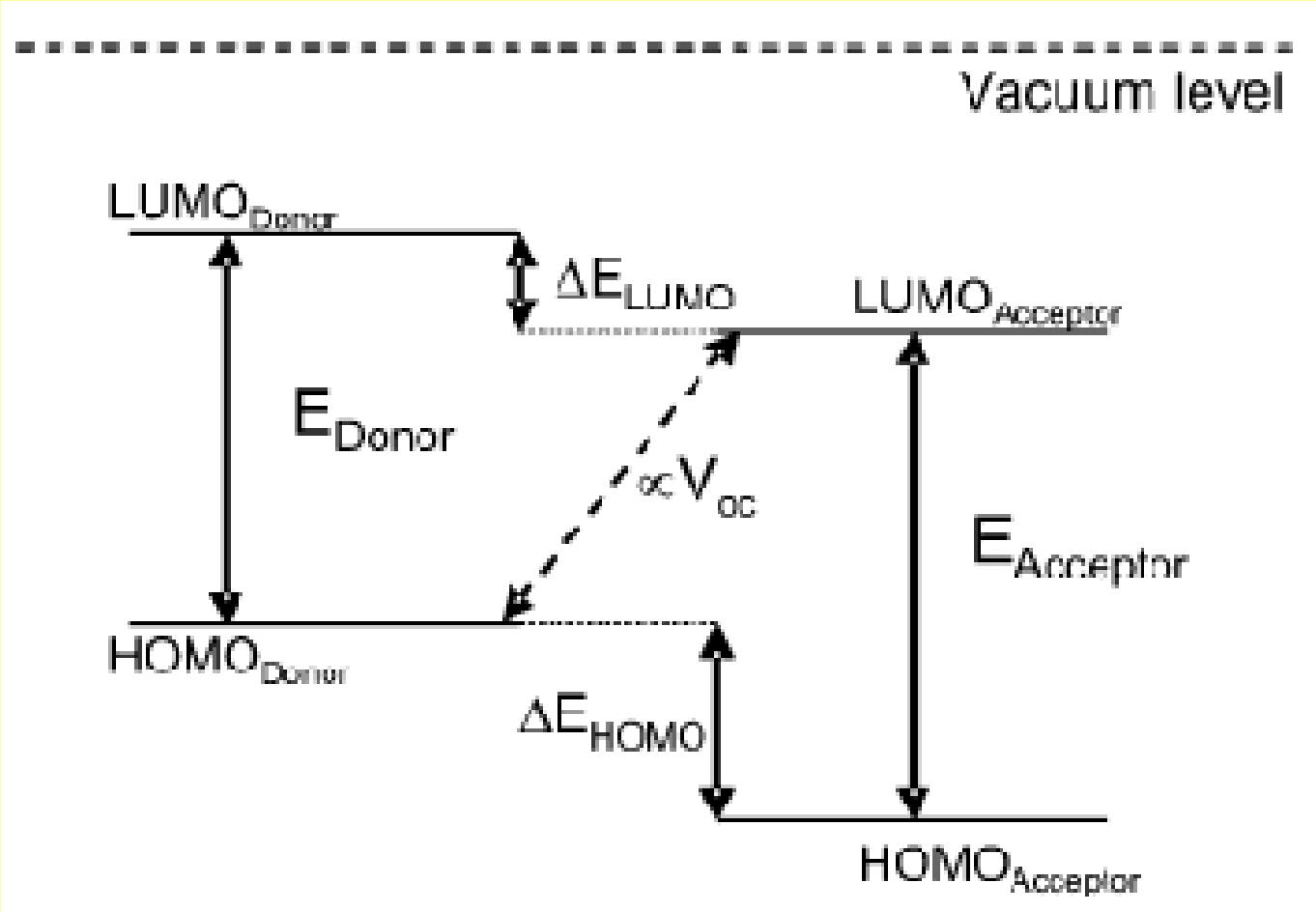

Voc vs LUMO of Acceptor

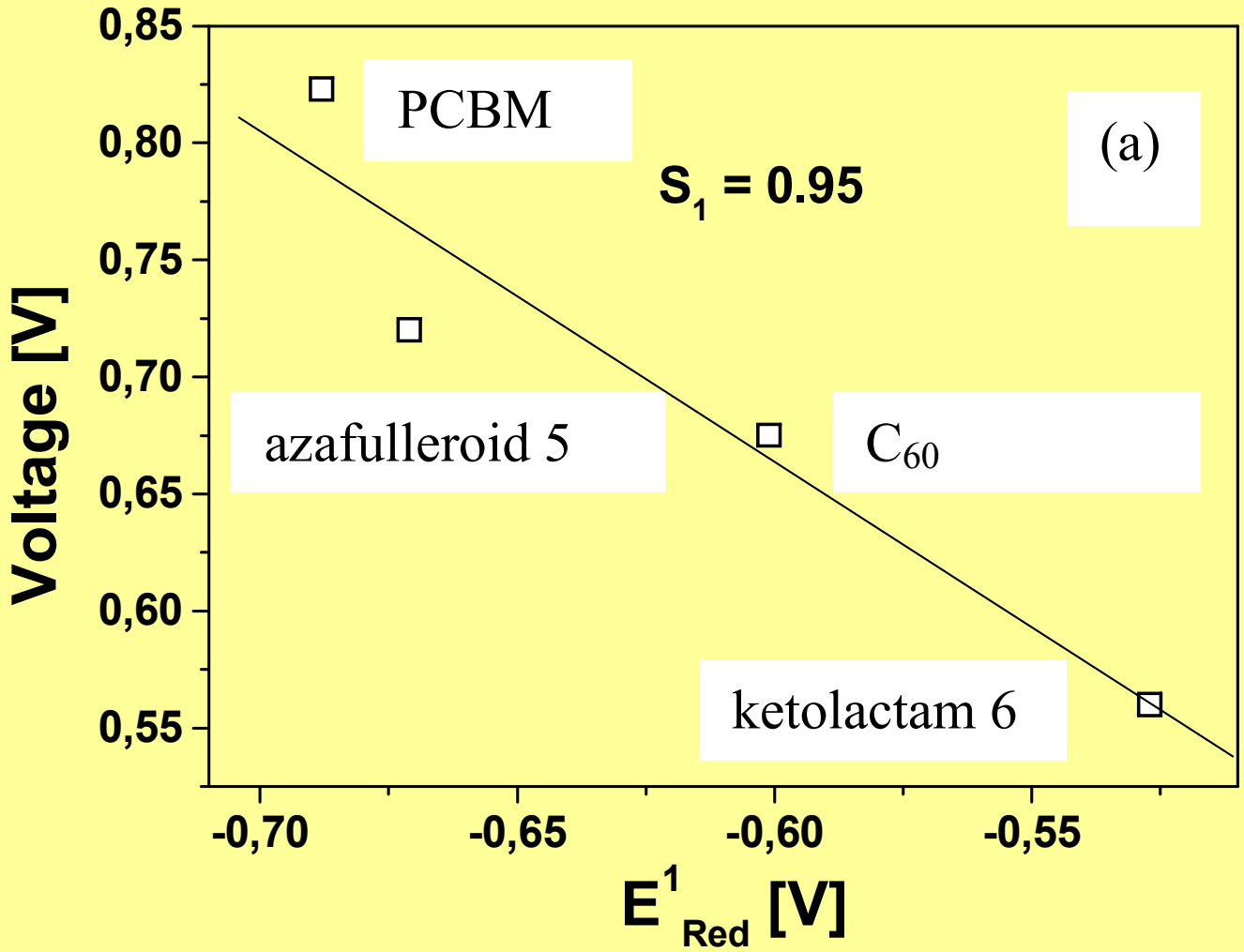

*Brabec et al., Advanced Functional Materials (2001), **11**, No.5, 374-380*

Voc vs HOMO of the Polymer Donor

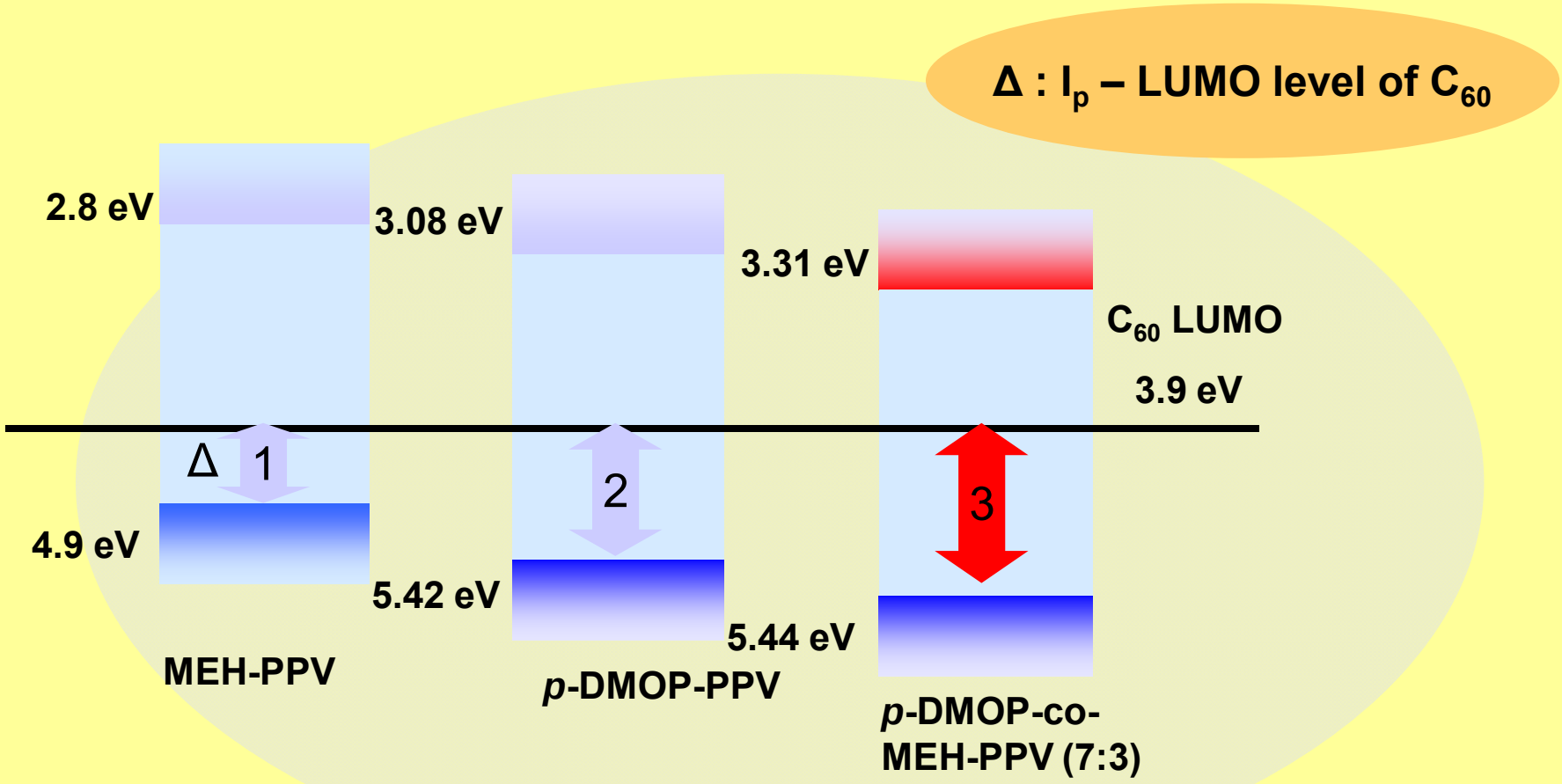

- High PL Quantum Efficiency Materials
- High Ionization Potential Materials

	1	2	3
Q.E.	10%	40%	23%

Kwanghee Lee et al, Pusan Univ. Korea

Voc vs HOMO of the Polymer Donor

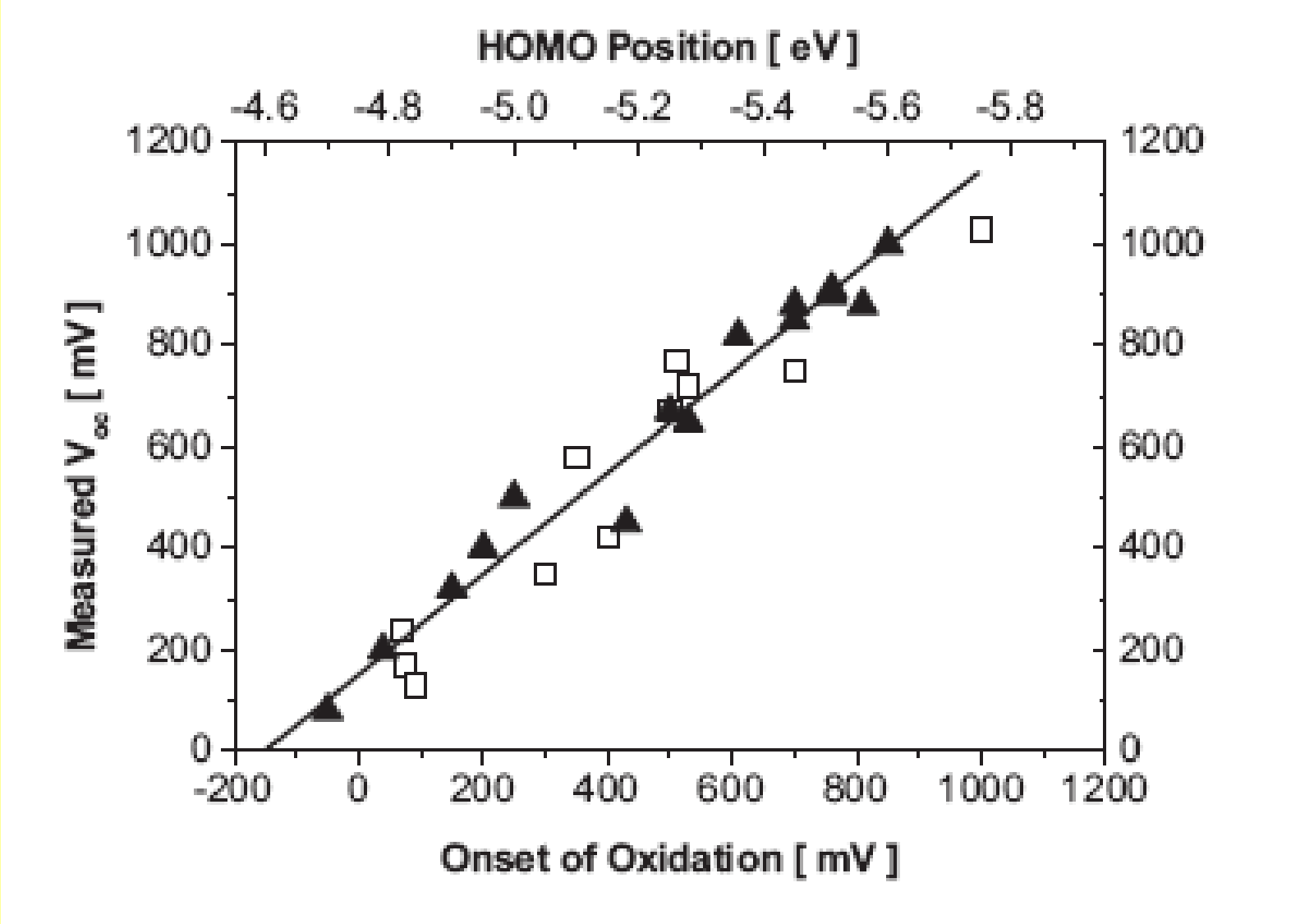

Markus Scharber *et al, Adv. Mater*. **18** (2006) 789

Polarons

Schematic energy diagram of a positive polaron

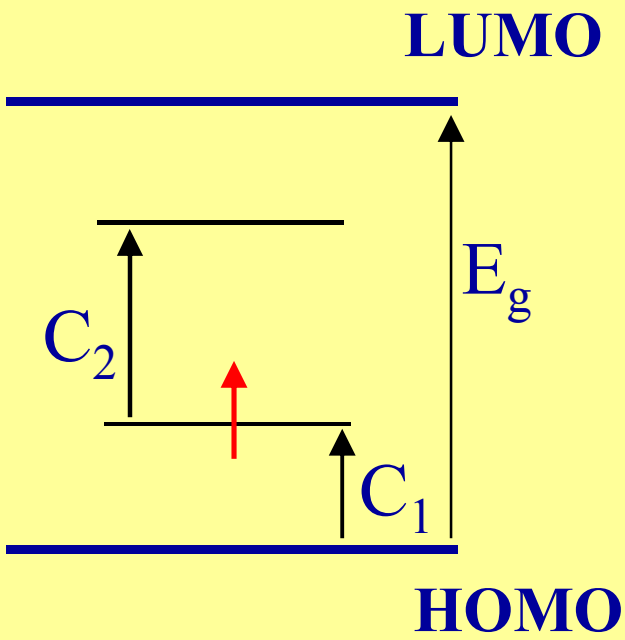

Typical PIA Spectrum

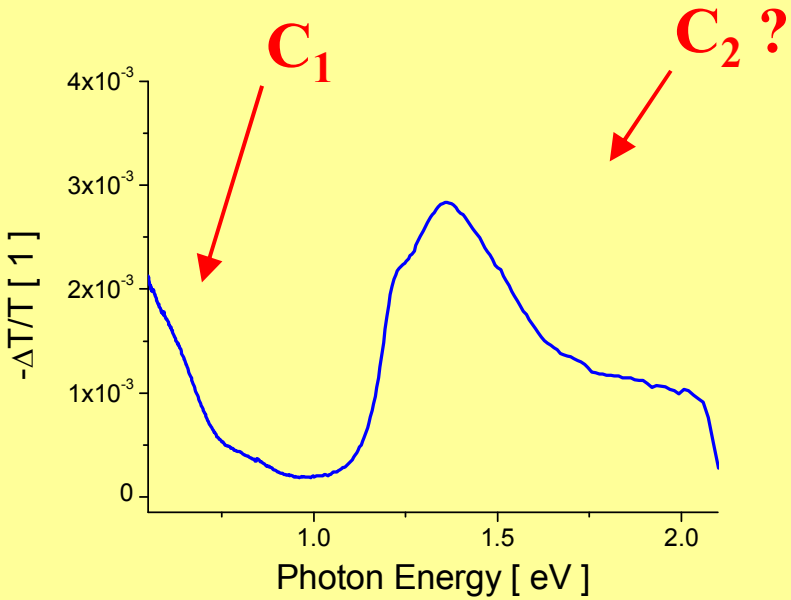

PIA Reflection-Setup

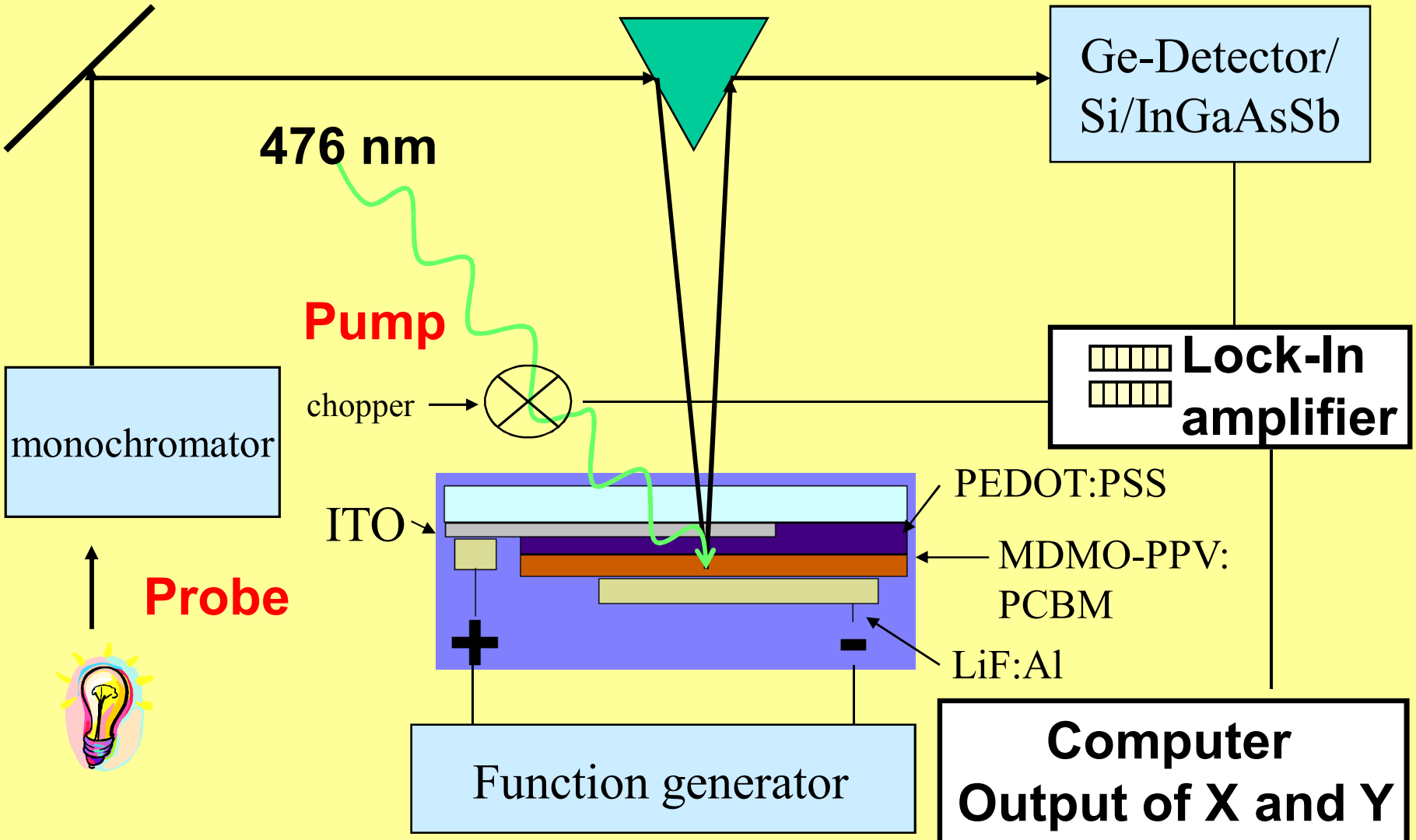

Photoinduced Absorption -Device

PIA of an MDMO-PPV/ PCBM 1:3 solar cell
under different applied voltages

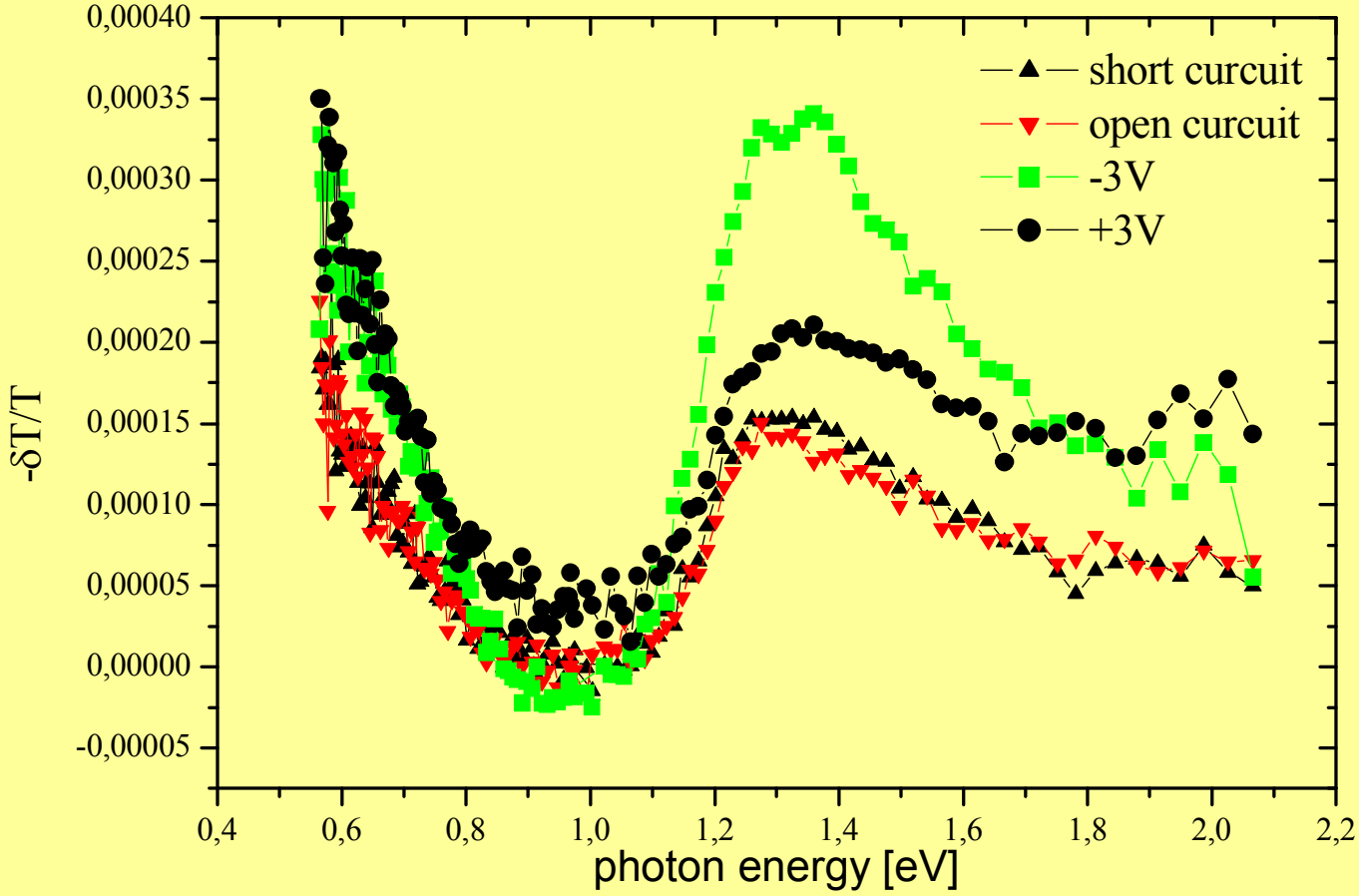

picture 3.7

Results

Different relaxation times for different spectral PIA bands

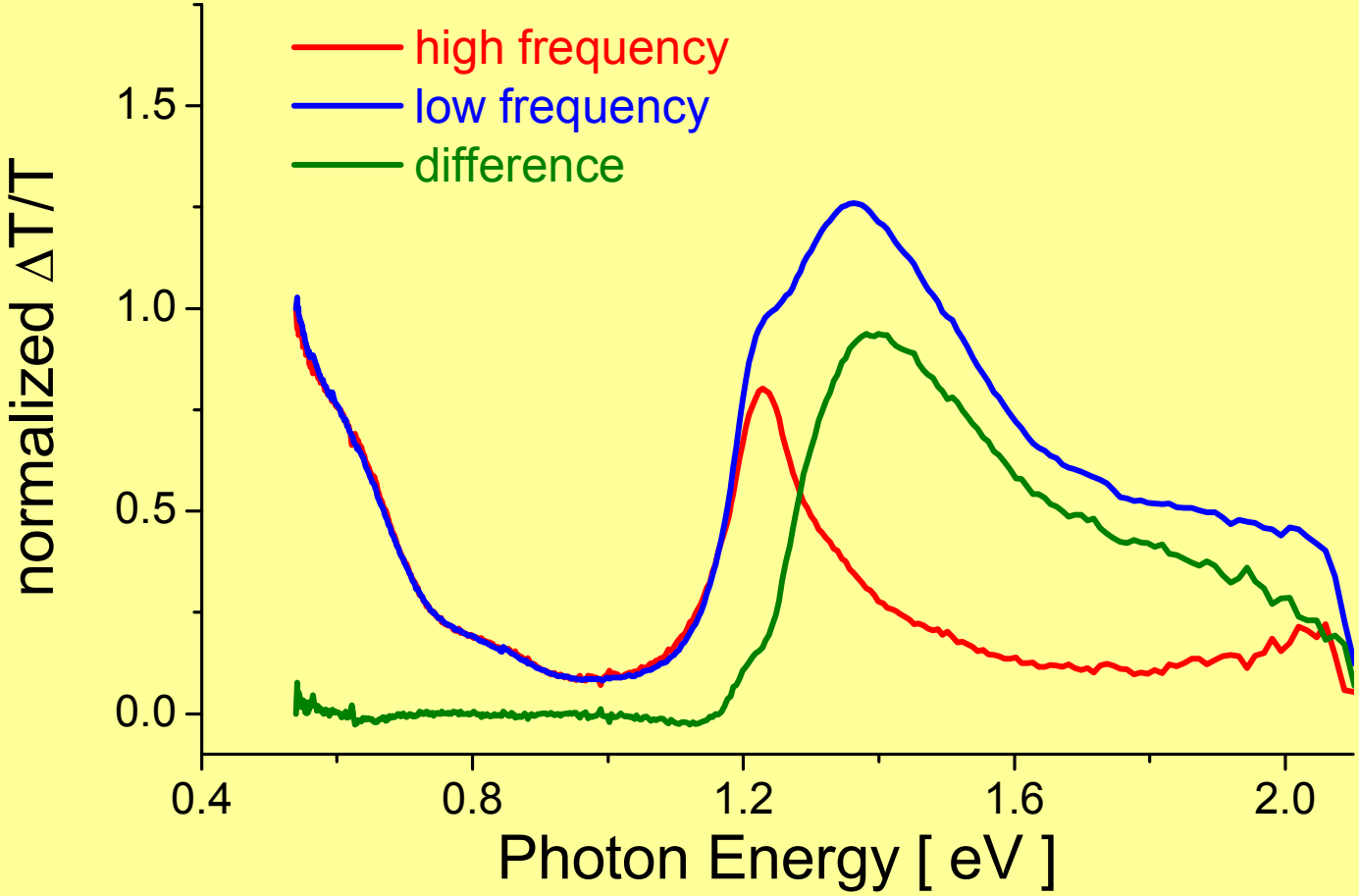

M. Scharber and N. S. Sariciftci, *Synth. Met.* **141**, (2004), Memorial Issue for Michael Rice

Linz Institute for Organic Solar Cells

Physics of Organic Semiconductors:

1.) Photoexcited spectroscopy
2.) Photoconductivity
3.) Thin film characterization
4.) Nanoscale engineering
5.) Nanoscale microscopy (AFM, STM...)
6.) In situ spectro-electrochemistry

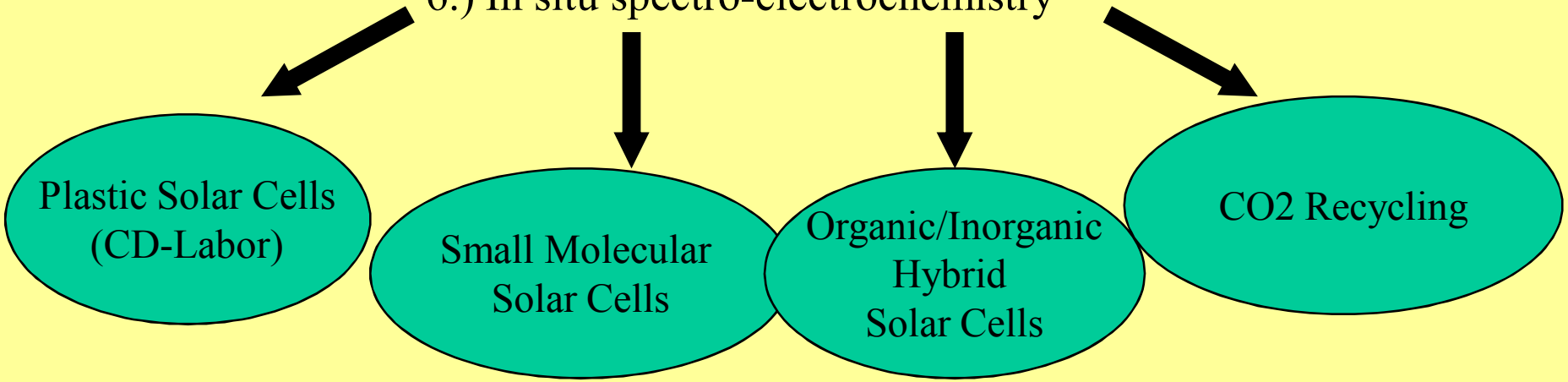

„Incubator“ for small high tech spin-off companies:
Konarka Austria (former QSEL), NanoIdent (insolv.), Botest, Isiqiri, Plastic Electronic GesmbH, Prelonic GesmbH , Solar Fuel GesmbH …

Acknowledgements

Members of LIOS:
Helmut Neugebauer, Mihai Irimia-Vladu, Elif Arici, Anita Fuchsbauer, Martin Egginger, Philipp Stadler, Alberto Montaign, Eric Glowacki, Engelbert Portenkirchner, Jacek Gasiorovski, Patchanita Thamyongkit, Almantas Pivrikas, Gerda Kalab, Beatrice Esteban-Meana, Kerstin Oppelt, Daniel Egbe, Stefan Schaur, Doris Sinwel, Sandra Kogler, Christoph Ulbricht, Matthew White, Mamatimin Abbas, Stefanie Schlager, Stefan Kraner, Valery Bliznyuk and many many more…

Uni. Linz, Collaborators.: Helmut Sitter, Thomas Fromherz, Siegfried Bauer, Reinhard Schwödiauer, Günther Knör

Spin-off companies:

Konarka Austria (plastic solar cells)
(NanoIdent) (insolv.)
Botest (plastic detector arrays)
Plastic Electronic (plastic pressure sensors)
Prelonic (printed batteries)
Isiqiri (intelligent display boards)
Solar Fuel (artificial fuels)

Funded by:
Solar Fuel Company
Austrian Foundation of Science (FWF)
European Commission